CHAPTER

11 Denoising

Removing noise from signals is possible only if some prior information is available. This information is encapsulated in an operator designed to reduce the noise while preserving the signal. Ideally, the joint probability distribution of the signal and the noise is known. Bayesian calculations then derive optimal operators that minimize the average estimation error. However, such probabilistic models are often not available for complex signals such as natural images.

Simpler signal models can be incorporated in the design of a basis or a frame, which takes advantage of known signal properties to build a sparse representation. Efficient nonlinear estimators are then computed by thresholding the resulting coefficients. For one-dimensional signals and images, thresholding estimators are studied in wavelet bases, time-frequency representations, and curvelet frames. Block thresholdings are introduced to regularize these operators, which improves the estimation of audio recordings and images.

The optimality of estimators is analyzed in a minimax framework, where the maximum estimation error is minimized over a predefined set of signals. When signals are not uniformly regular, nonlinear thresholding estimators in wavelet bases are shown to be much more efficient than linear estimators; they nearly reach the minimax risk over different signal classes, such as bounded variation signals and images.

11.1 ESTIMATION WITH ADDITIVE NOISE

Digital acquisition devices, such as cameras or microphones, output noisy measurements of an incoming analog signal $\bar{f}(x)$. These measurements can be modeled by a filtering of $\bar{f}(x)$ with the sensor responses $\bar{\phi}_n(x)$, to which is added a noise $W[n]$:

$$X[n] = \langle \bar{f}, \bar{\phi}_n \rangle + W[n] \quad \text{for} \quad 0 \leqslant n < N. \tag{11.1}$$

The noise W incorporates intrinsic physical fluctuations of the incoming signal. For example, an image intensity with low illumination has a random variation depending on the number of photons captured by each sensor. It also includes noises introduced by the measurement device, such as electronic noises or transmission errors. The aggregated noise W is modeled by a random vector that has a probability distribution that is supposed to be known a priori and is often Gaussian.

Let us denote the discretized signal by $f[n] = \langle \bar{f}, \bar{\phi}_n \rangle$. This analog-to-digital acquisition is supposed to be stable, so that, according to Section 3.1.3, an analog signal approximation of $\bar{f}(x)$ can be recovered from $f[n]$ with a linear projector. One must then optimize an estimation $\tilde{F}[n] = D\,X[n]$ of $f[n]$ calculated from the noisy measurements (11.1) that are rewritten as

$$X[n] = f[n] + W[n] \quad \text{for} \quad 0 \leqslant n < N.$$

The *decision operator* D is designed to minimize the estimation error $f - \tilde{F}$, measured by a *loss function*.

For audio signals or images, the loss function should measure the perceived audio or visual degradation. A mean-square distance is certainly not a perfect model of perceptual degradation, but it is mathematically simple and sufficiently precise in most applications. Throughout this chapter, the loss function is thus chosen to be a square Euclidean norm. The risk of the estimator $\tilde{F}$ of f is the average loss, calculated with respect to the probability distribution of the noise W:

$$r(D, f) = E\{\|f - DX\|^2\}. \tag{11.2}$$

The decision operator D is optimized with the prior information available on the signal. The Bayes framework supposes that signals are realizations of a random vector that has a known probability distribution, and a Bayes estimator minimizes the expected risk. A major difficulty is to acquire enough information to model this prior probability distribution. The minimax framework uses simpler deterministic models, which define signals as elements of a predefined set Θ. The expected risk cannot be computed, but the maximum risk can be minimized over Θ. Section 11.1.2 relates minimax and Bayes estimators through the minimax theorem.

11.1.1 Bayes Estimation

A Bayesian model considers signals f are realizations of a random vector F with a probability distribution π known a priori. This probability distribution is called the *prior distribution*. The noisy data are thus rewritten as

$$X[n] = F[n] + W[n] \quad \text{for} \quad 0 \leqslant n < N.$$

We suppose that noise and signal values $W[k]$ and $F[n]$ are independent for any $0 \leqslant k, n < N$. The joint distribution of F and W is thus the product of the distributions of F and W. It specifies the conditional probability distribution of F given the observed data X, also called the *posterior distribution*. This posterior distribution is used to optimize the decision operator D that computes an estimation $\tilde{F} = DX$ of F from the data X.

The *Bayes risk* is the expected risk calculated with respect to the prior probability distribution π of the signal:

$$r(D, \pi) = E_\pi\{r(D, F)\}.$$

By inserting (11.2), it can be rewritten as an expected value for the joint probability distribution of the signal and the noise:

$$r(D, \pi) = E\{\|F - \tilde{F}\|^2\} = \sum_{n=0}^{N-1} E\{|F[n] - \tilde{F}[n]|^2\}.$$

Let $\mathcal{O}_n$ be the set of all operators (linear and nonlinear) from $\mathbb{C}^N$ to $\mathbb{C}^N$. Optimizing D yields the *minimum Bayes risk*:

$$r_n(\pi) = \inf_{D \in \mathcal{O}_n} r(D, \pi).$$

Theorem 11.1 proves that there exist a *Bayes decision operator* D and a corresponding *Bayes estimator* $\tilde{F}$ that achieve this minimum risk.

Theorem 11.1. The Bayes estimator $\tilde{F}$ that yields the minimum Bayes risk $r_n(\pi)$ is the conditional expectation

$$\tilde{F}[n] = E\{F[n] \mid X[0], X[1], \ldots, X[N-1]\}. \tag{11.3}$$

Proof. Let $\pi_n(y)$ be the probability distribution of the value y of $F[n]$. The minimum risk is obtained by finding $\tilde{F}[n] = D_n(X)$ that minimizes $r(D_n, \pi_n) = E\{|F[n] - \tilde{F}[n]|^2\}$ for each $0 \leqslant n < N$. This risk depends on the conditional distribution $P_n(x|y)$ of the data $X = x$ given $F[n] = y$:

$$r(D_n, \pi_n) = \int \int (D_n(x) - y)^2 \, dP_n(x|y) \, d\pi_n(y).$$

Let $P(x) = \int P_n(x|y) \, d\pi_n(y)$ be the marginal distribution of X and $\pi_n(y|x)$ be the posterior distribution of $F[n]$ given X. The Bayes formula gives

$$r(D_n, \pi_n) = \int \left[\int (D_n(x) - y)^2 \, d\pi_n(y|x) \right] dP(x).$$

The double integral is minimized by minimizing the inside integral for each x. This quadratic form is minimum when its derivative vanishes:

$$\frac{\partial}{\partial D_n(x)} \int (D_n(x) - y)^2 \, d\pi_n(y|x) = 2 \int (D_n(x) - y) \, d\pi_n(y|x) = 0,$$

which implies that

$$D_n(x) = \int y \, d\pi_n(y|x) = E\{F[n] \mid X = x\},$$

so $D_n(X) = E\{F[n] \mid X\}$. ■

Linear Estimation

The conditional expectation (11.3) is generally a complicated nonlinear function of the data $\{X[k]\}_{0 \leqslant k < N}$, and is difficult to evaluate. To simplify this problem, we

restrict the decision operator D to be linear. Let $\mathcal{O}_l$ be the set of all linear operators from $\mathbb{C}^N$ to $\mathbb{C}^N$. The *linear minimum Bayes risk* is:

$$r_l(\pi) = \inf_{D \in \mathcal{O}_l} r(D, \pi).$$

The linear estimator $\tilde{F} = DX$ that achieves this minimum risk is called the *Wiener estimator*. Theorem 11.2 gives a necessary and sufficient condition that specifies this estimator. We suppose that $E\{F[n]\} = 0$, which can be enforced by subtracting $E\{F[n]\}$ from $X[n]$ to obtain a zero-mean signal.

Theorem 11.2. A linear estimator $\tilde{F}$ is a Wiener estimator if and only if

$$E\{(F[n] - \tilde{F}[n])\, X[k]\} = 0 \quad \text{for} \quad 0 \leq k, n < N. \tag{11.4}$$

Proof. For each $0 \leq n < N$, we must find a linear estimation

$$\tilde{F}[n] = D_n X = \sum_{k=0}^{N-1} h[n, k]\, X[k],$$

which minimizes

$$r(D_n, \pi_n) = E\left\{ \left(F[n] - \sum_{k=0}^{N-1} h[n, k]\, X[k] \right) \left(F[n] - \sum_{k=0}^{N-1} h[n, k]\, X[k] \right) \right\}. \tag{11.5}$$

The minimum of this quadratic form is reached if and only if for each $0 \leq k < N$,

$$\frac{\partial r(D_n, \pi_n)}{\partial h[n, k]} = -2\, E\left\{ \left(F[n] - \sum_{l=0}^{N-1} h[n, l]\, X[l] \right) X[k] \right\} = 0,$$

which verifies (11.4). ■

If F and W are independent Gaussian random vectors, then the linear optimal estimator is also optimal among nonlinear estimators. Indeed, two jointly Gaussian random vectors are independent if they are noncorrelated [53]. Since $F[n] - \tilde{F}[n]$ is jointly Gaussian with $X[k]$, the noncorrelation (11.4) implies that $F[n] - \tilde{F}[n]$ and $X[k]$ are independent for any $0 \leq k, n < N$. In this case, we can verify that $\tilde{F}$ is the Bayes estimator (11.3): $\tilde{F}[n] = E\{F[n] \mid X\}$. Theorem 11.3 computes the Wiener estimator from the covariance R_F and R_W of the signal F and of the noise W. The properties of covariance operators are described in Section A.6 of the Appendix.

Theorem 11.3: *Wiener.* If the signal F and the noise W are independent random vectors of covariance R_F and R_W, then the linear Wiener estimator $\tilde{F} = DF$ that minimizes $E\{\|\tilde{F} - F\|^2\}$ is

$$\tilde{F} = R_F\, (R_F + R_W)^{-1} X. \tag{11.6}$$

Proof. Let $\tilde{F}[n]$ be a linear estimator of $F[n]$:

$$\tilde{F}[n] = \sum_{l=0}^{N-1} h[n, l]\, X[l]. \tag{11.7}$$

This equation can be rewritten as a matrix multiplication by introducing the $N \times N$ matrix $H = (h[n,l])_{0 \leq n,l < N}$:

$$\tilde{F} = H\,X. \tag{11.8}$$

Theorem 11.2 proves that an optimal linear estimator satisfies the noncorrelation condition (11.4), which implies that for $0 \leq n, k < N$,

$$E\{F[n]\,X[k]\} = E\{\tilde{F}[n]\,X[k]\} = \sum_{l=0}^{N-1} h[n,l]\,E\{X[l]\,X[k]\}.$$

Since $X[k] = F[k] + W[k]$ and $E\{F[n]\,W[k]\} = 0$, it results that

$$E\{F[n]\,F[k]\} = \sum_{l=0}^{N-1} h[n,l]\,\Big(E\{F[l]\,F[k]\} + E\{W[l]\,W[k]\}\Big). \tag{11.9}$$

Let R_F and R_W be the covariance matrices of F and W, defined by $E\{F[n]\,F[k]\}$ and $E\{W[n]\,W[k]\}$, respectively. Equation (11.9) can be rewritten as a matrix equation:

$$R_F = H\,(R_F + R_W).$$

Inverting this equation gives

$$H = R_F\,(R_F + R_W)^{-1}. \qquad \blacksquare$$

The optimal linear estimator (11.6) is simple to compute since it only depends on second-order covariance moments of the signal and of the noise.

Estimation in a Karhunen-Loève Basis

Since a covariance operator is symmetric, it is diagonalized in an orthonormal basis that is called a *Karhunen-Loève basis* or a basis of *principal components*. If the covariance operators R_F and R_W are diagonal in the same Karhunen-Loève basis $\mathcal{B} = \{g_m\}_{0 \leq m < N}$, then Corollary 11.1 derives from Theorem 11.3 that the Wiener estimator is diagonal in this basis. We write

$$X_{\mathcal{B}}[m] = \langle X, g_m \rangle, \quad F_{\mathcal{B}}[m] = \langle F, g_m \rangle, \quad \tilde{F}_{\mathcal{B}}[m] = \langle \tilde{F}, g_m \rangle,$$

$$W_{\mathcal{B}}[m] = \langle W, g_m \rangle \quad \text{and} \quad \sigma_{\mathcal{B}}[m]^2 = E\{|\langle W, g_m \rangle|^2\}.$$

Corollary 11.1. If there exists a Karhunen-Loève basis $\mathcal{B} = \{g_m\}_{0 \leq m < N}$ that diagonalizes the covariance matrices R_F and R_W of F and W, then the Wiener estimator that minimizes $E\{\|\tilde{F} - F\|^2\}$ is

$$\tilde{F} = \sum_{m=0}^{N-1} \frac{E\{|F_{\mathcal{B}}[m]|^2\}}{E\{|F_{\mathcal{B}}[m]|^2\} + \sigma_{\mathcal{B}}[m]^2}\, X_{\mathcal{B}}[m]\, g_m. \tag{11.10}$$

The resulting minimum linear Bayes risk is

$$r_l(\pi) = \sum_{m=0}^{N-1} \frac{E\{|F_{\mathcal{B}}[m]|^2\}\,\sigma_{\mathcal{B}}[m]^2}{E\{|F_{\mathcal{B}}[m]|^2\} + \sigma_{\mathcal{B}}[m]^2}. \tag{11.11}$$

Proof. The diagonal values of R_F and R_W are $\langle R_F g_m, g_m\rangle = E\{|F_{\mathcal{B}}[m]|^2\}$ and $\langle R_W g_m, g_m\rangle = E\{|W_{\mathcal{B}}[m]|^2\} = \sigma^2_{\mathcal{B}}[m]$. Since R_F and R_W are diagonal in $\mathcal{B}$, the linear operator $R_F\,(R_F + R_W)^{-1}$ in (11.6) is also diagonal in $\mathcal{B}$, with diagonal values equal to $E\{|F_{\mathcal{B}}[m]|^2\}\,(E\{|F_{\mathcal{B}}[m]|^2\} + \sigma_{\mathcal{B}}[m]^2)^{-1}$. So (11.6) proves that the Wiener estimator is

$$\tilde{F}_{\mathcal{B}} = R_F\,(R_F + R_W)^{-1} X = \sum_{m=0}^{N-1} \frac{E\{|F_{\mathcal{B}}[m]|^2\}}{E\{|F_{\mathcal{B}}[m]|^2\} + \sigma_{\mathcal{B}}[m]^2}\, X_{\mathcal{B}}[m]\, g_m, \tag{11.12}$$

which proves (11.10).

The resulting risk is

$$E\{\|F - \tilde{F}\|^2\} = \sum_{m=0}^{N-1} E\left\{|F_{\mathcal{B}}[m] - \tilde{F}_{\mathcal{B}}[m]|^2\right\}. \tag{11.13}$$

Inserting (11.12) in (11.13) with $X_{\mathcal{B}}[m] = F_{\mathcal{B}}[m] + W_{\mathcal{B}}[m]$, where $F_{\mathcal{B}}[m]$ and $W_{\mathcal{B}}[m]$ are independent, yields (11.11). ■

This corollary proves that the Wiener estimator is implemented with a diagonal attenuation of each data coefficient $X_{\mathcal{B}}[m]$ by a factor that depends on the signal-to-noise ratio $E\{|F_{\mathcal{B}}[m]|^2\}/\sigma_{\mathcal{B}}[m]^2$ in the direction of g_m. The smaller the signal-to-noise ratio (SNR), the more attenuation is required. If F and W are Gaussian processes, then the Wiener estimator is optimal among linear and nonlinear estimators of F.

If W is a white noise, then its coefficients are uncorrelated with the same variance:

$$E\{W[n]\,W[k]\} = \sigma^2\,\delta[n-k].$$

Its covariance matrix is therefore $R_W = \sigma^2\,\mathrm{Id}$. It is diagonal in all orthonormal bases and, in particular, in a Karhunen-Loève basis of F. Thus, Theorem 11.1 can be applied with $\sigma_{\mathcal{B}}[m] = \sigma$ for $0 \leqslant m < N$.

Frequency Filtering

Suppose that F and W are zero-mean, wide-sense circular stationary random vectors. The properties of such processes are reviewed in Section A.6 of the Appendix. Their covariance satisfies

$$E\{F[n]\,F[k]\} = R_F[n-k], \quad E\{W[n]\,W[k]\} = R_W[n-k],$$

where $R_F[n]$ and $R_W[n]$ are N periodic. These matrices correspond to circular convolution operators and are therefore diagonal in the discrete Fourier basis

$$\left\{g_m[n] = \frac{1}{\sqrt{N}}\,\exp\left(\frac{i2m\pi n}{N}\right)\right\}_{0\leqslant m<N}.$$

The eigenvalues $E\{|F_{\mathcal{B}}[m]|^2\}$ and $\sigma_{\mathcal{B}}[m]^2$ are the discrete Fourier transforms of $R_F[n]$ and $R_W[n]$, also called *power spectra*:

$$E\{|F_{\mathcal{B}}[m]|^2\} = \sum_{n=0}^{N-1} R_F[n] \exp\left(\frac{-i2m\pi n}{N}\right) = \hat{R}_F[m],$$

$$\sigma_{\mathcal{B}}[m]^2 = \sum_{n=0}^{N-1} R_W[n] \exp\left(\frac{-i2m\pi n}{N}\right) = \hat{R}_W[m].$$

The Wiener estimator (11.10) is then a diagonal operator in the discrete Fourier basis, computed with the frequency filter

$$\hat{h}[m] = \frac{\hat{R}_F[m]}{\hat{R}_F[m] + \hat{R}_W[m]}. \tag{11.14}$$

It is therefore a circular convolution:

$$\tilde{F}[n] = DX = X \circledast h[n].$$

The resulting risk is calculated with (11.11):

$$r_l(\pi) = E\{\|F - \tilde{F}\|^2\} = \sum_{m=0}^{N-1} \frac{\hat{R}_F[m]\,\hat{R}_W[m]}{\hat{R}_F[m] + \hat{R}_W[m]}. \tag{11.15}$$

The numerical value of the risk is often specified by the signal-to-noise ratio, which is measured in decibels:

$$\mathrm{SNR}_{\mathrm{db}} = 10 \log_{10}\left(\frac{E\{\|F\|^2\}}{E\{\|F - \tilde{F}\|^2\}}\right). \tag{11.16}$$

EXAMPLE 11.1

Figure 11.1(a) shows a realization of a Gaussian process F obtained as a convolution of a Gaussian white noise B of variance β^2 with a low-pass filter g:

$$F[n] = B \circledast g[n],$$

with

$$g[n] = C \cos^2\left(\frac{\pi n}{2K}\right) \mathbf{1}_{[-K,K]}[n].$$

Theorem A.7 proves that

$$\hat{R}_F[m] = \hat{R}_B[m]\,|\hat{g}[m]|^2 = \beta^2\,|\hat{g}[m]|^2.$$

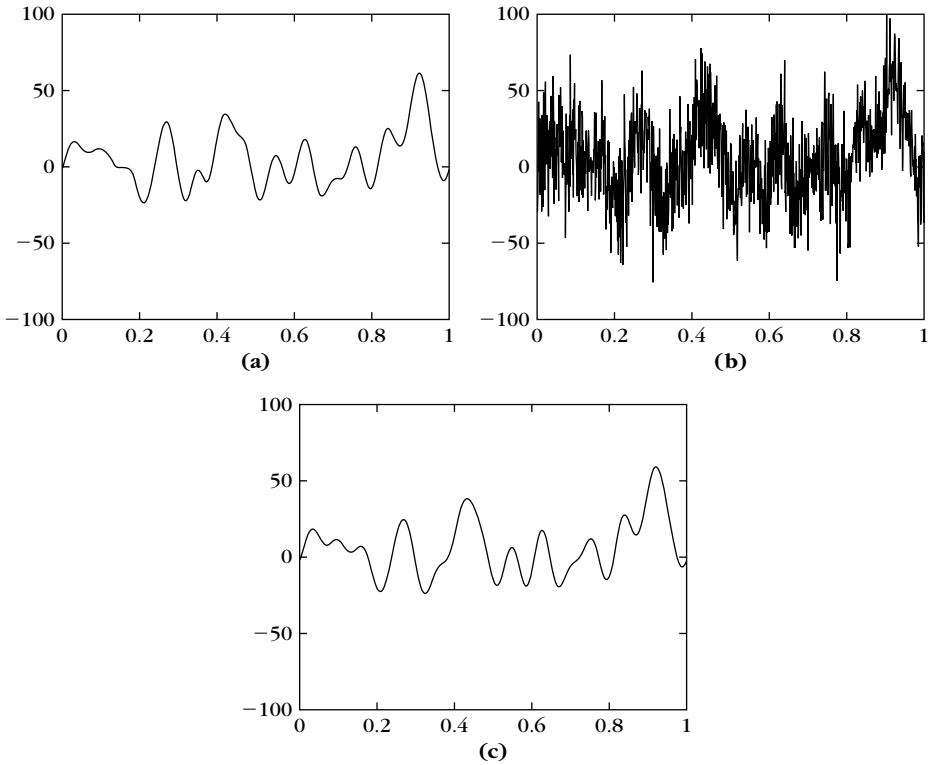

FIGURE 11.1

(a) Realization of a Gaussian process F. **(b)** Noisy signal obtained by adding a Gaussian white noise (SNR $= -0.48$ db). **(c)** Wiener estimation $\tilde{F}$ (SNR $= 15.2$ db).

The noisy signal X shown in Figure 11.1(b) is contaminated by a Gaussian white noise W of variance σ^2, so $\hat{R}_W[m] = \sigma^2$. The Wiener estimation $\tilde{F}$ is calculated with the frequency filter (11.14)

$$\hat{h}[m] = \frac{\beta^2 \, |\hat{g}[m]|^2}{\beta^2 \, |\hat{g}[m]|^2 + \sigma^2}.$$

This linear estimator is also an optimal nonlinear estimator because F and W are jointly Gaussian random vectors.

Piecewise Regular

The limitations of linear estimators appear clearly for processes with realizations that are piecewise regular signals. A simple example is a random-shift process F constructed by translating randomly a piecewise regular signal $f[n]$ of zero-mean, $\sum_{n=0}^{N-1} f[n] = 0$:

$$F[n] = f[(n - Q) \bmod N]. \qquad \textbf{(11.17)}$$

The translation variable Q is an integer random variable with a probability distribution on $[0, N-1]$. It is proved in (9.28) that F is a circular wide-sense stationary process with a power spectrum calculated in (9.29):

$$\hat{R}_F[m] = \frac{1}{N} |\hat{f}[m]|^2. \tag{11.18}$$

Figure 11.2 shows an example of a piecewise polynomial signal f of degree $d = 3$ contaminated by a Gaussian white noise W of variance σ^2. Assuming that we know $|\hat{f}[m]|^2$, the Wiener estimator $\tilde{F}$ is calculated as a circular convolution with the filter in (11.14). This Wiener filter is a low-pass filter that averages the noisy data to attenuate the noise in regions where the realization of F is regular, but this averaging is limited to avoid degrading the discontinuities too much. As a result, some noise is left in the smooth regions and the discontinuities are averaged a little. The risk

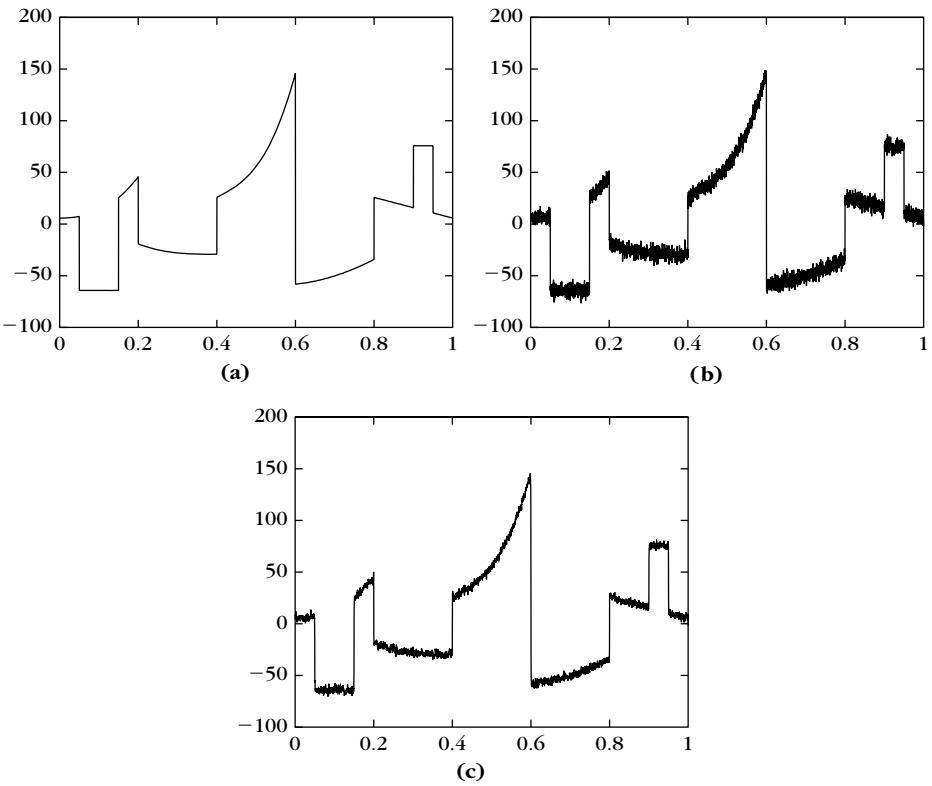

FIGURE 11.2

(a) Piecewise polynomial of degree 3. **(b)** Noisy signal degraded by a Gaussian white noise (SNR = 21.9 db). **(c)** Wiener estimation (SNR = 25.9 db).

calculated in (11.15) is normalized by the total noise energy $E\{\|W\|^2\} = N\sigma^2$:

$$\frac{r_I(\pi)}{N\sigma^2} = \sum_{m=0}^{N-1} \frac{N^{-1}\,|\hat{f}[m]|^2}{|\hat{f}[m]|^2 + N\sigma^2}. \tag{11.19}$$

Suppose that f has discontinuities of amplitude on the order of $C \geqslant \sigma$ and that the noise energy is not negligible: $N\,\sigma^2 \geqslant C^2$. Using the fact that $|\hat{f}[m]|$ decays typically like $C\,N\,m^{-1}$, a direct calculation of the risk (11.19) gives

$$\frac{r_I(\pi)}{N\sigma^2} \sim \frac{C}{\sigma\,N^{1/2}}. \tag{11.20}$$

The equivalence $\sim$ means that upper and lower bounds of the left side are obtained by multiplying the right side by two constants $A, B > 0$ that are independent of C, σ, and N.

The estimation of F can be improved by nonlinear operators, which average the data X over large domains where F is regular, but do not make any averaging where F is discontinuous. Many estimators have been studied [262, 380], to recover the position of the discontinuities of f in order to adapt the data averaging. These algorithms have long remained *ad hoc* implementations of intuitively appealing ideas. Wavelet thresholding estimators perform such an adaptive smoothing and Section 11.5.3 proves that the normalized risk decays like $N^{-1}(\log N)^2$ as opposed to $N^{-1/2}$ in (11.20).

11.1.2 Minimax Estimation

Although we may have some prior information, it is rare that we know the probability distribution of complex signals. Presently, there exists no stochastic model that takes into account the diversity of natural images. However, many images, such as the one in Figure 2.2, have some form of piecewise regularity, with a bounded total variation. Models are often defined over the original analog signal $\bar{f}$ that is measured with sensors having a response $\bar{\phi}_n$. The resulting discrete signal $f[n] = \langle \bar{f}, \bar{\phi}_n \rangle$ then belongs to a particular set Θ in $\mathbb{C}^N$ derived from the analog model. This prior information defines a signal set Θ, but it does not specify the probability distribution of signals in Θ. The more prior information, the smaller the set Θ.

Knowing that $f \in \Theta$, we want to estimate this signal from the noisy data

$$X[n] = f[n] + W[n].$$

The risk of an estimation $\tilde{F} = DX$ is $r(D, f) = E\{\|DX - f\|^2\}$. The expected risk over Θ cannot be computed because the probability distribution of signals in Θ is unknown. To control the risk for any $f \in \Theta$, we thus try to minimize the maximum risk:

$$r(D, \Theta) = \sup_{f \in \Theta} E\{\|DX - f\|^2\}.$$

The *minimax risk* is the lower bound computed over all linear and nonlinear operators D:

$$r_n(\Theta) = \inf_{D \in \mathcal{O}_n} r(D, \Theta).$$

In practice, we must find a decision operator D that is simple to implement and such that $r(D, \Theta)$ is close to the minimax risk $r_n(\Theta)$.

As a first step, as for Wiener estimators in the Bayes framework, the problem is simplified by restricting D to be a linear operator. The *linear minimax risk* over Θ is the lower bound:

$$r_l(\Theta) = \inf_{D \in \mathcal{O}_l} r(D, \Theta).$$

This strategy is efficient only if $r_l(\Theta)$ is of the same order as $r_n(\Theta)$.

Bayes Priors

A Bayes estimator supposes that we know the prior probability distribution π of signals in Θ. If available, this supplement of information can only improve the signal estimation. The central result of game and decision theory shows that minimax estimations are Bayes estimations for a "least-favorable" prior distribution.

Let F be the signal random vector with a probability distribution that is given by the prior π. For a decision operator D, the expected risk is $r(D, \pi) = E_\pi\{r(D, F)\}$. The minimum Bayes risks for linear and nonlinear operators are defined by:

$$r_l(\pi) = \inf_{D \in \mathcal{O}_l} r(D, \pi) \quad \text{and} \quad r_n(\pi) = \inf_{D \in \mathcal{O}_n} r(D, \pi).$$

Let Θ^* be the set of all probability distributions of random vectors with realizations in Θ. The minimax theorem (11.4) relates a minimax risk and the maximum Bayes risk calculated for priors in Θ^*.

Theorem 11.4: *Minimax.* For any subset Θ of $\mathbb{C}^N$,

$$r_l(\Theta) = \sup_{\pi \in \Theta^*} r_l(\pi) \quad \text{and} \quad r_n(\Theta) = \sup_{\pi \in \Theta^*} r_n(\pi). \tag{11.21}$$

Proof. For any $\pi \in \Theta^*$,

$$r(D, \pi) \leq r(D, \Theta) \tag{11.22}$$

because $r(D, \pi)$ is an average risk over realizations of F that are in Θ, whereas $r(D, \Theta)$ is the maximum risk over Θ. Let $\mathcal{O}$ be a convex set of operators (either $\mathcal{O}_l$ or $\mathcal{O}_n$). The inequality (11.22) implies that

$$\sup_{\pi \in \Theta^*} r(\pi) = \sup_{\pi \in \Theta^*} \inf_{D \in \mathcal{O}} r(D, \pi) \leq \inf_{D \in \mathcal{O}} r(D, \Theta) = r(\Theta). \tag{11.23}$$

The main difficulty is to prove the reverse inequality: $r(\Theta) \leq \sup_{\pi \in \Theta^*} r(\pi)$. When Θ is a finite set, the proof gives a geometrical interpretation of the minimum Bayes risk and the minimax risk. The extension to an infinite set Θ is sketched.

Suppose that $\Theta = \{f_i\}_{1 \leq i \leq p}$ is a finite set of signals. We define a risk set:

$$R = \{(y_1, \ldots, y_p) \in \mathbb{C}^p : \exists D \in \mathcal{O} \quad \text{with} \quad y_i = r(D, f_i) \text{ for } 1 \leq i \leq p\}.$$

This set is convex in $\mathbb{C}^p$ because $\mathcal{O}$ is convex. We begin by giving geometrical interpretations to the Bayes risk and the minimax risk.

A prior $\pi \in \Theta^*$ is a vector of discrete probabilities $(\pi_1, \ldots, \pi_p)$ and

$$r(\pi, D) = \sum_{i=1}^{p} \pi_i \, r(D, f_i). \tag{11.24}$$

The equation $\sum_{i=1}^{p} \pi_i y_i = b$ defines a hyperplane P_b in $\mathbb{C}^p$. Computing $r(\pi) = \inf_{D \in \mathcal{O}} r(D, \pi)$ is equivalent to finding the infimum $b_0 = r(\pi)$ of all b for which P_b intersects R. The plane P_{b_0} is tangent to R as shown in Figure 11.3.

The minimax risk $r(\Theta)$ has a different geometrical interpretation. Let $Q_c = \{(y_1, \ldots, y_p) \in \mathbb{C}^p : y_i \leqslant c\}$. One can verify that $r(\Theta) = \inf_{D \in \mathcal{O}} \sup_{f_i \in \Theta} r(D, f_i)$ is the infimum $c_0 = r(\Theta)$ of all c such that Q_c intersects R.

To prove that $r(\Theta) \leqslant \sup_{\pi \in \Theta^*} r(\pi)$, we look for a prior distribution $\tau \in \Theta^*$ such that $r(\tau) = r(\Theta)$. Let $\tilde{Q}_{c_0}$ be the interior of Q_{c_0}. Since $\tilde{Q}_{c_0} \cap R = \emptyset$ and both $\tilde{Q}_{c_0}$ and R are convex sets, the hyperplane separation theorem says that there exists a hyperplane of equation

$$\sum_{i=1}^{p} \tau_i y_i = \tau \,.\, y = b, \tag{11.25}$$

with $\tau \,.\, y \leqslant b$ for $y \in \tilde{Q}_{c_0}$ and $\tau \,.\, y \geqslant b$ for $y \in R$. Each $\tau_i \geqslant 0$, for if $\tau_j < 0$, then for $y \in \tilde{Q}_{c_0}$, we obtain a contradiction by taking y_j to $-\infty$ with the other coordinates being fixed. Indeed, $\tau \,.\, y$ goes to $+\infty$ and since y remains in $\tilde{Q}_{c_0}$, it contradicts the fact that $\tau \,.\, y \leqslant b$. We can normalize $\sum_{i=1}^{p} \tau_i = 1$ by dividing each side of (11.25) by $\sum_{i=1}^{p} \tau_i > 0$. So τ corresponds to a probability distribution. By letting $y \in \tilde{Q}_{c_0}$ converge to the corner point $(c_0, \ldots, c_0)$, since $y \,.\, \tau \leqslant b$, we derive that $c_0 \leqslant b$. Moreover, since $\tau \,.\, y \geqslant b$ for all $y \in R$,

$$r(\tau) = \inf_{D \in \mathcal{O}} \sum_{i=1}^{p} \tau_i \, r(D, f_i) \geqslant c \geqslant c_0 = r(\Theta).$$

So, $r(\Theta) \leqslant \sup_{\pi \in \Theta^*} r(\pi)$, which, together with (11.23), proves that $r(\Theta) = \sup_{\pi \in \Theta^*} r(\pi)$.

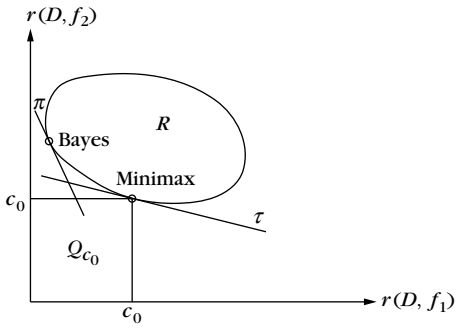

FIGURE 11.3

At the Bayes point, a hyperplane defined by the prior π is tangent to the risk set R. The least-favorable prior τ defines a hyperplane that is tangential to R at the minimax point.

The extension of this result to an infinite set of signals Θ is done with a compactness argument. When $\mathcal{O} = \mathcal{O}_l$ or $\mathcal{O} = \mathcal{O}_n$, for any prior $\pi \in \Theta^*$, we know from Theorems 11.1 and 11.2 that $\inf_{D \in \mathcal{O}} r(D, \pi)$ is reached by some Bayes decision operator $D \in \mathcal{O}$. One can verify that there exists a subset of operators $\mathcal{C}$ that includes the Bayes operator for any prior $\pi \in \Theta^*$, and such that $\mathcal{C}$ is compact for an appropriate topology. When $\mathcal{O} = \mathcal{O}_l$, one can choose $\mathcal{C}$ to be the set of linear operators of norm smaller than 1, which is compact because it belongs to a finite-dimensional space of linear operators. Moreover, the risk $r(f, D)$ can be shown to be continuous in this topology with respect to $D \in \mathcal{C}$.

Let $c < r(\Theta)$. For any $f \in \Theta$, we consider the set of operators $\mathcal{S}_f = \{D \in \mathcal{C} : r(D, f) > c\}$. The continuity of r implies that $\mathcal{S}_f$ is an open set. For each $D \in \mathcal{C}$ there exists $f \in \Theta$ such that $D \in \mathcal{S}_f$, so $\mathcal{C} = \cup_{f \in \Theta} \mathcal{S}_f$. Since $\mathcal{C}$ is compact, there exists a finite covering $\mathcal{C} = \cup_{1 \leqslant i \leqslant p} \mathcal{S}_{f_i}$. The minimax risk over $\Theta_c = \{f_i\}_{1 \leqslant i \leqslant p}$ satisfies

$$r(\Theta_c) = \inf_{D \in \mathcal{O}} \sup_{1 \leqslant i \leqslant p} r(D, f_i) \geqslant c.$$

Since Θ_c is a finite set, we proved that there exists $\tau_c \in \Theta_c^* \subset \Theta^*$ such that $r(\tau_c) = r(\Theta_c)$. But $r(\Theta_c) \geqslant c$, so letting c go to $r(\Theta)$ implies that $\sup_{\pi \in \Theta^*} r(\pi) \geqslant r(\Theta)$. Together with (11.23) this shows that $\inf_{\tau \in \Theta^*} r(\tau) = r(\Theta)$. ■

A distribution $\tau \in \Theta^*$ such that $r(\tau) = \inf_{\pi \in \Theta^*} r(\pi)$ is called a *least-favorable* prior distribution. The minimax theorem proves that the minimax risk is the minimum Bayes risk for a least-favorable prior.

In signal processing, minimax calculations are often hidden behind apparently orthodox Bayes estimations. Let us consider an example involving images. It has been observed that histograms of the wavelet coefficients of "natural" images can be modeled with generalized Gaussian distributions [361, 440]. This means that natural images belong to a certain set Θ, but it does not specify a prior distribution over this set. To compensate for the lack of knowledge about the dependency of wavelet coefficients spatially and across scales, one may be tempted to create a "simple probabilistic model" where all wavelet coefficients are considered to be independent. This model is clearly simplistic since images have geometrical structures that create strong dependencies both spatially and across scales (see Figure 7.24). However, calculating a Bayes estimator with this inaccurate prior model may give valuable results when estimating images. Why? Because this "simple" prior is often close to a least-favorable prior. The resulting estimator and risk are thus good approximations of the minimax optimum. If not chosen carefully, a "simple" prior may yield an optimistic risk evaluation that is not valid for real signals.

On the other hand, the minimax approach may seem very pessimistic since we always consider the maximum risk over Θ; this is sometimes the case. However, when the set Θ is large, one can often verify that a "typical" signal of Θ has a risk of the order of the maximum risk over Θ. A minimax calculation attempts to isolate the class of signals that are the most difficult to estimate, and one can check whether these signals are indeed typically encountered in an application. If this is not the case, then it indicates that the model specified by Θ is not well adapted to this application.

11.2 DIAGONAL ESTIMATION IN A BASIS

It is generally not possible to compute the optimal Bayes or minimax estimator that minimizes the risk among all possible operators. To manage this complexity, the most classical strategy limits the choice of operators among linear operators. This comes at a cost, because the minimum risk among linear estimators may be well above the minimum risk obtained with nonlinear estimators. Figure 11.2 is an example where the linear Wiener estimation can be considerably improved with a nonlinear averaging. This section studies a particular class of nonlinear estimators that are diagonal in a basis $\mathcal{B}$. If the basis $\mathcal{B}$ defines a sparse signal representation, then such diagonal estimators are nearly optimal among all nonlinear estimators.

Section 11.2.1 computes a lower bound for the risk when estimating an arbitrary signal f with a diagonal operator. Donoho and Johnstone [221] made a fundamental breakthrough by showing that thresholding estimators have a risk that is close to this lower bound. The general properties of thresholding estimators are introduced in Sections 11.2.2 and 11.2.3.

11.2.1 Diagonal Estimation with Oracles

We consider estimators computed with a diagonal operator in an orthonormal basis $\mathcal{B} = \{g_m\}_{0 \leqslant m < N}$. Lower bounds for the risk are computed with "oracles," which simplify the estimation by providing information about the signal that is normally not available. These lower bounds are closely related to errors when approximating signals from a few vectors selected in $\mathcal{B}$.

The noisy data

$$X[n] = f[n] + W[n] \quad \text{for} \quad 0 \leqslant n < N \tag{11.26}$$

are decomposed in $\mathcal{B}$. We write

$$X_{\mathcal{B}}[m] = \langle X, g_m \rangle, \quad f_{\mathcal{B}}[m] = \langle f, g_m \rangle \quad \text{and} \quad W_{\mathcal{B}}[m] = \langle W, g_m \rangle.$$

The inner product of (11.26) with g_m gives

$$X_{\mathcal{B}}[m] = f_{\mathcal{B}}[m] + W_{\mathcal{B}}[m].$$

We suppose that W is a zero-mean *white noise* of variance σ^2, which means

$$E\{W[n]\, W[k]\} = \sigma^2\, \delta[n-k].$$

The noise coefficients

$$W_{\mathcal{B}}[m] = \sum_{n=0}^{N-1} W[n]\, g_m^*[n]$$

also define a white noise of variance σ^2. Indeed,

$$E\{W_{\mathcal{B}}[m]\, W_{\mathcal{B}}[p]\} = \sum_{n=0}^{N-1} \sum_{k=0}^{N-1} g_m[n]\, g_p[k]\, E\{W[n]\, W[k]\}$$
$$= \sigma^2\, \langle g_p, g_m \rangle = \sigma^2\, \delta[p-m].$$

Since the noise remains white in all bases, it does not influence the choice of basis.

A *diagonal operator* independently estimates each $f_{\mathcal{B}}[m]$ by multiplying $X_{\mathcal{B}}[m]$ by a factor $a_m(X_{\mathcal{B}}[m])$. The resulting estimator is

$$\tilde{F} = D\,X = \sum_{m=0}^{N-1} a_m(X_{\mathcal{B}}[m])\, X_{\mathcal{B}}[m]\, g_m. \tag{11.27}$$

The operator D is linear when $a_m(X_{\mathcal{B}}[m])$ is a constant independent of $X_{\mathcal{B}}[m]$.

Oracle Attenuation

For a given signal f let us find the constant $a_m = a_m(X_{\mathcal{B}}[m])$ that minimizes the risk $r(D,f)$ of the estimator (11.27):

$$r(D,f) = E\left\{ \|f - \tilde{F}\|^2 \right\} = \sum_{m=0}^{N-1} E\{|f_{\mathcal{B}}[m] - a_m\, X_{\mathcal{B}}[m]|^2\}. \tag{11.28}$$

We shall see that $|a_m| \leqslant 1$, which means that the diagonal operator D should attenuate the noisy coefficients.

Since $X_{\mathcal{B}} = f_{\mathcal{B}} + W_{\mathcal{B}}$ and $E\{|W_{\mathcal{B}}[m]|^2\} = \sigma^2$, and since a_m is a constant that does not depend on the noise, it follows that

$$E\{|f_{\mathcal{B}}[m] - X_{\mathcal{B}}[m]\, a_m|^2\} = |f_{\mathcal{B}}[m]|^2\, (1-a_m)^2 + \sigma^2\, a_m^2. \tag{11.29}$$

This risk is minimum for

$$a_m = \frac{|f_{\mathcal{B}}[m]|^2}{|f_{\mathcal{B}}[m]|^2 + \sigma^2}, \tag{11.30}$$

in which case

$$r_{\inf}(f) = E\{\|f - \tilde{F}\|^2\} = \sum_{m=0}^{N-1} \frac{|f_{\mathcal{B}}[m]|^2\, \sigma^2}{|f_{\mathcal{B}}[m]|^2 + \sigma^2}. \tag{11.31}$$

Observe that the attenuation factor a_m and the resulting risk have the same structure as the Wiener filter (11.10). However, the Wiener filter is a linear operator that depends on the expected SNRs that are constant values. This attenuation factor depends on the unknown original signal-to-noise ratio $|f_{\mathcal{B}}[m]|^2/\sigma^2$. Since $|f_{\mathcal{B}}[m]|$ is unknown, the attenuation factor a_m cannot be computed. It is considered as an *oracle* information. The resulting oracle risk $r_{\inf}(f)$ is a lower bound that is normally not reachable. However, Section 11.2.2 shows that one can get close to $r_{\inf}(f)$ with a simple thresholding.

Oracle Projection

The analysis of diagonal estimators can be simplified by restricting $a_m \in \{0, 1\}$. When $a_m = 1$, the estimator $\tilde{F} = DX$ selects the coefficient $X_{\mathcal{B}}[m]$, and it removes it if $a_m = 0$. The operator D is then an orthogonal projector on a selected subset of vectors of the basis $\mathcal{B}$.

The nonlinear projector that minimizes the risk (11.29) is defined by

$$a_m = \begin{cases} 1 & \text{if } |f_{\mathcal{B}}[m]| \geqslant \sigma \\ 0 & \text{if } |f_{\mathcal{B}}[m]| < \sigma. \end{cases} \tag{11.32}$$

The resulting oracle projector is

$$DX = \sum_{m \in \Lambda_\sigma} X_{\mathcal{B}}[m]\, g_m \quad \text{with} \quad \Lambda_\sigma = \{0 \leqslant m < N \,:\, |f_{\mathcal{B}}[m]| \geqslant \sigma\}. \tag{11.33}$$

It is an orthogonal projection on the set $\{g_m\}_{m \in \Lambda_\sigma}$ of basis vectors that best approximate f. This "oracle" projector cannot either be implemented because a_m and Λ_σ depend on $f_{\mathcal{B}}[m]$ instead of $X_{\mathcal{B}}[m]$. The resulting risk is computed with (11.29):

$$r_{\mathrm{pr}}(f) = E\{\|f - \tilde{F}\|^2\} = \sum_{m=0}^{N-1} \min(|f_{\mathcal{B}}[m]|^2, \sigma^2). \tag{11.34}$$

Since for any $(x, y) \in \mathbb{R}^2$,

$$\min(x, y) \geqslant \frac{x\,y}{x+y} \geqslant \frac{1}{2} \min(x, y),$$

the risk of the oracle projector (11.34) is of the same order as the risk of an oracle attenuation (11.31):

$$r_{\mathrm{pr}}(f) \geqslant r_{\mathrm{inf}}(f) \geqslant \frac{1}{2}\, r_{\mathrm{pr}}(f). \tag{11.35}$$

The risk of an oracle projector can also be related to the approximation error of f in the basis $\mathcal{B}$. Let $M = |\Lambda_\sigma|$ be the number of coefficients such that $|f_{\mathcal{B}}[m]| \geqslant \sigma$. The best M-term approximation of f, defined in Section 9.2.1, is the orthogonal projection on the M vectors $\{g_m\}_{m \in \Lambda_\sigma}$ that yield the largest-amplitude coefficients:

$$f_M = \sum_{m \in \Lambda_\sigma} f_{\mathcal{B}}[m]\, g_m.$$

The nonlinear oracle projector risk can be rewritten as

$$r_{\mathrm{pr}}(f) = \sum_{m=0}^{N-1} \min(|f_{\mathcal{B}}[m]|^2, \sigma^2) = \sum_{m \notin \Lambda_\sigma} |f_{\mathcal{B}}[m]|^2 + M\,\sigma^2 \tag{11.36}$$

$$= \varepsilon_n(M, f) + M\,\sigma^2, \tag{11.37}$$

where

$$\varepsilon_n(M,f) = \|f - f_M\|^2 = \sum_{m \notin \Lambda_\sigma} |f_{\mathcal{B}}[m]|^2$$

is the best M-term approximation error. It is the bias produced by setting signal coefficients to zero, and $M\sigma^2$ is the variance of the remaining noise on the M coefficients that are kept. Theorem 11.5 proves that when σ decreases, the decay of this risk is characterized by the decay of the nonlinear approximation error $\varepsilon_n(M,f)$ as M increases.

Theorem 11.5. If $\varepsilon_n(M,f) \leqslant C^2 M^{1-2s}$ with $1 \leqslant C/\sigma \leqslant N^s$, then

$$r_{\mathrm{pr}}(f) \leqslant 3\, C^{1/s}\, \sigma^{2-1/s}. \tag{11.38}$$

Proof. Observe that

$$r_{\mathrm{pr}}(f) = \min_{0 \leqslant M \leqslant N} \Big(\varepsilon_n(M,f) + M\sigma^2 \Big). \tag{11.39}$$

Let M_0 be defined by $2M_0\,\sigma^2 > C^2 M_0^{1-2s} \geqslant M_0\,\sigma^2$. Since $1 \leqslant C/\sigma \leqslant N^s$, necessarily $1 \leqslant M_0 \leqslant N$. Inserting $\varepsilon_n(M_0,f) \leqslant C^2 M_0^{1-2s}$ with $s > 1/2$ and $M_0 \leqslant C^{1/s}\,\sigma^{-1/s}$ yields

$$r_{\mathrm{pr}}(f) \leqslant \varepsilon_n(M_0,f) + M_0\sigma^2 \leqslant 3\, M_0\, \sigma^2 \leqslant 3C^{1/s}\, \sigma^{2-1/s}, \tag{11.40}$$

which proves (11.38). ■

Linear Projection

Oracle estimators cannot be implemented because a_m is a constant that depends on the unknown signal f. Let us consider linear projectors obtained by setting a_m to be equal to 1 on the first M vectors and 0 otherwise:

$$\tilde{F} = D_M X = \sum_{m=0}^{M-1} X_{\mathcal{B}}[m]\, g_m. \tag{11.41}$$

The risk (11.28) becomes

$$r(D_M,f) = \sum_{m=M}^{N-1} |f_{\mathcal{B}}[m]|^2 + M\,\sigma^2 = \varepsilon_l(M,f) + M\,\sigma^2, \tag{11.42}$$

where $\varepsilon_l(M,f)$ is the linear approximation error computed in (9.3). The two terms $\varepsilon_l(M,f)$ and $M\,\sigma^2$ are, respectively, the bias and the variance components of the estimator. To minimize $r(D_M,f)$, the parameter M is adjusted so that the bias is of the same order as the variance. When the noise variance σ^2 decreases, Theorem 11.6 proves that resulting risk depends on the decay of $\varepsilon_l(M,f)$ as M increases.

Theorem 11.6. If $\varepsilon_l(M,f) \leqslant C^2 M^{1-2s}$ with $1 \leqslant C/\sigma \leqslant N^s$, then

$$r(D_{M_0},f) \leqslant 3\, C^{1/s}\, \sigma^{2-1/s} \quad \text{for} \quad (C/(2\sigma))^{1/s} < M_0 \leqslant (C/\sigma)^{1/s}. \tag{11.43}$$

Proof. As in (11.40), we verify that

$$r(D_{M_0}, f) = \varepsilon_l(M_0, f) + M_0\sigma^2 \leqslant 3C^{1/s}\,\sigma^{2-1/s},$$

for $(C/(2\sigma))^{1/s} < M_0 \leqslant (C/\sigma)^{1/s}$, which proves (11.43). ■

Theorems 11.5 and 11.6 prove that the performances of oracle projection estimators and optimized linear projectors depend, respectively, on the precision of nonlinear and linear approximations in the basis $\mathcal{B}$. Having an approximation error that decreases quickly means that one can then construct a sparse and precise signal representation with only a few vectors in $\mathcal{B}$. Section 9.2 shows that nonlinear approximations can be much more precise, in which case the risk of a nonlinear oracle projection is much smaller than the risk of a linear projection. The next section shows that thresholding estimators are nonlinear projection estimators that have a risk close to the oracle projection risk.

11.2.2 Thresholding Estimation

In a basis $\mathcal{B} = \{g_m\}_{0 \leqslant m < N}$, a diagonal estimator of f from $X = f + W$ can be written as

$$\tilde{F} = DX = \sum_{m=0}^{N-1} a_m(X_{\mathcal{B}}[m])\, X_{\mathcal{B}}[m]\, g_m. \tag{11.44}$$

We suppose that W is a Gaussian white noise of variance σ^2. When a_m are thresholding functions, the risk of this estimator is shown to be close to the lower bounds obtained with oracle estimators.

Hard Thresholding

A hard-thresholding estimator is implemented with

$$a_m(x) = \begin{cases} 1 & \text{if } |x| \geqslant T \\ 0 & \text{if } |x| < T, \end{cases} \tag{11.45}$$

and can thus be rewritten as

$$\tilde{F} = DX = \sum_{m \in \tilde{\Lambda}_T} X_{\mathcal{B}}[m]\, g_m \quad \text{with} \quad \tilde{\Lambda}_T = \{0 \leqslant m < N \,:\, |X_{\mathcal{B}}[m]| \geqslant T\}. \tag{11.46}$$

It is an orthogonal projection of X on the set of basis vectors $\{g_m\}_{m \in \tilde{\Lambda}_T}$. This estimator can also be rewritten with a hard-thresholding function

$$\tilde{F} = \sum_{m=0}^{N-1} \rho_T(X_{\mathcal{B}}[m])\, g_m \quad \text{with} \quad \rho_T(x) = \begin{cases} x & \text{if } |x| > T \\ 0 & \text{if } |x| \leqslant T. \end{cases} \tag{11.47}$$

The risk of this thresholding is

$$r_{\text{th}}(f) = r(D, f) = \sum_{m=0}^{N-1} E\{|f_{\mathcal{B}}[m] - \rho_T(X_{\mathcal{B}}[m])|^2\},$$

with $X_{\mathcal{B}}[m] = f_{\mathcal{B}}[m] + W_{\mathcal{B}}[m]$, and thus

$$|f_{\mathcal{B}}[m] - \rho_T(X_{\mathcal{B}}[m])|^2 = \begin{cases} |W_{\mathcal{B}}[m]|^2 & \text{if } |X_{\mathcal{B}}[m]| > T \\ |f_{\mathcal{B}}[m]|^2 & \text{if } |X_{\mathcal{B}}[m]| \leqslant T. \end{cases}$$

Since a hard thresholding is a nonlinear projector in the basis $\mathcal{B}$, the thresholding risk is larger than the risk (11.34) of an oracle projector:

$$r_{\text{th}}(f) \geqslant r_{\text{pr}}(f) = \sum_{m=0}^{N-1} \min(|f_{\mathcal{B}}[m]|^2, \sigma^2).$$

Soft Thresholding

An oracle attenuation (11.30) yields a risk $r_{\text{inf}}(f)$ that is smaller than the risk $r_{\text{pr}}(f)$ of an oracle projection, by slightly decreasing the amplitude of all coefficients in order to reduce the added noise. A soft attenuation, although nonoptimal, is implemented by

$$0 \leqslant a_m(x) = \max\left(1 - \frac{T}{|x|},\ 0\right) \leqslant 1. \tag{11.48}$$

The resulting diagonal estimator $\tilde{F}$ in (11.44) can be written as in (11.47) with a soft-thresholding function, which decreases the amplitude of all noisy coefficients by T:

$$\rho_T(x) = \begin{cases} x - T & \text{if } x \geqslant T \\ x + T & \text{if } x \leqslant -T \\ 0 & \text{if } |x| \leqslant T. \end{cases} \tag{11.49}$$

The threshold T is generally chosen so that there is a high probability that it is just above the maximum level of the noise coefficients $|W_{\mathcal{B}}[m]|$. Reducing the amplitude of all noisy coefficients by T thus ensures that the amplitude of an estimated coefficient is smaller than the amplitude of the original one:

$$|\rho_T(X_{\mathcal{B}}[m])| \leqslant |f_{\mathcal{B}}[m]|. \tag{11.50}$$

In a wavelet basis where large-amplitude coefficients are created by sharp signal variations, this estimation restores a signal that is at least as regular as the original signal f, without adding sharp transitions due to the noise.

Thresholding Risk

Theorem 11.7 [221] proves that for an appropriate choice of T, the risk of a thresholding is close to the risk of an oracle projector $r_{\text{pr}}(f) = \sum_{m=0}^{N-1} \min(|f_{\mathcal{B}}[m]|^2, \sigma^2)$. We denote by $\mathcal{O}_d$ the set of all linear or nonlinear operators that are diagonal in $\mathcal{B}$.

Theorem 11.7: *Donoho, Johnstone.* Let $T = \sigma\sqrt{2\log_{\text{e}} N}$. The risk $r_{\text{th}}(f)$ of a hard- or soft-thresholding estimator satisfies for all $N \geqslant 4$,

$$r_{\text{th}}(f) \leqslant (2\log_{\text{e}} N + 1)\left(\sigma^2 + r_{\text{pr}}(f)\right). \tag{11.51}$$

The factor $2\log_{\mathrm{e}} N$ is optimal among diagonal estimators in $\mathcal{B}$:

$$\lim_{N\to+\infty} \inf_{D\in\mathcal{O}_d} \sup_{f\in\mathbb{C}^N} \frac{E\{\|f-\tilde{F}\|^2\}}{\sigma^2 + r_{\mathrm{pr}}(f)} \frac{1}{2\log_{\mathrm{e}} N} = 1. \tag{11.52}$$

Proof. The proof of (11.51) is given for a soft thresholding. For a hard thresholding, the proof is similar although slightly more complicated. For a threshold λ, a soft thresholding is computed with

$$\rho_\lambda(x) = (x - \lambda\,\mathrm{sign}(x))\,\mathbf{1}_{|x|>\lambda}.$$

Let X be a Gaussian random variable of mean μ and variance 1. The risk when estimating μ with a soft thresholding of X is

$$r(\lambda,\mu) = E\{|\rho_\lambda(X)-\mu|^2\} = E\{|(X-\lambda\,\mathrm{sign}(X))\,\mathbf{1}_{|X|>\lambda}-\mu|^2\}. \tag{11.53}$$

If X has a variance σ^2 and a mean μ, then by considering $\tilde{X} = X/\sigma$, we verify that

$$E\{|\rho_\lambda(X)-\mu|^2\} = \sigma^2\, r\left(\frac{\lambda}{\sigma}, \frac{\mu}{\sigma}\right).$$

Since $f_{\mathcal{B}}[m]$ is a constant, $X_{\mathcal{B}}[m] = f_{\mathcal{B}}[m] + W_{\mathcal{B}}[m]$ is a Gaussian random variable of mean $f_{\mathcal{B}}[m]$ and variance σ^2. The risk of the soft-thresholding estimator $\tilde{F}$ with a threshold T is thus

$$r_{\mathrm{th}}(f) = \sigma^2 \sum_{m=0}^{N-1} r\left(\frac{T}{\sigma}, \frac{f_{\mathcal{B}}[m]}{\sigma}\right). \tag{11.54}$$

An upper bound of this risk is calculated with Lemma 11.1.

Lemma 11.1. If $\mu \geqslant 0$, then

$$r(\lambda,\mu) \leqslant r(\lambda,0) + \min(1+\lambda^2, \mu^2). \tag{11.55}$$

To prove (11.55), we first verify that if $\mu \geqslant 0$, then

$$0 \leqslant \frac{\partial r(\lambda,\mu)}{\partial \mu} = 2\mu \int_{-\lambda+\mu}^{\lambda-\mu} \phi(x)\,dx \leqslant 2\mu, \tag{11.56}$$

where $\phi(x)$ is the normalized Gaussian probability density

$$\phi(x) = \frac{1}{\sqrt{2\pi}} \exp\left(-\frac{x^2}{2}\right).$$

Indeed (11.53) shows that

$$r(\lambda,\mu) = \mu^2 \int_{-\lambda+\mu}^{\lambda-\mu} \phi(x)\,dx + \int_{\lambda-\mu}^{+\infty} (x-\lambda)^2\,\phi(x)\,dx + \int_{-\infty}^{-\lambda+\mu} (x+\lambda)^2\,\phi(x)\,dx. \tag{11.57}$$

We obtain (11.56) by differentiating with respect to μ.

Since $\int_{-\infty}^{+\infty} \phi(x)\,dx = \int_{-\infty}^{+\infty} x^2\,\phi(x)\,dx = 1$ and $\frac{\partial r(\lambda,\mu)}{\partial \mu} \geqslant 0$, necessarily

$$r(\lambda,\mu) \leqslant \lim_{\mu \to +\infty} r(\lambda,\mu) = 1 + \lambda^2. \tag{11.58}$$

Moreover, since $\frac{\partial r(\lambda,s)}{\partial s} \leqslant 2s$,

$$r(\lambda,\mu) - r(\lambda,0) = \int_0^{\mu} \frac{\partial r(\lambda,s)}{\partial s}\,ds \leqslant \mu^2. \tag{11.59}$$

The inequality (11.55) of the lemma is finally derived from (11.58) and (11.59):

$$r(\lambda,\mu) \leqslant \min(r(\lambda,0) + \mu^2,\, 1+\lambda^2) \leqslant r(\lambda,0) + \min(1+\lambda^2,\, \mu^2).$$

By inserting the inequality (11.55) of the lemma in (11.54), we get

$$r_{\mathrm{th}}(f) \leqslant N\sigma^2 r\left(\frac{T}{\sigma}, 0\right) + \sigma^2 \sum_{m=0}^{N-1} \min\left(\frac{T^2+\sigma^2}{\sigma^2}, \frac{|f_{\mathcal{B}}[m]|^2}{\sigma^2}\right). \tag{11.60}$$

The expression (11.57) shows that $r(\lambda,0) = 2\int_0^{+\infty} x^2\,\phi(x+\lambda)\,dx$. For $T = \sigma\sqrt{2\log_{\mathrm{e}} N}$ and $N \geqslant 4$, one can verify that

$$N\, r\left(\frac{T}{\sigma}, 0\right) \leqslant 2\log_{\mathrm{e}} N + 1. \tag{11.61}$$

Moreover,

$$\begin{aligned}\sigma^2\ \min\left(\frac{T^2+\sigma^2}{\sigma^2}, \frac{|f_{\mathcal{B}}[m]|^2}{\sigma^2}\right) &= \min(2\sigma^2\log_{\mathrm{e}} N + \sigma^2,\, |f_{\mathcal{B}}[m]|^2) \\ &\leqslant (2\log_{\mathrm{e}} N + 1)\ \min(\sigma^2,\, |f_{\mathcal{B}}[m]|^2).\end{aligned} \tag{11.62}$$

Inserting (11.61) and (11.62) in (11.60) proves (11.51).

Since the soft- and hard-thresholding estimators are particular instances of diagonal estimators, the inequality (11.51) implies that

$$\lim_{N\to+\infty} \inf_{D\in\mathcal{O}_d} \sup_{f\in\mathbb{C}^N} \frac{E\{\|f-\tilde{F}\|^2\}}{\sigma^2 + r_{\mathrm{pr}}(f)}\ \frac{1}{2\log_{\mathrm{e}} N} \leqslant 1. \tag{11.63}$$

To prove that the limit is equal to 1, for N fixed, we compute a lower bound by replacing the supremum over all signals f by an expected value over the distribution of a particular signal process F. The coefficients $F_{\mathcal{B}}[m]$ are chosen to define a very sparse sequence. They are independent random variables having a high probability $1-\alpha_N$ to be equal to 0 and a low probability α_N to be equal to a value μ_N that is on the order of $\sigma\sqrt{2\log_{\mathrm{e}} N}$, but smaller. By adjusting μ_N and α_N, Donoho and Johnstone [221] prove that the Bayes estimator $\tilde{F}$ of F tends to zero as N increases and they derive a lower bound of the left side of (11.63) that tends to 1. ■

The upper bound (11.51) proves that the risk $r_{\mathrm{th}}(f)$ of a thresholding estimator is at most $2\log_{\mathrm{e}} N$ times larger than the risk $r_{\mathrm{pr}}(f)$ of an oracle projector. Moreover, (11.52) proves that the $2\log_{\mathrm{e}} N$ factor cannot be improved by any other diagonal estimator. For $r_{\mathrm{pr}}(f)$ to be small, (11.37) shows that f must be well approximated

by a few vectors in $\mathcal{B}$. One can verify [221] that the theorem remains valid if $r_{\mathrm{pr}}(f)$ is replaced by the risk $r_{\mathrm{inf}}(f)$ of an oracle attenuation, which is smaller.

Choice of Threshold

The threshold T must be chosen just above the maximum level of the noise. Indeed, if $f = 0$ and thus $X_{\mathcal{B}} = W_{\mathcal{B}}$, then to ensure that $\tilde{F} \approx 0$, the noise coefficients $|W_{\mathcal{B}}[m]|$ must have a high probability of being below T. However, if $f \neq 0$, then T must not be too large, so that we do not set to zero too many coefficients such that $|f_{\mathcal{B}}[m]| \geqslant \sigma$. Since $W_{\mathcal{B}}$ is a vector of N independent Gaussian random variables of variance σ^2, one can prove [7] that the maximum amplitude of the noise has a very high probability of being just below $T = \sigma\sqrt{2\log_{\mathrm{e}} N}$:

$$\lim_{N \to +\infty} \mathrm{pr}\left(T - \frac{\sigma \log_{\mathrm{e}} \log_{\mathrm{e}} N}{\log_{\mathrm{e}} N} \leqslant \max_{0 \leqslant m < N} |W_{\mathcal{B}}[m]| \leqslant T \right) = 1. \tag{11.64}$$

This explains why the theorem chooses this value. That the threshold T increases with N may seem counterintuitive. This is due to the tail of the Gaussian distribution, which creates larger-and-larger-amplitude noise coefficients when the sample size increases. The threshold $T = \sigma\sqrt{2\log_{\mathrm{e}} N}$ is not optimal and, in general, a lower threshold reduces the risk.

A soft thresholding computed for $T = \sigma\sqrt{2\log_{\mathrm{e}} N}$ often produces a risk that is larger than with a hard thresholding. A soft thresholding reduces to nearly 0 the amplitude of coefficients just above T or just below $-T$, whereas a hard thresholding leaves them as is. To obtain nearly the same risk for a hard thresholding and a soft thresholding, it is often necessary to reduce by two the threshold of the soft thresholding. Section 11.2.3 explains how to adapt the threshold T to the data X.

Upper-Bound Interpretation

Despite the technicality of the proof, the factor $2\log_{\mathrm{e}} N$ of the upper bound (11.51) can be easily explained. The ideal coefficient selection (11.32) sets $X_{\mathcal{B}}[m]$ to zero if and only if $|f_{\mathcal{B}}[m]| \leqslant \sigma$, whereas a hard thresholding sets $X_{\mathcal{B}}[m]$ to zero when $|X_{\mathcal{B}}[m]| \leqslant T$. If $|f_{\mathcal{B}}[m]|| \leqslant \sigma$, then it is very likely that $|X_{\mathcal{B}}[m]| \leqslant T$, because T is above the noise level. In this case, the hard thresholding sets $X_{\mathcal{B}}[m]$ to zero as the oracle projector (11.32) does. If $|f_{\mathcal{B}}[m]| \geqslant 2T$, then it is likely that $|X_{\mathcal{B}}[m]| \geqslant T$ because $|W_{\mathcal{B}}[m]| \leqslant T$. In this case, the hard thresholding and the oracle projector retain $X_{\mathcal{B}}[m]$.

The hard thresholding may behave differently from the ideal coefficient selection when $|f_{\mathcal{B}}[m]|$ is on the order of T. The ideal selection yields a risk: $\min(\sigma^2, |f_{\mathcal{B}}[m]|^2) = \sigma^2$. If we are unlucky and $|X_{\mathcal{B}}[m]| \leqslant T$, then the thresholding sets $X_{\mathcal{B}}[m]$ to zero, which produces a risk

$$|f_{\mathcal{B}}[m]|^2 \sim T^2 = 2\log_{\mathrm{e}} N \sigma^2.$$

In this worst case, the thresholding risk is $2\log_{\mathrm{e}} N$ times larger than the ideal selection risk. Since the proportion of coefficients $|f_{\mathcal{B}}[m]|$ on the order of T is often

small, the ratio between the hard-thresholding risk and the oracle projection risk is generally significantly smaller than $2 \log_e N$.

Colored Noise

Thresholding estimators can be adapted when the noise W is not white. We suppose that $E\{W[n]\} = 0$. Since W is not white, $\sigma_{\mathcal{B}}[m]^2 = E\{|W_{\mathcal{B}}[m]|^2\}$ depends on each vector g_m of the basis. As in (11.32) and (11.34), we verify that an oracle projector that keeps all coefficients such that $|f_{\mathcal{B}}[m]| \geqslant \sigma_{\mathcal{B}}[m]$ and sets to zero all others has a risk

$$r_{\mathrm{pr}}(f) = \sum_{m=0}^{N-1} \min(|f_{\mathcal{B}}[m]|^2, \sigma_{\mathcal{B}}^2[m]). \tag{11.65}$$

Any linear or nonlinear projector in the basis $\mathcal{B}$ has a risk larger than $r_{\mathrm{pr}}(f)$.

Since the noise variance depends on m, a thresholding estimator must vary the threshold T_m as a function of m. Such a hard- or soft-thresholding estimator can be written as

$$\tilde{F} = DX = \sum_{m=0}^{N-1} \rho_{T_m}(X_{\mathcal{B}}[m])\, g_m. \tag{11.66}$$

Theorem 11.8 generalizes Theorem 11.7 to compute the thresholding risk $r_{\mathrm{th}}(f) = E\{\|f - \tilde{F}\|^2\}$.

Theorem 11.8: *Donoho, Johnstone.* Let $\tilde{F}$ be a hard- or soft-thresholding estimator with

$$T_m = \sigma_{\mathcal{B}}[m]\sqrt{2 \log_e N} \quad \text{for } 0 \leqslant m < N.$$

Let $\bar{\sigma}^2 = N^{-1} \sum_{m=0}^{N-1} \sigma_{\mathcal{B}}[m]^2$. For any $N \geqslant 4$,

$$r_{\mathrm{th}}(f) \leqslant (2 \log_e N + 1)\left(\bar{\sigma}^2 + r_{\mathrm{pr}}(f)\right). \tag{11.67}$$

The proof of (11.67) is identical to the proof of (11.51). The thresholds T_m are chosen to be just above the amplitude of each noisy coefficient $W_{\mathcal{B}}[m]$.

Frame Thresholding Estimators

The properties of thresholding estimators remain valid for nonorthogonal Riesz bases and frames. The redundancy of frames often produces a smaller risk than with an orthogonal basis, thanks to their redundancy. They are thus most often used in numerical applications.

Let us recall that $\{\phi_p\}_{0 \leqslant p < P}$ with $P \geqslant N$ is a frame of $\mathbb{C}^N$ if there exists $0 < A \leqslant B$, such that for any $f \in \mathbb{C}^N$

$$A \|f\|^2 \leqslant \sum_{p=0}^{P-1} |\langle f, \phi_p \rangle|^2 \leqslant B \|f\|^2.$$

When $P = N$, the frame is a Riesz basis, otherwise it is redundant. In the following, we consider that all frame vectors are normalized $\|\phi_p\| = 1$. Theorem 5.2 then proves that $A \leqslant P/N \leqslant B$.

Theorem 5.5 proves that there exists a dual frame $\{\tilde{\phi}_p\}_{0 \leqslant p < P}$ such that

$$f = \sum_{p=0}^{P-1} \langle f, \phi_p \rangle \, \tilde{\phi}_p.$$

A signal f can be estimated from noisy coefficients $X = f + W$ by thresholding its frame coefficients

$$\tilde{F} = \sum_{p=0}^{P-1} \rho_T(\langle X, \phi_p \rangle) \, \tilde{\phi}_p. \tag{11.68}$$

The resulting risk is $r_{\text{th}}(f) = E\{\|\tilde{F} - f\|^2\}$. Let us write

$$r_{\text{pr}}(f) = \sum_{p=0}^{P-1} \min(|\langle f, \phi_p \rangle|^2, \sigma^2).$$

Using an oracle, we verify in Exercise 11.12 that $r_{\text{th}}(f) \geqslant r_{\text{pr}}(f)/B$. Moreover, for a threshold $T = \sigma \sqrt{2 \log_{\text{e}} P}$, with the same derivation steps as in the proof of Theorem 11.8, one can prove that for any $P \geqslant 4$,

$$r_{\text{th}}(f) \leqslant \frac{2 \log_{\text{e}} P + 1}{A} \Big(\sigma^2 + r_{\text{pr}}(f) \Big). \tag{11.69}$$

This proves that thresholding estimators in frames behave like thresholding estimators in orthogonal bases. The threshold $T = \sigma \sqrt{2 \log_{\text{e}} P}$ is a conservative upper bound that is too large in most numerical experiments. For a tight frame, $A = B = P/N$. The thresholding estimator then behaves as the average of A estimators in A orthogonal bases. This averaging often reduces the resulting risk.

11.2.3 Thresholding Improvements

The thresholding risk is often reduced by choosing a threshold smaller than $\sigma \sqrt{2 \log_{\text{e}} N}$. A threshold adapted to the data is calculated by minimizing an estimation of the risk. Different thresholding functions are also considered, and an important improvement is introduced with a translation-invariant thresholding algorithm.

Sure Thresholds

To study the impact of the threshold on the risk, we denote by $r_{\text{th}}(f, T)$ the risk of a soft-thresholding estimator calculated with a threshold T. An estimate of $r_{\text{th}}(f, T)$ is calculated from the noisy data X, and T is optimized by minimizing the estimated risk.

To estimate the risk $r_{\text{th}}(f,T)$, observe that if $|X_{\mathcal{B}}[m]|<T$, then the soft thresholding sets this coefficient to zero, which produces a risk equal to $|f_{\mathcal{B}}[m]|^2$. Since

$$E\{|X_{\mathcal{B}}[m]|^2\}=|f_{\mathcal{B}}[m]|^2+\sigma^2,$$

one can estimate $|f_{\mathcal{B}}[m]|^2$ with $|X_{\mathcal{B}}[m]|^2-\sigma^2$. If $|X_{\mathcal{B}}[m]|\geqslant T$, the soft thresholding subtracts T from the amplitude of $X_{\mathcal{B}}[m]$. The expected risk is the sum of the noise energy plus the bias introduced by the reduction of the amplitude of $X_{\mathcal{B}}[m]$ by T. It is estimated by σ^2+T^2. The resulting estimator of $r_{\text{th}}(f,T)$ is

$$\textit{Sure}(X,T)=\sum_{m=0}^{N-1} C(X_{\mathcal{B}}[m]), \tag{11.70}$$

with

$$C(u)=\begin{cases} u^2-\sigma^2 & \text{if } u\leqslant T \\ \sigma^2+T^2 & \text{if } u>T. \end{cases} \tag{11.71}$$

Theorem 11.9 [222] proves that $\textit{Sure}(X,T)$ is a unbiased risk estimator. It is called a *Stein unbiased risk estimator* (Sure) [445].

Theorem 11.9: *Donoho, Johnstone.* For a soft thresholding, the risk estimator $\textit{Sure}(X,T)$ is unbiased:

$$E\{\textit{Sure}(X,T)\}=r_{\text{th}}(f,T). \tag{11.72}$$

Proof. A soft-thresholding estimator performs a soft thresholding of each noisy coordinate. As in (11.54), we thus derive that the resulting risk is the sum of the soft-thresholding risk for each coordinate

$$r_{\text{th}}(f,T)=E\{\|f-\tilde{F}\|^2\}=\sigma^2\sum_{m=0}^{N-1} r(T,f_{\mathcal{B}}[m],\sigma), \tag{11.73}$$

where $r(\lambda,\mu,\sigma)$ is the risk when estimating μ by soft thresholding a Gaussian random variable X of mean μ and variance σ^2:

$$r(\lambda,\mu,\sigma)=E\{|\rho_\lambda(X)-\mu|^2\}=E\{|(X-\lambda\,\text{sign}(X))\,\mathbf{1}_{|X|>\lambda}-\mu|^2\}. \tag{11.74}$$

Let us rewrite

$$r(T,\mu,\sigma)=E\{(X-g(X)-\mu)^2\}, \tag{11.75}$$

where $g(x)=T\,\text{sign}(x)+(x-T\,\text{sign}(x))\,\mathbf{1}_{|x|<T}$ is a weakly differentiable function (in the sense of distributions). This risk is calculated by the following Stein formula [445].

Lemma 11.1: *Stein.* Let $g(x)$ be a weakly differentiable function. If X is a Gaussian random vector of mean μ and variance σ^2, then

$$E\{|X+g(X)-\mu|^2\}=\sigma^2+E\{|g(X)|^2\}+2\sigma^2E\{g'(X)\}. \tag{11.76}$$

To prove this lemma, let us develop (11.76)

$$E\{|X+g(X)-\mu|^2\} = E\{(X-\mu)^2\} + E\{|g(X)|^2\} - 2E\{(X-\mu)\,g(X)\}. \quad \textbf{(11.77)}$$

The probability density of X is the Gaussian $\phi_\sigma(y-\mu)$. The change of variable $x = y-\mu$ shows that

$$E\{(X-\mu)\,g(X)\} = \int_{-\infty}^{+\infty} x\,g(x+\mu)\,\phi_\sigma(x)\,dx.$$

Since $x\,\phi_\sigma(x) = -\sigma^2\,\phi'_\sigma(x)$, an integration by parts gives

$$\begin{aligned} E\{(X-\mu)g(X)\} &= -\sigma^2 \int_{-\infty}^{+\infty} g(x+\mu)\,\phi'_\sigma(x)\,dx \\ &= \sigma^2 \int_{-\infty}^{+\infty} g'(x)\,\phi_\sigma(x-\mu)\,dx = E\{g'(X)\}. \end{aligned}$$

Inserting this result in (11.77) proves (11.76).

For the soft-thresholding risk, $g(x) = T\,\mathrm{sign}(x) + (x - T\,\mathrm{sign}(x))\,\mathbf{1}_{|x|<T}$, and thus $g'(x) = \mathbf{1}_{|x|\geq T}$. Using the fact that $E\{\mathbf{1}_{|X|\geq T}\} + E\{\mathbf{1}_{|X|<T}\} = 1$, the Stein unbiased risk formula (11.76) implies that

$$r(T,\mu,\sigma) = (\sigma^2+T^2)\,E\{\mathbf{1}_{|X|\geq T}\} + E\left\{(|X|^2-\sigma^2)\,\mathbf{1}_{|X|\leq T}\right\} = E\left\{C(|X|^2)\right\}, \quad \textbf{(11.78)}$$

where $C(x)$ is defined in (11.71). Inserting this expression in (11.73) proves (11.72). ■

These results suggest choosing the threshold that minimizes the Sure estimator

$$\tilde{T} = \operatorname*{argmin}_T \mathit{Sure}(X,T).$$

Although the estimator $\mathit{Sure}(X,T)$ of $r_{\mathrm{th}}(f,T)$ is unbiased, its variance may induce errors leading to a threshold $\tilde{T}$ that is too small. This happens if the signal energy is small relative to the noise energy: $\|f\|^2 \ll E\{\|W\|^2\} = N\sigma^2$. In this case, one must impose $T = \sigma\sqrt{2\log_{\mathrm{e}} N}$ in order to remove all the noise. Since $E\{\|X\|^2\} = \|f\|^2 + N\sigma^2$, we estimate $\|f\|^2$ with $\|X\|^2 - N\sigma^2$ and compare this value with a minimum energy level $\varepsilon_N = \sigma^2 N^{1/2}(\log_{\mathrm{e}} N)^{3/2}$. The resulting Sure threshold is

$$T = \begin{cases} \sigma\sqrt{2\log_{\mathrm{e}} N} & \text{if } \|X\|^2 - N\sigma^2 \leq \varepsilon_N \\ \tilde{T} & \text{if } \|X\|^2 - N\sigma^2 > \varepsilon_N. \end{cases} \quad \textbf{(11.79)}$$

Let Θ be a signal set and $\min_T r_{\mathrm{th}}(\Theta)$ be the minimax risk of a soft thresholding obtained by optimizing the choice of T depending on Θ. Donoho and Johnstone [222] prove that the threshold empirically computed with (11.79) yields a risk $r_{\mathrm{th}}(\Theta)$ equal to $\min_T r_{\mathrm{th}}(\Theta)$, plus a corrective term that decreases rapidly when N increases if $\varepsilon_N = \sigma^2 N^{1/2}(\log_{\mathrm{e}} N)^{3/2}$.

Exercise 11.13 studies a similar risk estimator for hard thresholding. However, this risk estimator is biased. We cannot guarantee that the threshold that minimizes this estimated risk is nearly optimal for hard-thresholding estimations.

Other Thresholdings and Masking Noise

Besides hard and soft thresholdings, other diagonal attenuation functions in (11.66) can improve a diagonal signal estimation. A whole family of diagonal attenuations is defined by

$$a_m(x) = \max\left(1 - \frac{T^\beta}{|x|^\beta},\ 0\right) \quad \text{with} \quad \beta > 0.$$

For $\beta = 1$, it corresponds to the soft thresholding (11.48). When β tends to $+\infty$, it yields the hard thresholding (11.45).

If $\beta = 2$, then $a_m(x)$ is a James-Stein shrinkage [445]. It is intermediate between a hard and a soft attenuation. Since $E\{|X_{\mathcal{B}}[m]|^2\} = |f_{\mathcal{B}}[m]|^2 + \sigma^2$, for $T = \sigma$ the attenuation

$$a_m(X_{\mathcal{B}}[m]) = \max\left(\frac{|X_{\mathcal{B}}[m]|^2 - \sigma^2}{|X_{\mathcal{B}}[m]|^2},\ 0\right)$$

can be interpreted as an empirical estimation of the oracle attenuation factor $a_m = |f_{\mathcal{B}}[m]|^2/(|f_{\mathcal{B}}[m]|^2 + \sigma^2)$. Is also called an *empirical Wiener attenuation*.

Thresholding signal coefficients can introduce perceptual artifacts that reduce the perceived quality of the estimation. The next section shows that in wavelet bases, thresholding noisy image coefficients removes fine texture and can produce cartoonlike images with no textures. Other artifacts can be created by thresholding estimators. Leaving some noise reduces our perceptual sensitivity to these artifacts and can thus improve the perceived signal quality, although it may increase the mean-square norm of the error. It is implemented with attenuation factors that remain strictly positive:

$$a_m(x) = \max\left(1 - \frac{T^\beta}{|x|^\beta},\ \varepsilon\right) \quad \text{with} \quad \varepsilon > 0. \tag{11.80}$$

If $|X_{\mathcal{B}}[m]| \leqslant T$, then $a_m(X_{\mathcal{B}}[m]) = \varepsilon$, so this thresholding leaves a reduced noise of variance $\varepsilon^2\,\sigma^2$, which masks potential artifacts.

Translation-Invariant Thresholding

In many applications, signal models are translation invariant. This is often the case for audio signals, where the recording beginning may be arbitrarily shifted, or for images that are translated by changing the camera position. For stochastic signal models with random processes, translation invariance means that the process is stationary. For a deterministic model that specifies a set Θ where the signal belongs, it means that any $f \in \Theta$ remains in Θ after a translation. For signals embedded in additive noise, if the noise is stationary and Θ is translation invariant, then the minimization of the maximum risk over Θ is achieved with translation-invariant estimators. Theorem 11.12 proves this result for linear minimax estimators, which is also valid for nonlinear estimators.

Coifman and Donoho [179] have introduced translation-invariant thresholding estimators that reduce the risk for translation-invariant sets Θ. For signals of finite

length N, to avoid boundary issues, we consider circular translations modulo N: $f_p[n] = f[(n-p) \bmod N]$. Observe that if $\mathcal{B} = \{g_m\}_{0 \leq m < N}$ is an orthonormal basis of $\mathbb{C}^N$, then the translated basis $\mathcal{B}_p = \{g_{p,m}[n] = g_m[(n-p) \bmod N]\}_{0 \leq m < N}$ is also an orthogonal basis of $\mathbb{C}^N$ for any $0 \leq p < N$. If there is no translation information on the signal, all the bases $\{\mathcal{B}_p\}_{0 \leq p < N}$ are a priori equivalent for thresholding estimations. Coifman and Donoho [179] thus proposed to average the thresholding estimations obtained in these N bases. This is equivalent to decompose the signal in a translation-invariant dictionary that is a union of these N translated orthonormal bases:

$$\mathcal{D} = \cup_{p=0}^{N-1} \mathcal{B}_p = \{g_{p,m}\}_{0 \leq m,p < N}. \tag{11.81}$$

The energy conservation in each orthogonal basis $\mathcal{B}_p$ implies a global energy conservation over the N^2 dictionary vectors

$$\|f\|^2 = \frac{1}{N} \sum_{m=0}^{N-1} \sum_{p=0}^{N-1} |\langle f, g_{p,m} \rangle|^2,$$

which proves that this dictionary is a tight frame.

The resulting translation-invariant estimator of f from noisy data $X = f + W$ is obtained by thresholding the translation-invariant tight frame coefficients of X:

$$\tilde{F}[n] = \frac{1}{N} \sum_{p=0}^{N-1} \sum_{m=0}^{N-1} \rho_T(\langle X, g_{p,m} \rangle)\, g_{p,m}[n], \tag{11.82}$$

where ρ_T is a hard- or a soft-thresholding operator. Since this estimator is obtained by averaging N thresholding estimators in orthogonal bases, the resulting thresholding risk satisfies the same upper bound as in Theorem 11.7.

A priori, this translation-invariant thresholding requires N times more operations than a thresholding estimation in the original basis $\mathcal{B}$. However, this is not the case when the original basis $\mathcal{B}$ includes translated vectors. In this case, the translation-invariant dictionary $\mathcal{D}$ has less than N^2 different vectors. For example, a wavelet orthogonal basis yields a translation-invariant dyadic wavelet dictionary that has only $N \log_2 N$ different wavelets.

Translation-invariant tight frames are not necessarily derived from an orthogonal basis. Theorem 5.12 proves that a translation-invariant dictionary obtained by translating Q generators $\{g_q\}_{0 \leq q < Q}$ is a tight frame if and only if their discrete Fourier transforms satisfy $\sum_{q=0}^{Q-1} |\hat{g}_q[k]|^2 = Q$ for all $0 \leq k < N$. The simplicity of this condition offers more flexibility to build translation-invariant thresholding estimators then from orthogonal bases.

11.3 THRESHOLDING SPARSE REPRESENTATIONS

Thresholding estimators are particularly efficient in a basis that can precisely approximate signals with few nonzero coefficients. The basis must therefore be chosen from prior information on signal properties in order to obtain sparse representations.

Wavelet bases are particularly efficient to estimate piecewise regular signals. Noise removal from images is studied in Section 11.3.2, with wavelet bases and curvelet frames. For audio signals, sparse representations are obtained with localized time-frequency transforms. An important limitation of diagonal-thresholding operators is illustrated in Section 11.3.3, with the creation of a "musical noise" when thresholding windowed Fourier coefficients for audio noise removal.

11.3.1 Wavelet Thresholding

Thresholding wavelet coefficients implements an adaptive signal averaging with a kernel that is locally adapted to the signal regularity [4]. Numerical examples illustrate the properties of these estimators for piecewise regular one-dimensional signals. The minimax optimality of wavelet thresholding estimators is studied in Section 11.5.3.

A filter bank of conjugate mirror filters decomposes a discrete signal in a discrete orthogonal wavelet basis, defined in Section 7.3.3. The discrete wavelets $\psi_{j,m}[n] = \psi_j[n - N2^j m]$ are translated modulo modifications near the boundaries, which are explained in Section 7.5. The support of the signal is normalized to [0, 1] with N samples spaced by N^{-1}. The scale parameter 2^j thus varies from $2^L = N^{-1}$ up to $2^J < 1$:

$$\mathcal{B} = \left[\{\psi_{j,m}[n]\}_{L<j\leqslant J,\, 0\leqslant m<2^{-j}},\ \{\phi_{J,m}[n]\}_{0\leqslant m<2^{-J}} \right]. \tag{11.83}$$

A thresholding estimator in this wavelet basis can be written as

$$\tilde{F} = \sum_{j=L+1}^{J} \sum_{m=0}^{2^{-j}} \rho_T\Big(\langle X, \psi_{j,m}\rangle\Big)\, \psi_{j,m} + \sum_{m=0}^{2^{-J}} \rho_T\Big(\langle X, \phi_{J,m}\rangle\Big)\, \phi_{J,m}, \tag{11.84}$$

where ρ_T is a hard thresholding (11.47) or a soft thresholding (11.49). The upper bound (11.51) proves that the estimation risk is small if the energy of f is absorbed by a few wavelet coefficients.

Adaptive Smoothing

The thresholding sets all coefficients $|\langle X, \psi_{j,m}\rangle| \leqslant T$ to zero. This performs an adaptive smoothing that depends on the regularity of the signal f. Since T is above the maximum amplitude of the noise coefficients $|\langle W, \psi_{j,m}\rangle|$, if

$$|\langle X, \psi_{j,m}\rangle| = |\langle f, \psi_{j,m}\rangle + \langle W, \psi_{j,m}\rangle| \geqslant T,$$

then $|\langle f, \psi_{j,m}\rangle|$ has a high probability of being at least of the order T. At fine scales 2^j, these coefficients are in the neighborhood of sharp signal transitions, as shown in Figure 11.4(b). By keeping them, we avoid smoothing these sharp variations. In the regions where $|\langle X, \psi_{j,m}\rangle| < T$, the coefficients $\langle f, \psi_{j,m}\rangle$ are likely to be small, which means that f is locally regular. Setting wavelet coefficients to zero is equivalent to locally averaging the noisy data X, which is done only if the underlying signal f appears to be regular.

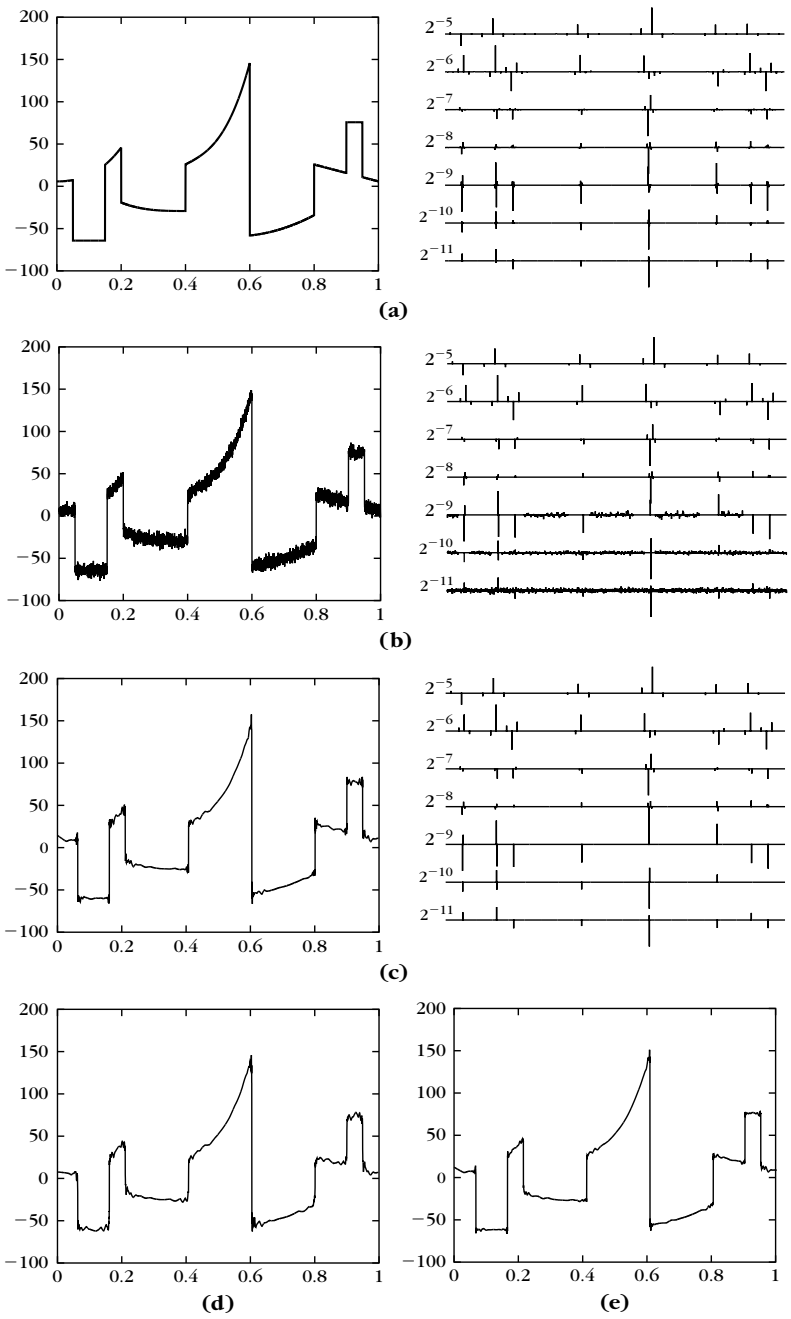

FIGURE 11.4

(a) Piecewise polynomial signal (*left*) and its wavelet transform (*right*). **(b)** Noisy signal (SNR = 21.9 db) (*left*) and its wavelet transform (*right*). **(c)** Estimation reconstructed from wavelet coefficients above the threshold (*right*) (SNR = 30.8 db). **(d)** Estimation with wavelet soft thresholding (SNR = 23.8 db). **(e)** Estimation with translation-invariant hard thresholding (SNR = 33.7 db).

Noise Variance Estimation

To estimate the variance σ^2 of the noise $W[n]$ from the data $X[n] = W[n] + f[n]$, we need to suppress the influence of $f[n]$. When f is piecewise smooth, a robust estimator is calculated from the median of the finest-scale wavelet coefficients [221].

The signal X of size N has $N/2$ wavelet coefficients $\{\langle X, \psi_{l,m}\rangle\}_{0 \leq m < N/2}$ at the finest scale $2^l = 2N^{-1}$. The coefficient $|\langle f, \psi_{l,m}\rangle|$ is small if f is smooth over the support of $\psi_{l,m}$, in which case $\langle X, \psi_{l,m}\rangle \approx \langle W, \psi_{l,m}\rangle$. In contrast, $|\langle f, \psi_{l,m}\rangle|$ is large if f has a sharp transition in the support of $\psi_{l,m}$. A piecewise regular signal has few sharp transitions, and thus produces a number of large coefficients that is small compared to $N/2$. At the finest scale, the signal f thus influences the value of a small portion of large-amplitude coefficients $\langle X, \psi_{l,m}\rangle$ that are considered to be "outliers." All others are approximately equal to $\langle W, \psi_{l,m}\rangle$, which are independent Gaussian random variables of variance σ^2.

A robust estimator of σ^2 is calculated from the median of $\{\langle X, \psi_{l,m}\rangle\}_{0 \leq m < N/2}$. The median of P coefficients $\mathrm{Med}(\alpha_p)_{0 \leq p < P}$ is the value of the middle coefficient α_{n_0} of rank $P/2$. As opposed to an average, it does not depend on the specific values of coefficients $\alpha_p > \alpha_{n_0}$. If M is the median of the absolute value of P independent Gaussian random variables of zero mean and variance σ_0^2, then one can show that

$$E\{M\} \approx 0.6745\, \sigma_0.$$

The variance σ^2 of the noise W is estimated from the median M_X of $\{|\langle X, \psi_{l,m}\rangle|\}_{0 \leq m < N/2}$ by neglecting the influence of f:

$$\tilde{\sigma} = \frac{M_X}{0.6745}. \tag{11.85}$$

Indeed, f is responsible for few large-amplitude outliers, and these have little impact on M_X.

Hard or Soft Thresholding

If $T = \sigma\sqrt{2\log_e N}$, then (11.50) shows that a soft thresholding guarantees with a high probability that

$$|\langle \tilde{F}, \psi_{j,m}\rangle| = |\rho_T(\langle X, \psi_{j,m}\rangle)| \leq |\langle f, \psi_{j,m}\rangle|.$$

The estimator $\tilde{F}$ is at least as regular as f because its wavelet coefficients have a smaller amplitude. This is not true for the hard-thresholding estimator, which leaves the coefficients above T unchanged, and which can therefore be larger than those of f because of the additive noise component.

Figure 11.4(a) shows a piecewise polynomial signal of degree at most 3, and its wavelet coefficients calculated with a symmlet 4. Figure 11.4(c) gives an estimation computed with a hard thresholding of the noisy wavelet coefficients in Figure 11.4(b). An estimator $\tilde{\sigma}^2$ of the noise variance σ^2 is calculated with the median (11.85) and the threshold is set to $T = \tilde{\sigma}\sqrt{2\log_e N}$. Thresholding wavelet

coefficients remove the noise in the domain where f is regular but some traces of the noise remain in the neighborhood of singularities. The resulting SNR is 30.8 db. The soft-thresholding estimation of Figure 11.4(d) attenuates the noise effect at the discontinuities but the reduction by T of the coefficient amplitude is much too strong, which reduces the SNR to 23.8 db. As already explained, to obtain comparable SNR values, the threshold of the soft thresholding must be about half the size of the hard-thresholding one. In this example, reducing the threshold by 2 increases the SNR of the soft thresholding to 28.6 db.

Multiscale Sure Thresholds

Piecewise regular signals have a proportion of large coefficients $|\langle f, \psi_{j,m}\rangle|$ that increases when the scale 2^j increases. Indeed, a singularity creates the same number of large coefficients at each scale, whereas the total number of wavelet coefficients increases when the scale decreases. To use this prior information, one can adapt the threshold choice to the scale 2^j. At large scale 2^j the threshold T_j should be smaller in order to avoid setting too many large-amplitude signal coefficients to zero, which would increase the risk.

Section 11.2.3 explains how to compute the threshold value for a soft thresholding from the coefficients of the noisy data. We first compute an estimate $\tilde{\sigma}^2$ of the noise variance σ^2 with the median formula (11.85) at the finest scale. At each scale 2^j, a different threshold is calculated from the 2^{-j} noisy coefficients $\{\langle X, \psi_{j,m}\rangle\}_{0 \leq m < 2^{-j}}$ with the algorithm of Section 11.2.3. A Sure threshold T_j is calculated with (11.79) at each scale 2^j. A soft thresholding is then applied at each scale 2^j, with a threshold T_j. For a hard thresholding, we have no reliable formula to estimate the risk and thus compute an adapted threshold by minimizing the estimated risk. However, ad hoc hard thresholds may be computed by multiplying by 2 the Sure threshold calculated for a soft thresholding.

Figure 11.5(c) is a hard-thresholding estimation calculated with the same threshold $T = \tilde{\sigma}\sqrt{2\log_e N}$ at all scales 2^j. The SNR is 23.3 db. Figure 11.5(d) is obtained by a soft thresholding with Sure thresholds T_j adapted at each scale 2^j. The SNR is 24.1 db. A soft thresholding with the threshold $T = \tilde{\sigma}/2\sqrt{2\log_e N}$ at all scales gives a smaller SNR equal to 21.7 db. The adaptive calculation of thresholds clearly improves the estimation.

Translation Invariance

Thresholding noisy wavelet coefficients creates small ripples near discontinuities, as seen in Figures 11.4(c,d) and 11.5(c,d). Indeed, setting a coefficient $\langle f, \psi_{j,m}\rangle$ to zero subtracts $\langle f, \psi_{j,m}\rangle\, \psi_{j,m}$ from f, which introduces oscillations whenever $\langle f, \psi_{j,m}\rangle$ is nonnegligible. Figures 11.4(e) and 11.5(e, f) show that averaging the signal estimation over translated wavelet bases reduces these oscillations, significantly improving the SNR.

A translation-invariant wavelet thresholding estimator decomposes the noisy data X over a dictionary obtained by translating each orthogonal wavelet $\psi_{j,m}[n] = \psi_j[n - N2^j m]$ by any factor $0 \leq p < N$ modulo N. Suppose that each of the $J - L$

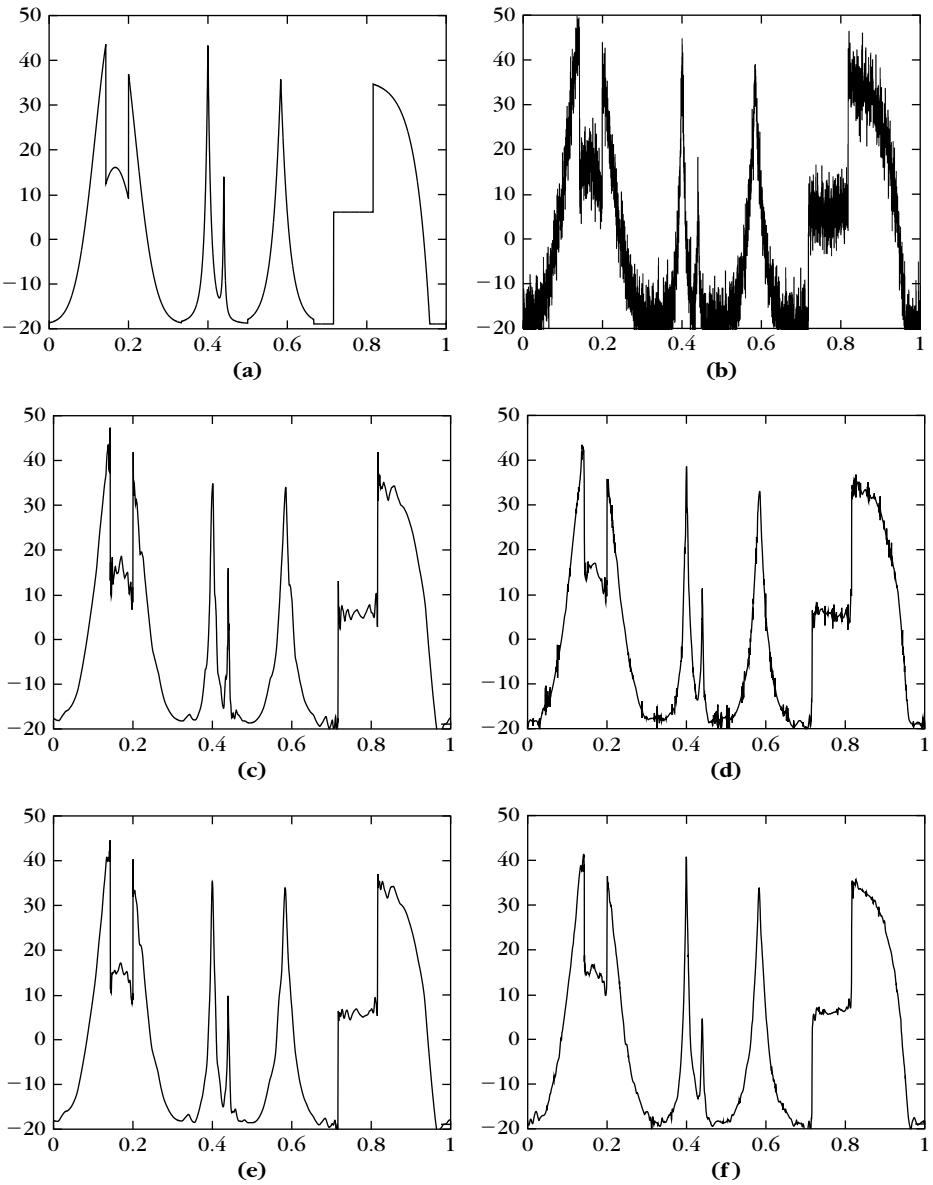

FIGURE 11.5

(a) Original signal. **(b)** Noisy signal ($\mathrm{SNR} = 13.1$ db). **(c)** Estimation by a hard thresholding in a wavelet basis (symmlet 4) with $T = \tilde{\sigma}\sqrt{2\log_e N}$ ($\mathrm{SNR} = 23.3$ db). **(d)** Soft thresholding calculated with Sure thresholds T_j adapted to each scale 2^j ($\mathrm{SNR} = 24.5$ db). **(e)** Translation-invariant hard thresholding with $T = \tilde{\sigma}\sqrt{2\log_e N}$ ($\mathrm{SNR} = 25.7$ db). **(f)** Translation-invariant soft thresholding with Sure thresholds ($\mathrm{SNR} = 25.6$ db).

wavelet $\psi_j[n]$ is N periodic. This yields a translation-invariant dyadic wavelet tight frame including $(J-L)\,N$ wavelets:

$$\mathcal{D} = \{\psi_j[n-p], \quad \phi_J[n-p]\}_{L<j\leqslant J, 0\leqslant p<N},$$

and the resulting translation-invariant thresholding estimator can be written as

$$\tilde{F}[n] = \sum_{j=L+1}^{J} \sum_{p=0}^{N-1} \rho_T(\langle X[q], \psi_j[q-p]\rangle)\, \psi_j[n-p] + \sum_{p=0}^{N-1} \rho_T(\langle X[q], \phi_J[q-p]\rangle)\, \phi_J[n-p].$$

The decomposition coefficients of X in this dictionary are provided by the dyadic wavelet transform defined in Section 5.2:

$$WX[2^j, p] = \langle X[n], \psi_j[n-p]\rangle \quad \text{for} \quad 0\leqslant p<N.$$

The *algorithme à trous* from Section 5.2.2 computes these $(J-L)N$ coefficients for $L<j\leqslant J$ with $O(N\,(J-L))$ operations and reconstructs a signal from the thresholded coefficients with the same number of operations. Since $(J-L)\leqslant \log_2 N$, the total number of operations is bounded by $O(N\,\log_2 N)$.

11.3.2 Wavelet and Curvelet Image Denoising

Reducing noise by thresholding wavelet coefficients is particularly effective for piecewise regular images, which have sparse wavelet representations. When images include edges or textures that have a regular geometry, then curvelet frames can improve wavelet thresholding estimators.

Wavelet Bases

Figure 11.6(b) shows an example of an image contaminated by an additive Gaussian white noise of variance σ^2. This image is decomposed in a separable two-dimensional biorthogonal wavelet basis, generated by a 7/9 mother wavelet. As in one dimension, an estimator $\tilde{\sigma}$ of σ is computed from the median M_X of the finest-scale noisy wavelet coefficient amplitudes with (11.85). For images of $N = 512^2$ pixels, the universal threshold of Theorem 11.7 is $T = \tilde{\sigma}\sqrt{2\log_e N} \approx 5\tilde{\sigma}$. Wavelet hard-thresholding estimators are improved by choosing $T = 3\tilde{\sigma}$, which significantly increases the SNR and the visual quality of the image. Figure 11.6(c) gives an example. Figure 11.6(d) shows a soft-thresholding estimation with $T = 3\tilde{\sigma}/2$ from the same wavelet coefficients. For hard- and soft-thresholdings estimations, low-frequency scaling coefficients are not thresholded. A hard thresholding at T and a soft thresholding at $T/2$ set the same wavelet coefficients to zero, which are shown in white in Figure 11.6(f). A hard thresholding does not modify the other coefficients shown in black, whereas a soft thresholding reduces their amplitude by $T/2$. Coefficients are mostly kept near edges, but some isolated noise coefficients above $3\tilde{\sigma}$ remain in regular regions.

These isolated noise wavelet coefficients above the threshold produce small wavelet oscillation artifacts that are more visible with a hard thresholding. The visual quality of edges is also affected by small Gibbs-like oscillations, which also

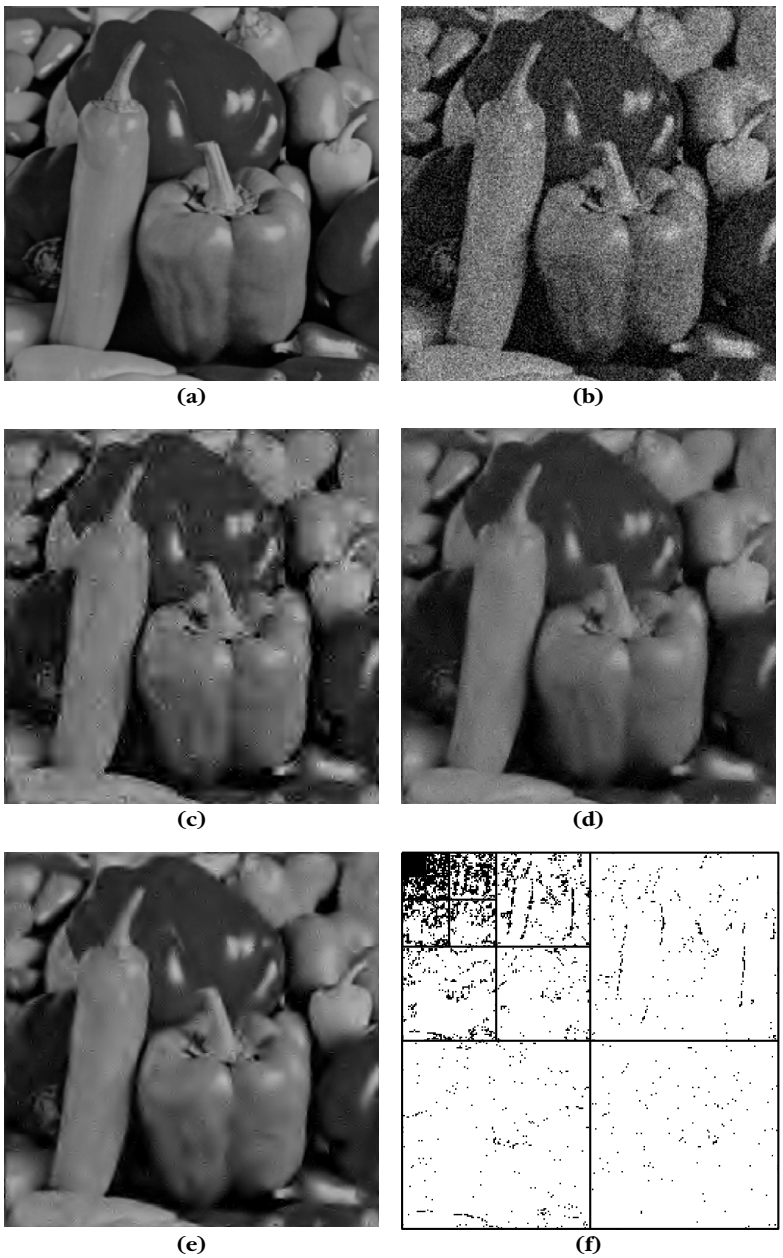

FIGURE 11.6

(a) Original image. **(b)** Noisy image ($\text{SNR} = 18\,\text{db}$). **(c)** Hard thresholding in a 7/9 separable wavelet basis ($\text{SNR} = 21.6\,\text{db}$). **(d)** Soft thresholding ($\text{SNR} = 22.6\,\text{db}$). **(e)** Translation-invariant hard thresholding ($\text{SNR} = 24.7\,\text{db}$). **(f)** Wavelet coefficients above $T = 3\tilde{\sigma}$ are shown in black. All other coefficients are set to zero by the hard and soft thresholding.

appear in the one-dimensional estimations in Figure 11.4(c) and Figure 11.5(c). The soft thresholding improves the SNR by 1 db relatively to the hard thresholding, and for most images an improvement between 0.5 db and 1 db is observed, with or without finer optimizations of thresholds. A Sure optimization of thresholds at each scale with (11.79) further increases the soft thresholding SNR by over 0.5 db.

A translation-invariant wavelet thresholding estimator is computed by decomposing the image in a two-dimensional translation-invariant dyadic wavelet tight frame. A fast dyadic wavelet transform is implemented with a separable filter bank, similar to the two-dimensional fast orthogonal transform described in Section 7.7.3. The one-dimension filterings and subsamplings along the image rows and columns are replaced by the filterings of the *algorithm à trous* in Section 5.2.2. It requires $O(N \log_2 N)$ operations. Figure 11.6(e) is calculated with translation-invariant hard thresholding, which gives a much higher SNR of 24.7 db and a better visual quality. A translation-invariant soft thresholding gives an SNR of 23.6 db. Although a soft thresholding is typically better than a hard thresholding in an orthogonal or biorthogonal basis, a hard thresholding improves a soft-thresholding SNR in a translation-invariant wavelet frame and yields the best results. A translation-invariant hard thresholding often removes fine textures that affect the visual image quality. By maintaining a small masking noise with $\rho_T(x) = |x|$ if $|x| \geqslant T$ and $\rho_T(x) = \varepsilon\,|x|$ if $|x| > T$, the restored image can look more natural.

In Section 11.5.3 we prove that a thresholding in a wavelet basis has a nearly minimax risk for bounded variation images. When the noise variance σ^2 decreases to zero, the wavelet thresholding risk is bounded by $O(\sigma\,\log\sigma)$. Irregular or oscillatory textures are not as well estimated because they do not have a sparse wavelet representation and create many nonnegligible wavelet coefficients. Block thresholding algorithms, presented in Section 11.4.2, can improve texture estimation with wavelets.

Curvelet Frames

Section 9.3.3 shows that images including structures that are geometrically regular, such as $\mathbf{C}^2$ piecewise regular images, have a representation that is asymptotically more sparse with curvelets than with wavelets. Thresholding curvelet coefficients can then improve wavelet thresholding estimators. This is also valid for textures including geometrically regular structures.

Curvelet tight frames $\{c^{\alpha}_{j,m}\}_{j,m,\alpha}$, presented in Section 5.5.2, are composed of anisotropic waveforms with different scales and directions. Curvelets have an elongated support proportional to $2^{j/2}$ in a direction $\alpha \in [0,\, \pi)$ and a width proportional to 2^j in the perpendicular direction. They are translated along a grid with intervals that are, respectively, $2^{j/2}$ in the direction α and 2^j in the direction $\alpha + \pi/2$. In numerical implementations, normalized curvelets have a frame bound $A = B \geqslant 5$, which corresponds to a minimum redundancy factor of 5. A thresholding curvelet estimation of f from a noisy observation $X = f + W$ can be written as

$$\tilde{F} = \sum_{j,m,\alpha} \rho_T(\langle X,\, c^{\alpha}_{j,m}\rangle)\, c^{\alpha}_{j,m}.$$

Suppose that f is obtained by discretizing a $\mathbf{C}^2$ piecewise regular image with $\mathbf{C}^2$ edge curves, as specified by Definition 9.1. Theorem 9.20 proves that a nonlinear curvelet approximation error has a decay bounded by $O(M^{-2}(\log M)^3)$, which improves the asymptotic error decay of wavelet approximations. Theorem 11.5 for $s = 3/2$ proves that a nonlinear approximation error $\varepsilon_n(M, f) = O(M^{-2})$ yields an oracle projection risk that satisfies $r_{\mathrm{pr}}(f) = O(\sigma^{4/3})$. A thresholding estimator has the same decay up to a $\log_e P$ factor where $P = AN$ is the total number of curvelets.

Taking into account the $(\log M)^3$ factor, Candès and Donoho [141] derive that the risk of a curvelet thresholding of a $\mathbf{C}^2$ piecewise regular image satisfies

$$E\{\|\tilde{F} - f\|^2\} = O(|\log \sigma|^2 \sigma^{4/3}),$$

when the noise variance σ decreases to zero. This improves the risk decay $O(|\log \sigma|\sigma)$ of a wavelet thresholding estimator. We later prove in (11.152), with $\alpha = 2$, that the nonlinear minimax risk over uniformly $\mathbf{C}^2$ Lipschitz images decays like $\sigma^{4/3}$. A curvelet thresholding estimator nearly achieves this decay despite the presence of edges, and is therefore asymptotically minimax for the class of $\mathbf{C}^2$ piecewise regular images, up to the $|\log \sigma|^2$ factor.

The threshold $T = \sigma\sqrt{\log_e P}$ is conservative and Figure 11.7 gives an example with $T = 3\sigma$, which improves the SNR. When the image has textures with regular stripes as in Lena's hat, a curvelet thresholding gives a better SNR than a translation-invariant wavelet thresholding. However, despite the asymptotic improvements of curvelets on $\mathbf{C}^2$ piecewise regular images, the pepper image in Figure 11.6 is better estimated with wavelets than with curvelets. As opposed to wavelets, curvelets do not have a compact spatial support and their decay is not exponential because their Fourier transform has a compact support. This increases the number of high-amplitude curvelet coefficients created by edges, which impacts the image estimation.

Irregular textures or pointwise singularities have a representation that is more sparse with wavelets than with curvelets, and are thus better estimated by a wavelet thresholding. Other image representations may also be used. A thresholding in a best bandlet basis, presented in Section 12.2.4, adapts the basis to the geometric image regularity, and chooses wavelets when there is no such regularity.

11.3.3 Audio Denoising by Time-Frequency Thresholding

Audio signals, whether music or speech, often have a sparse time-frequency representation. Such signals are well approximated by relatively few coefficients in appropriate time-frequency bases or frames. Thus, one may expect that thresholding these time-frequency representations yields effective noise-removal algorithms. Although this is true from a SNR point of view, diagonal thresholding algorithms degrade the audio signal quality by introducing a "musical noise." This musical noise is produced by isolated noisy time-frequency coefficients above the threshold.

Sparse audio representations are obtained in wavelet packet and local cosine orthogonal bases that have the time-frequency localization that can be adapted to

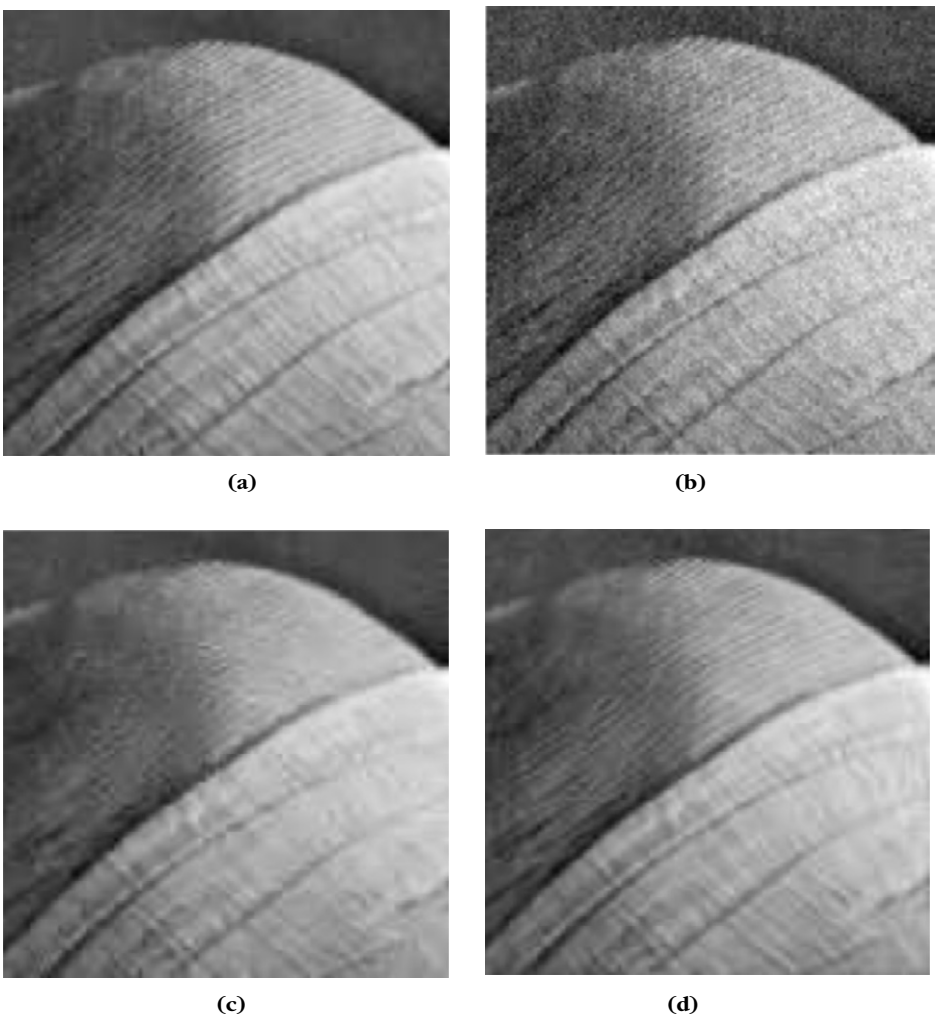

(a) **(b)**

(c) **(d)**

FIGURE 11.7

(a) Original image. **(b)** Noisy image (SNR = 22 db). **(c)** Translation-invariant wavelet hard thresholding (SNR = 25.3 db). **(d)** Curvelet tight frame hard thresholding (SNR = 26 db).

the signal properties. Window Fourier frames also have a time-frequency localization that can be adjusted by choosing an appropriate window size. Thresholding the complex modulus of windowed Fourier frame coefficients seems to better preserve perceptual sound quality than thresholding real wavelet packet or local cosine coefficients. This could be explained by a better restoration of the phase, which is perceptually important for sounds. We shall thus concentrate on windowed Fourier frame thresholding.

A discrete windowed Fourier tight frame of $\mathbb{C}^N$ is constructed in Section 5.4 by translating and modulating a window $g[n]$, which has a support included in $[-K/2, K/2-1]$. If M divides N and

$$\sum_{m=0}^{N/M-1} |g[n-mM]|^2 = \frac{A}{K} \quad \text{for} \quad 0 \leqslant n < N$$

then Theorem 5.18 proves that

$$\{g_{m,k}[n] = g[n-mM]\, \mathrm{e}^{i2\pi kn/K}\}_{0\leqslant k<K, 0\leqslant m<N/M}$$

is a tight frame of $\mathbb{C}^N$, with a frame bound equal to A. Numerical experiments in Figure 11.8 are performed using a square root Hanning window $g[n] = \sqrt{2/K}\, \cos(\pi n/K)$ with $M = K/2$ and thus $A = 2$. The resulting windowed Fourier frame coefficients for $0 \leqslant k < K$, $0 \leqslant m < N/M$ are

$$Sf[m,k] = \langle f, g_{m,k}\rangle = \sum_{n=-K/2}^{K/2-1} f[n]\, g[n-mM]\, \mathrm{e}^{-i2\pi kn/K}.$$

Audio noises are often stationary but not necessarily white. The time-frequency noise variance thus only depends on the frequency and depends on the noise power spectrum $\sigma_{\mathcal{B}}^2[m,k] = \sigma_{\mathcal{B}}^2[k]$. A windowed Fourier thresholding estimator can then be written as

$$\tilde{F} = \sum_{m=0}^{N/M-1} \sum_{k=0}^{K-1} \rho_{T_k}(\langle X, g_{m,k}\rangle)\, g_{m,k} \tag{11.86}$$

with a threshold $T_k^2 = \lambda\, \sigma_{\mathcal{B}}^2[k]$. Since the early work on time-frequency audio denoising [109], many types of thresholding functions have been studied for time-frequency audio noise removal [430]. The James-Stein estimator, called empirical Wiener estimator or "power subtraction" in audio noise removal, is often used,

$$a_{k,m}(\langle X, g_{m,k}\rangle) = \frac{\rho_{T_k}(\langle X, g_{m,k}\rangle)}{\langle X, g_{m,k}\rangle} = \max\left(1 - \frac{T_k^2}{|\langle X, g_{m,k}\rangle|^2}\,,\ \varepsilon\right), \tag{11.87}$$

with a masking noise factor ε that is often nonzero.

To illustrate the musical noise produced by a spectrogram thresholding, Figure 11.8 shows the denoising of a short recording of a Mozart oboe concerto with a white Gaussian noise. Figures 11.8(c, d) give, respectively, the log spectrograms $\log|Sf[m,k]|$ and $\log|SX[m,k]|$ of the original signal f and of the noisy sound X. Figure 11.8(g) displays the attenuation factors $a_{k,m}$ in (11.87) with $\varepsilon = 0$. Black points correspond to $a_{k,m} = 1$ and white points to $a_{k,m} = 0$. For this Mozart recording, when the noisy signal has a SNR that ranges between -2 db up to 15 db, the SNR improvement of this time-frequency soft-thresholding estimator is between 8 db and 10 db, which is important. However, as it can be observed in the zoom in Figure 11.8(h), there are isolated attenuation coefficients $a_{k,m} \approx 1$ corresponding to black points, which retain noise coefficients in time-frequency regions where the signal has no energy. Similar isolated points appear in the estimation support

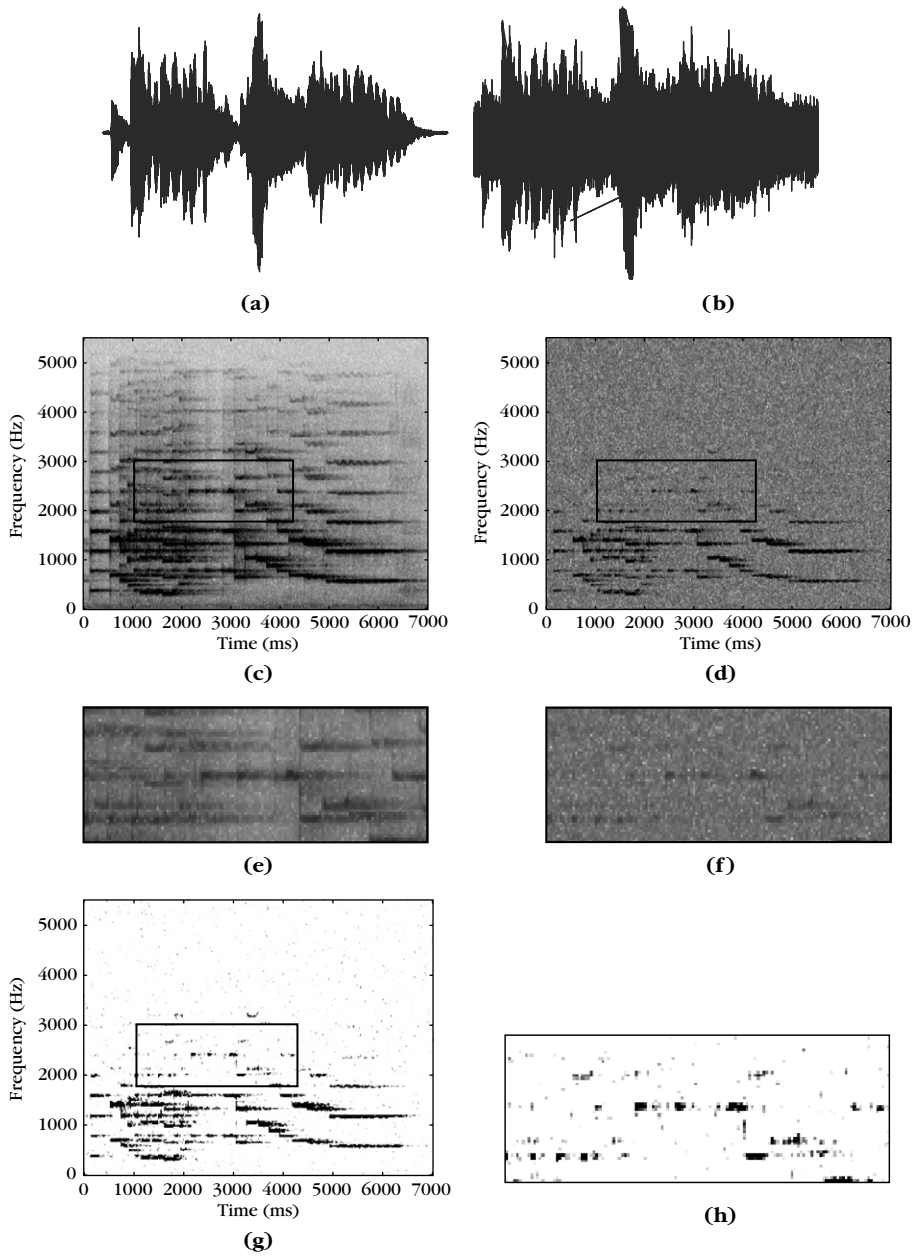

FIGURE 11.8

(a, b) Original and noisy "Mozart" recording (0 db). **(c, d)** Log spectrograms of the original and noisy signals. **(e, f)** Zoom on the spectrograms in (c, d). **(g)** Attenuation factors (11.87) computed from noisy coefficients in (d). Black and white pixels correspond, respectively, to 1 and 0. **(h)** Zoom in on the attenuation factors in (g).

$\tilde{\Lambda}_T$ of Figure 11.6(f) for a wavelet image estimation. Because of these isolated attenuation coefficients $a_{k,m} \approx 1$, the estimator (11.86) restores windowed Fourier vectors $g_{m,k}[n]$ that are perceived as a "musical noise." Despite its small energy, this musical noise is clearly perceived because it is not masked by a sound component at a close frequency and time. Audio masking properties are explained in Section 10.3.3. Despite the SNR improvement, this "musical noise" can be more annoying than the original white noise. Translation-invariant spectrogram thresholding barely improves the musical noise problem. It can be reduced by increasing thresholds, but this attenuates too much audio signal information, and thus also degrades the sound quality. A nonzero masking noise factor ε, which maintains a background noise, can be used to reduce the perception of musical noises.

Section 11.4 shows that effective musical noise reduction requires using nondiagonal time-frequency estimators, which regularize the time-frequency estimation by processing coefficients in groups.

11.4 NONDIAGONAL BLOCK THRESHOLDING

A diagonal estimator in a basis processes each coefficient independently and thus does not take advantage of potential dependencies between neighbor coefficients. Ideally, an optimized representation takes advantage of all structural signal correlations to improve the signal sparsity. In practice, this is not the case. When a coefficient has a large amplitude, it is likely that some other neighborhood coefficients are also nonnegligible, because of signal dependencies that are not fully taken into account by the representation. For example, wavelet image transforms do not capture the geometric regularity of edges, which produce large wavelet coefficients along curves.

Block thresholding estimators introduced by Cai [129] take advantage of such properties by grouping coefficients in blocks and by taking a decision over these blocks. This grouping regularizes thresholding estimators, which improves the resulting risk. It also avoids leaving isolated noise coefficients above the threshold, perceived as "musical noises" in audio signals and that appear as isolated oscillations in images.

Block thresholding estimators are introduced in Section 11.4.1 together with their mathematical properties. Section 11.4.2 studies the improvements of block thresholding estimations in wavelet bases for piecewise regular signals and images. For audio noise, we show in Section 11.4.3 that time-frequency block thresholdings are effective estimators that avoid introducing musical noises.

11.4.1 Block Thresholding in Bases and Frames

A block thresholding estimator implements thresholding decisions over groups of coefficients. The input noisy signal $X = f + W$ is decomposed in an orthonormal basis $\mathcal{B} = \{g_m\}_{0 \leq m < M}$ of $\mathbb{C}^N$, and we write

$$X_{\mathcal{B}}[m] = \langle X, g_m \rangle, \quad f_{\mathcal{B}}[m] = \langle f, g_m \rangle, \quad W_{\mathcal{B}}[m] = \langle W, g_m \rangle, \quad \text{and} \quad \sigma^2_{\mathcal{B}}[m] = E\{|W_{\mathcal{B}}[m]|^2\}.$$

The interval $[0, N-1]$ of all indexes m is partitioned in Q disjoint blocks $\{B_q\}_{1 \leqslant q \leqslant Q}$ of indexes that are grouped together. A block diagonal estimator multiplies all coefficients in B_q with the same attenuation factor a_q

$$\tilde{F} = DX = \sum_{q=1}^{Q} a_q \sum_{m \in B_q} X_{\mathcal{B}}[m]\, g_m, \tag{11.88}$$

where each a_q depends on all coefficients $X_{\mathcal{B}}[m]$ for $m \in B_q$. If all blocks are reduced to a single coefficient, then a block thresholding is a diagonal estimator, otherwise this estimator is not diagonal. Lower bounds of the risk are first computed with "oracles."

Oracle Block Attenuations

If a_q is a constant in the block B_q, then the risk $r(D, f)$ of the block estimator (11.88) is

$$r(D,f) = E\left\{ \|f - \tilde{F}\|^2 \right\} = \sum_{q=1}^{Q} \sum_{m \in B_q} E\{|f_{\mathcal{B}}[m] - a_q X_{\mathcal{B}}[m]|^2\}. \tag{11.89}$$

Since $X_{\mathcal{B}} = f_{\mathcal{B}} + W_{\mathcal{B}}$ and $E\{|W_{\mathcal{B}}[m]|^2\} = \sigma^2_{\mathcal{B}}[m]$, it follows that

$$\sum_{m \in B_q} E\{|f_{\mathcal{B}}[m] - a_q X_{\mathcal{B}}[m]|^2\} = (1-a_q)^2 \, \|f_{\mathcal{B}}\|^2_{B_q} + a_q^2 \, \|\sigma_{\mathcal{B}}\|^2_{B_q}, \tag{11.90}$$

with

$$\|f_{\mathcal{B}}\|^2_{B_q} = \sum_{m \in B_q} |f_{\mathcal{B}}[m]|^2 \quad \text{and} \quad \|\sigma_{\mathcal{B}}\|^2_{B_q} = \sum_{m \in B_q} \sigma^2_{\mathcal{B}}[m].$$

This error is minimized by an oracle attenuation factor,

$$a_q = \frac{\|f_{\mathcal{B}}\|^2_{B_q}}{\|f_{\mathcal{B}}\|^2_{B_q} + \|\sigma_{\mathcal{B}}\|^2_{B_q}}. \tag{11.91}$$

In a Bayesian framework, estimating this coefficient amounts to estimating an a priori SNR $\|f_{\mathcal{B}}\|^2_{B_q} / \|\sigma_{\mathcal{B}}\|^2_{B_q}$ regularized over a block.

An oracle block projection estimator simplifies the estimation by imposing that $a_q \in \{0, 1\}$. The minimization of the risk (11.90) gives

$$a_q = \begin{cases} 1 & \text{if } \|f_{\mathcal{B}}\|_{B_q} \geqslant \|\sigma_{\mathcal{B}}\|_{\mathcal{B}_q} \\ 0 & \text{if } \|f_{\mathcal{B}}\|_{B_q} < \|\sigma_{\mathcal{B}}\|_{\mathcal{B}_q}. \end{cases} \tag{11.92}$$

This oracle estimator is thus an orthogonal projection of X

$$DX = \sum_{m \in \overline{\Lambda}_\sigma} X_{\mathcal{B}}[m]\, g_m,$$

where $\overline{\Lambda}_\sigma$ is the union of all blocks B_q such that $\|f_{\mathcal{B}}\|_{B_q} \geqslant \|\sigma_{\mathcal{B}}\|_{B_q}$. It is a block approximation of the set of coefficients $\Lambda_\sigma = \{0 \leqslant m < N : |f_{\mathcal{B}}[m]| \geqslant \sigma_{\mathcal{B}}[m]\}$, which defines the diagonal oracle projector (11.33). The resulting minimum projection risk is

$$\overline{r}_{\mathrm{pr}}(f) = E\{\|f - \tilde{F}\|^2\} = \sum_{q=1}^{Q} \min(\|f_{\mathcal{B}}\|^2_{B_q},\ \|\sigma_{\mathcal{B}}\|^2_{B_q}). \tag{11.93}$$

The risk $\overline{r}_{\mathrm{pr}}(f)$ of an oracle block projector is always larger that the risk $r_{\mathrm{pr}}(f)$ of a diagonal oracle projector calculated in (11.65),

$$\overline{r}_{\mathrm{pr}}(f) \geqslant r_{\mathrm{pr}}(f) = \sum_{m=0}^{N-1} \min(|f_{\mathcal{B}}[m]|^2, \sigma_{\mathcal{B}}[m]^2), \tag{11.94}$$

because a single thresholding decision is taken over a whole block B_q and not for each coefficient. Both risks are equal if the thresholding decisions are the same, which means that within each block B_q, all coefficients are below the noise or all coefficients are above the noise:

$$\forall m \in B_q\ \sigma_{\mathcal{B}}[m] \leqslant |f_{\mathcal{B}[m]}| \quad \text{or} \quad \forall m \in B_q\ \sigma_{\mathcal{B}}[m] > |f_{\mathcal{B}[m]}|.$$

It is nearly the case if large coefficients are aggregated together, and if the blocks are not too large.

Block Thresholding

To approximate oracle block projections, block thresholding decisions are computed from the empirical noisy signal energy on each block

$$\|X_{\mathcal{B}}\|^2_{B_q} = \sum_{m \in B_q} |X_{\mathcal{B}}[m]|^2.$$

The resulting block thresholding estimator is

$$\tilde{F} = DX = \sum_{q=1}^{Q} a_q(\|X_{\mathcal{B}}\|_{B_q}) \sum_{m \in B_q} X_{\mathcal{B}}[n]\, g_m. \tag{11.95}$$

The soft block thresholding of Cai [129, 130] is implemented with the James-Stein thresholding rule:

$$0 \leqslant a_q(x) = a_{T_q}(x) = \max\left(1 - \frac{T_q^2}{x^2},\ 0\right) \leqslant 1 \tag{11.96}$$

for a threshold $T_q^2 = \lambda \|\sigma_{\mathcal{B}}\|^2_{B_q}$ that is proportional to the noise energy. A hard block thresholding is implemented with a hard-thresholding decision:

$$a_q(x) = a_{T_q}(x) = \begin{cases} 1 & \text{if } |x| > T_q \\ 0 & \text{if } |x| \leqslant T_q, \end{cases} \tag{11.97}$$

with $T_q^2 = \lambda \|\sigma_{\mathcal{B}}\|^2_{B_q}$, but it is usually not used because its mathematical and numerical properties are not as effective as a soft James-Stein block thresholding.

Thresholding Risk

Let us denote $\overline{r}_{\mathrm{th}}(f) = E\{\|\tilde{F} - f\|^2\}$ as the risk of a soft block thresholding estimator. Suppose that W is a Gaussian white noise of variance σ^2 and that all blocks have the same size L. The noise energy in each block is then $\|\sigma_{\mathcal{B}}\|^2_{B_q} = L\,\sigma^2$. Theorem 11.10 [129] computes an upper bound of the block thresholding risk, which is related to the risk $\overline{r}_{\mathrm{pr}}(f)$ of an oracle block projector.

Theorem 11.10: *Cai.* Let $T^2 = \lambda\, L\,\sigma^2$. The risk $\overline{r}_{\mathrm{th}}(f)$ of a soft block thresholding estimator satisfies

$$\overline{r}_{\mathrm{th}}(f) \leqslant \lambda\, \overline{r}_{\mathrm{pr}}(f) + 4N\,\sigma^2\, P(\chi^2_L > \lambda L). \tag{11.98}$$

If $L = \log_{\mathrm{e}} N$ and $T = \sigma\sqrt{\lambda_*\, \log_{\mathrm{e}} N}$ with $\lambda_* = 4.50524$, then

$$\overline{r}_{\mathrm{th}}(f) \leqslant \lambda_*\, \overline{r}_{\mathrm{pr}}(f) + 2\sigma^2. \tag{11.99}$$

Proof. The noisy coefficient $X_{\mathcal{B}}[m] = f_{\mathcal{B}}[m] + W_{\mathcal{B}}[m]$ is a Gaussian random variable of mean $f_{\mathcal{B}}[m]$ and variance σ^2. Over a block B of size L the soft block thresholding estimator can be written as

$$\tilde{F}_{\mathcal{B}} = X_{\mathcal{B}} + g(X_{\mathcal{B}}),$$

where g is defined over any vector $x[m]$ for $m \in B$ by

$$g(x) = (1 - \frac{\lambda L\sigma^2}{\|x\|^2_B})_+\, x - x.$$

The resulting block thresholding risk can thus be computed with a sure estimation, using the following Stein lemma 11.2 which generalizes the one-dimensional lemma (11.1).

Lemma 11.2: *Stein.* Let $g(x) = (g_1(x), ..., g_L(x))$ be a weakly differentiable function from $\mathbb{R}^L$ to $\mathbb{R}^L$. Let us write $\nabla \cdot g(x) = \sum_{l=1}^{L} \frac{\partial g_l(x)}{\partial x[l]}$. If X is a Gaussian random vector of mean $\mu \in \mathbb{R}^L$ and covariance matrix $\sigma^2\,\mathrm{Id}$, then

$$E\{\|X + g(X) - \mu\|^2_B\} = E\{L\,\sigma^2 + \|g(X)\|^2_B + 2\sigma^2\, \nabla \cdot g(X)\}. \tag{11.100}$$

The proof is a multidimensional extension of the one-dimensional proof given for Lemma 11.1 and can be found in [445]. For $g(x) = (1 - \frac{\lambda L\sigma^2}{\|x\|^2_B})_+\, x - x$, Lemma 11.2 implies that

$$E\{\|\tilde{F}_{\mathcal{B}} - f_{\mathcal{B}}\|^2_B\} = E\{\mathit{Sure}(X_{\mathcal{B}}, T, L, \sigma)\}, \tag{11.101}$$

and applying (11.100) with an algebraic calculation gives

$$\begin{aligned}\mathit{Sure}(X_{\mathcal{B}}, \lambda, L, \sigma) = \sigma^2 \Bigg(& L + \frac{\lambda^2 L^2 - 2\lambda L(L-2)}{\|X_{\mathcal{B}}\|^2_B/\sigma^2}\, \mathbf{1}_{(\|X_{\mathcal{B}}\|^2_B > \lambda L\sigma^2)} \\ & + (\|X_{\mathcal{B}}\|^2_B/\sigma^2 - 2L)\, \mathbf{1}_{(\|X_{\mathcal{B}}\|^2_B \leqslant \lambda L\sigma^2)} \Bigg).\end{aligned} \tag{11.102}$$

Since $\|\sigma^{-1}\, X_{\mathcal{B}}\|^2$ is a sum of L independent squared normal random variables, it has a χ^2_L distribution with L degrees of freedom.

The overall thresholding risk is

$$\overline{r}_{\mathrm{th}}(f) = \sum_{q=1}^{Q} E\{\|\tilde{F}_{\mathcal{B}} - f_{\mathcal{B}}\|_{B_q}^2\}.$$

By inserting (11.101) and (11.102), through several technical lemma that are not reproduced here, Cai [129] derives that

$$\overline{r}_{\mathrm{th}}(f) \leq \sum_{q=1}^{Q} \min(\|f_{\mathcal{B}}\|_{B_q}^2 , T^2) + 4N\sigma^2 P(\chi_L^2 > \lambda L). \tag{11.103}$$

Since each block has a size L, $T^2 = \lambda L\sigma^2 = \lambda \|\sigma_{\mathcal{B}}\|_{B_q}^2$, so (11.103) implies (11.98). Cai also proves in [129] that $P(\chi_L^2 > \lambda L) \leq 1/(2N)$ if $L = \log_e N$ and $\lambda = \lambda_*$ with $\lambda_* - \log_e \lambda_* = 3$. Inserting this result in (11.98) proves (11.99). ■

The upper bound (11.98) of the block thresholding risk $\overline{r}_{\mathrm{th}}(f)$ has two terms that balance the bias and variance of this estimator. The second term $N\sigma^2 P(\chi_L^2 > \lambda L)$ is the average error produced by blocks of noisy coefficients above the threshold when the signal is zero. For a diagonal thresholding ($L = 1$), this residual noise corresponds to the "musical noise" that appears when thresholding time-frequency representations of noisy audio recordings. When the block size L increases, this residual noise energy decreases. However, the bias of the oracle risk $\overline{r}_{\mathrm{pr}}(f)$, and thus of $\overline{r}_{\mathrm{th}}(f)$, increases with L. Indeed, larger blocks reduce the flexibility of block thresholding, which computes a single attenuation factor over each block. If large signal coefficients have a tendency to be aggregated, then increasing L up to a maximum value reduces the residual noise energy more than it increases the bias of $\overline{r}_{\mathrm{pr}}(f)$. This is why a block thresholding can reduce the risk of a diagonal thresholding. Setting $L = \log_e N$ and $\lambda = \lambda_*$ gives in (11.99) a block thresholding risk that is of the same order as the oracle risk $\overline{r}_{\mathrm{pr}}(f)$, but it may not minimize the thresholding risk $\overline{r}_{\mathrm{th}}(f)$ because it may increase the oracle risk too much.

For a given block size L, the threshold T and thus λ are adjusted to balance the error produced by signal coefficients set to zero and the remaining noise energy of coefficients above the threshold. It can be computed by maximizing a Sure estimation of the SNR, as described in the next subsection. One can also set a priori the residual noise probability

$$P(\chi_L^2 > \lambda L) = \delta. \tag{11.104}$$

This strategy is used when this residual noise affects the perceived signal quality more than the SNR, as is the case for time-frequency audio denoising. For $\delta = 0.1\%$, Table 11.1 gives the values of λ depending on L.

Sure Block Size Estimation

To optimize the choice of thresholds and block sizes, as in Section 11.2.3, the Sure approach by Cai and Zhou [131] minimizes the Stein unbiased risk estimator. The

Table 11.1 Thresholding Parameter λ Calculated for Different Block Size L, with a Residual Noise Probability $\delta = 0.1\%$

L	4	8	16	32	64	128
λ	4.7	3.5	2.5	2.0	1.8	1.5

Sure risk estimator of a soft block thresholding over a block B of L coefficient is calculated in (11.102) by supposing that the noise is Gaussian and has a constant variance σ^2 in the directions of all the vectors of B. The block noise energy is then $\|\sigma_{\mathcal{B}}\|_B^2 = L\sigma^2$. A global risk estimator is obtained by inserting this expression in (11.102) and by summing over the $Q = N/L$ blocks of a signal of size N:

$$\begin{aligned} Sure(X_{\mathcal{B}}, \lambda, L, \sigma_{\mathcal{B}}) &= \|\sigma_{\mathcal{B}}\|^2 \\ &+ \sum_{q=1}^{Q} \left(\frac{\lambda^2 \|\sigma_{\mathcal{B}}\|_{B_q}^2 - 2\lambda \|\sigma_{\mathcal{B}}\|_{B_q}^2 (L-2)}{\|X_{\mathcal{B}}\|_{B_q}^2 / \|\sigma_{\mathcal{B}}\|_{B_q}^2} \mathbf{1}_{\left(\|X_{\mathcal{B}}\|_{B_q}^2 > \lambda \|\sigma_{\mathcal{B}}\|_{B_q}^2\right)} \right. \\ &+ \left. \left(\|X_{\mathcal{B}}\|_{B_q}^2 - 2\|\sigma_{\mathcal{B}}\|_{B_q}^2 \right) \mathbf{1}_{\left(\|X_{\mathcal{B}}\|_{B_q}^2 \leqslant \lambda \|\sigma\|_{B_q}^2\right)} \right). \end{aligned} \tag{11.105}$$

If the noise is Gaussian white with a variance σ^2, then $\|\sigma_{\mathcal{B}}\|_{B_q}^2 = L\sigma^2$ for all blocks $1 \leqslant q \leqslant Q$. If the noise is not white but its covariance is nearly diagonalized in $\mathcal{B}$, then this formula remains approximately valid as long as the noise coefficient variances remain nearly constant over each block B_q. Indeed, over each block the noise behaves as a white noise.

The Sure minimization approach by Cai and Zhou [131] computes the block size and threshold parameters that minimize the Sure estimated risk:

$$(\tilde{L}, \tilde{\lambda}) = \arg\min_{L,\lambda} Sure(X_{\mathcal{B}}, \lambda, L, \sigma_{\mathcal{B}}). \tag{11.106}$$

In applications, the minimization is performed over a limited set of possible values for the block size L and for λ. A different λ may also be chosen with (11.104) by adjusting the probability δ of the residual noise.

In Section 11.2.3 we explain that when the signal is small relative to the noise energy, the variance of the Sure risk estimator is large and the resulting computed thresholds may be too small. As in (11.79), this case is avoided by estimating the signal energy $\|f\|^2$ with $\|X\|^2 - N\sigma^2$ and comparing it with $\varepsilon_N = \sigma^2 N^{1/2} (\log_{\mathrm{e}} N)^{3/2}$. When the noise energy is too small, the block size is set to 1 and we use the universal threshold $\sigma\sqrt{2\log_{\mathrm{e}} N}$. The resulting threshold and block sizes are derived from the Sure minimization parameters (11.106) with:

$$(T, L) = \begin{cases} (\sigma\sqrt{2\log_{\mathrm{e}} N},\ 1) & \text{if } \|X\|^2 - N\sigma^2 \leqslant \varepsilon_N \\ (\sigma\sqrt{\tilde{\lambda}\tilde{L}},\ \tilde{L}) & \text{if } \|X\|^2 - N\sigma^2 > \varepsilon_N. \end{cases} \tag{11.107}$$

Frame Block Thresholding and Translation Invariance

Block thresholding results extend from orthogonal bases to general frames, by thresholding blocks of frame coefficients with the same thresholding formula. Since Theorem 11.10 is proved with a calculation on a single block, this theorem can be extended from orthogonal bases to frames with minor modifications. Optimal block sizes may also be estimated with the Sure procedure previously described.

Similar to diagonal thresholding, block thresholding can be improved with a translation-invariant procedure that decomposes the signal over a translation-invariant tight frame (11.81)

$$\mathcal{D} = \{g_{m,p}[n] = g_m[(n-p) \bmod N]\}_{0 \leqslant m,p < N}. \tag{11.108}$$

A fully translation-invariant block thresholding requires using overlapping blocks of equal sizes that are translated. A block $B_{m,p}$ obtained by translating by p the block $B_{m,0}$ is associated to each coefficient $X_{\mathcal{B}}[m,p] = \langle X, g_{m,p} \rangle$. The resulting block thresholding estimator is

$$\tilde{F}[n] = \sum_{m=0}^{N-1} \sum_{p=0}^{N-1} a_{T_{m,p}}(\|X_{\mathcal{B}}\|_{B_{m,p}})\, X_{\mathcal{B}}[m,p]\, g_{m,p}[n], \tag{11.109}$$

where a_T is the soft attenuation (11.96). In this case, a thresholding decision is performed for each coefficient, but this thresholding decision is regularized by the block energy averaging.

11.4.2 Wavelet Block Thresholding

Block thresholding improves wavelet thresholding estimations when large-amplitude wavelet coefficients are often aggregated together. With appropriate block sizes, block thresholds are smaller than diagonal thresholds, which preserves more signal information with less residual noise. The Sure block thresholding chooses a threshold and block size that is fixed at each scale 2^j, but that varies with 2^j.

One-Dimensional Signals

In one dimension, a pointwise signal singularity produces at each scale 2^j about three large-amplitude orthogonal wavelet coefficients and even more of smaller relative amplitude. This suggests using blocks of size $L_j \approx 3$ for piecewise regular signals that have isolated singularities. This block size adjustment is performed automatically by the Sure block size and threshold optimizations (11.106) and (11.107). For the piecewise regular signals in Figures 11.4 and 11.5, the block sizes are indeed between 2 and 4. Since the blocks are small, the improvement of this block thresholding over a diagonal thresholding with $L_j = 1$ is marginal, of about 0.3 db for the signals in Figures 11.4 and 11.5.

Images

In images, sharp transitions are often distributed along edge curves or in texture regions. Large-amplitude wavelet coefficients are thus not only aggregated because

(a) (b) (c)

FIGURE 11.9

(a) Noisy image zoom (SNR = 28.1 db on the whole image). **(b)** Denoising with a Sure diagonal soft thresholding of orthogonal wavelet coefficients (SNR = 33.4 db). **(c)** Denoising with a Sure soft block thresholding estimation (SNR = 34.2 db).

of the wavelet support but also because of the geometric image regularity. Block thresholding algorithms take advantage of this geometric property to reduce the estimation risk.

For two-dimensional wavelet bases, blocks have a fixed size of $L_j \times L_j$ pixels that are optimized at each scale 2^j with the Sure optimization together with the thresholds. The resulting soft block thresholding improves the SNR by about 1 db over images such as Lena. Figure 11.9(b) shows a diagonal soft-thresholding estimation ($L_j = 1$) over orthogonal wavelet coefficients with a Sure estimation that adapts thresholds at each scale. The Sure threshold optimization improves the SNR by 0.7 db relative to a soft thresholding with $T = 3\sigma/2$ at all scales. Figure 11.9(c) gives a Sure block thresholding estimation over orthogonal wavelet coefficients. Block width L_j is typically equal to 3 or 4 and λ remains nearly equal to 1. Thus, blocks include between 9 and 16 coefficients. Sure block thresholding restores the texture on Lena's hat much better because of block averaging. On the whole Lena image, the SNR of the noisy image is 28.1 db. A Sure diagonal wavelet soft thresholding gives an SNR of 33.4 db, and a Sure soft block thresholding an SNR of 34.2 db.

With a translation-invariant wavelet transform, a diagonal hard thresholding with $T = 3\sigma$ yields an SNR of 34.5 db, which is better than with a soft thresholding, and a soft Sure block thresholding gives an SNR of 35 db. A Sure block thresholding chooses block sizes L_j between 3×2^j and 4×2^j with λ remaining around 1. The improvement is then only 0.5 db, but the image quality is visually improved because textures are better restored.

11.4.3 Time-Frequency Audio Block Thresholding

Most effective audio denoising algorithms are implemented with nondiagonal adaptive attenuations of time-frequency signal coefficients. Section 11.3.3 explains

that diagonal thresholding algorithms introduce a "musical noise" corresponding to the residual noise above the threshold in time-frequency regions where there is no signal energy. To regularize this estimation, Ephraim and Malah [247, 248] have introduced a time-recursive filtering of time-frequency coefficients that considerably reduces the musical noise. This has led to a large body of complex time-frequency estimators regularized with a time-frequency averaging [147, 176].

Time-frequency block thresholdings also avoid introducing musical noise due to the block averaging that regularizes the thresholding decision. Yu, Mallat, and Bacry [495] showed that automatic parameter adjustments by minimizing the Sure estimated risk produce a low-risk and high-audio perceptual quality.

In Section 11.3.3, on audio time-frequency thresholding, the noisy signal X is decomposed in a windowed Fourier tight frame of $\mathbb{C}^N$

$$SX[m,k] = \langle X, g_{m,k} \rangle = \sum_{n=-K/2}^{K/2-1} X[n]\, g[n - mM]\, \mathrm{e}^{-i2\pi kn/K},$$

for $0 \leqslant k < K$ and $0 \leqslant m < N/M$. A block thresholding computes the noisy spectrogram signal energy over blocks B_q that define a partition of the time-frequency index plane:

$$\|X_{\mathcal{B}}\|^2_{B_q} = \sum_{(m,k)\in B_q} |SX[m,k]|^2.$$

The resulting soft block thresholding estimator is

$$\tilde{F} = \sum_{q=1}^{Q} a_{T_k}(\|X_{\mathcal{B}}\|_{B_q}) \sum_{m\in B_q} SX[m,k]\, g_m, \tag{11.110}$$

where a_{T_k} implements the soft James-Stein attenuation (11.96). The audio noise is often stationary, in which case its variance only depends on the frequency index $\sigma^2_{\mathcal{B}}[m,k] = \sigma^2_{\mathcal{B}}[k]$.

To nearly remove all musical noise, the residual noise probability $P(\chi^2_L > \lambda L) = \delta$ is set to a low value, for example, $\delta = 0.1\%$ [495]. The block size L is adjusted by minimizing the resulting Sure estimated risk. Section 11.4.1 explains that ideally a block includes either signal coefficients that are all above the threshold or all below the threshold in order to minimize the bias error. Thus, block estimation can be improved by adjusting their shape. In regions where the signal includes attacks, it is preferable to use blocks that are narrow in time with a larger frequency width, because the signal energy is delocalized in frequency but concentrated in time. This eliminates "pre-echo" artifacts on signal onsets and results in less distortion on signal transients. For a musical signal, including precise harmonics that have a narrow frequency width, blocks should be narrow in frequency and more elongated in time in order to match the signal time-frequency resolution.

If (L_m, L_k) are the time and frequency widths of a block, its total size is $L = L_m \times L_k$. Sure parameter estimation independently adjusts the time and frequency widths of time-frequency blocks B_q. Long audio signals are divided into segments of N coefficients, and over each subpiece of size N the block sizes and thresholds are computed by minimizing the Sure risk estimator (11.105) with $L = L_m \times L_k$. This Sure risk is calculated over a set of possible time and frequency widths (L_m, L_k), and for each of them λ is computed by adjusting the residual noise probability $P(\chi_L^2 > \lambda L) = \delta$.

Numerical experiments are performed with 15 possible block sizes $L_m \times L_k$ with $L_m = 8, 4, 2$ and $L_k = 16, 8, 4, 2, 1$. Figure 11.10 compares the attenuation coefficients $a_{m,k}$ of a diagonal thresholding in (a) and of a block thresholding in (b). The zoom in Figures 11.10(c, d) shows that nondiagonal block thresholding attenuation factors are more regular and do not include isolated points corresponding to a residual noise above the threshold, perceived as a musical noise [495]. When the SNR of the noisy Mozart recording ranges between -2 db and 15 db, the SNR improvement of a block thresholding relative to a soft diagonal thresholding is between 1 db and 1.5 db [495]. More signal components are recovered because the thresholding factors λ of a block thresholding are at least twice smaller than

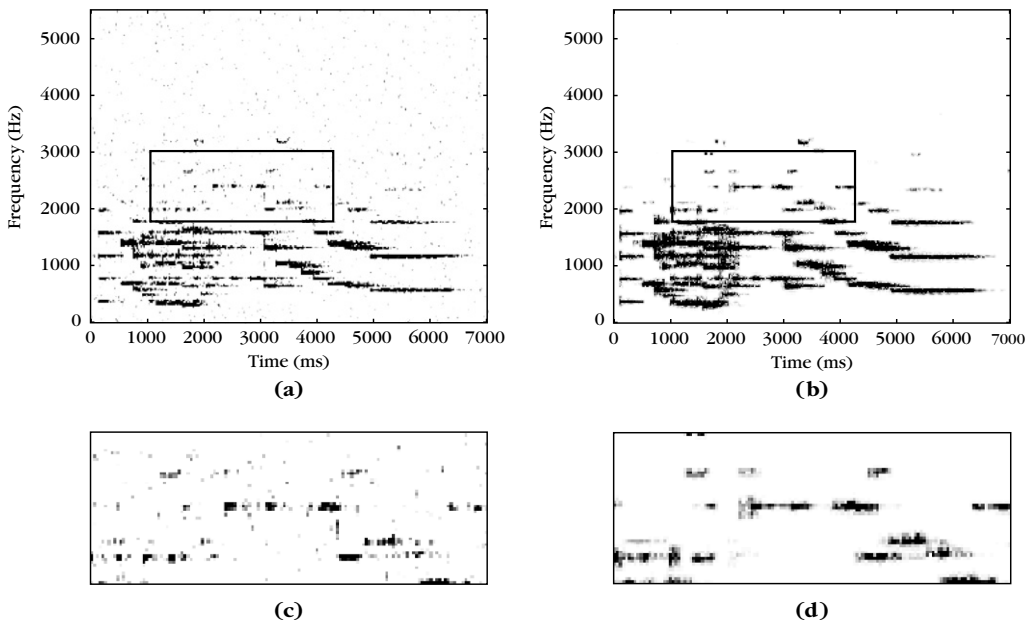

FIGURE 11.10

(a, b) Attenuation coefficients calculated, respectively, with a soft thresholding and a block thresholding on the spectrogram of the noisy "Mozart" signal in Figure 11.8. Black pixels correspond to 1 and white to 0. **(c, d)** Zooms over rectangular regions indicated in (a, b).

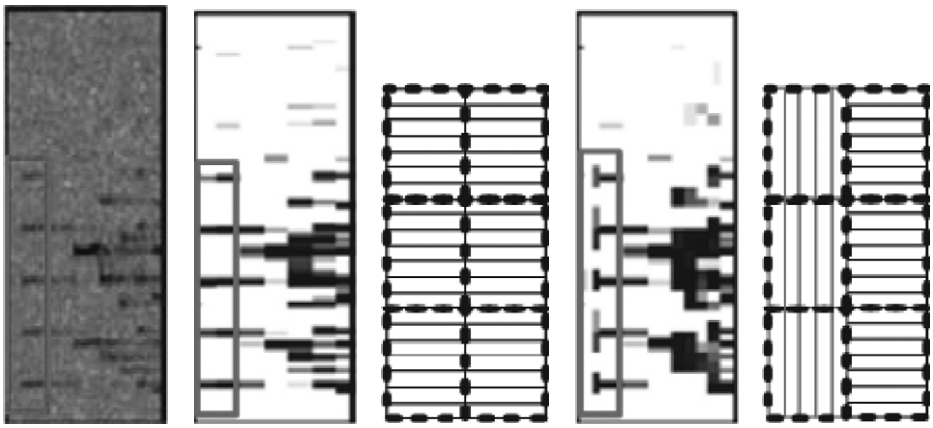

FIGURE 11.11

Zoom on the onset of "Mozart." **(a)** Log spectrogram. **(b)** Attenuation coefficients of a fixed block thresholding. **(c)** Block sizes ($L_m = 8, L_k = 1$) at the signal onset indicated by a vertical rectangle in (b). **(d)** Attenuation coefficients of an adaptive block thresholding. **(e)** Adapted block sizes ($L_m = 2, L_k = 9$) at the signal onset and ($L_m = 16, L_k = 1$) afterwards.

with a diagonal thresholding. Besides this SNR improvement, the audio quality is considerably improved because of the musical noise removal. Better SNR is also obtained with a block thresholding than with classical Ephraim and Malah–type algorithms [247, 248].

Figure 11.11(a) zooms on the onset of the "Mozart" signal that has a log spectrogram shown in Figure 11.8(b). The attenuation factors of block thresholding with a fixed block size $L_m = 8$ and $L_k = 1$ are displayed in Figure 11.11(b). At the beginning of the harmonics, blocks of large attenuation factors spread before the signal's onset. Figure 11.11(c) illustrates the horizontal blocks used to compute the block attenuation factors in Figure 11.11(b). In the time interval where the blocks exceed the signal onset, a moderate attenuation is performed, and since noise is not eliminated, a transient noise component is heard before the signal begins, which is perceived as a "pre-echo" artifact. In Figures 11.11(c, d), the minimization of the Sure estimation risk chooses blocks of shorter length L just before and after the onset, which nearly eliminates the "pre-echo" artifact. After onset, more narrow horizontal blocks are selected ($L_m = 16$, $L_k = 1$) to better capture narrow harmonic signal structures.

11.5 DENOISING MINIMAX OPTIMALITY

Section 11.2.2 proves that a thresholding estimator in an orthogonal basis is nearly optimal compared to any diagonal estimator in this basis. It remains to be understood how these estimators compare to all possible linear and nonlinear estimators.

There is often no appropriate stochastic model for complex signals. Thus, we use deterministic models where any prior information is used to specify the smallest possible set Θ of potential signals. In this minimax framework, our goal is to minimize the maximum risk over Θ and understand under which conditions linear or nonlinear diagonal estimators in a basis $\mathcal{B}$ can nearly reach this minimax risk.

Discrete Minimax Risk

Given noisy data $X[n] = f[n] + W[n]$ for $0 \leq n < N$, where W is a Gaussian white noise of variance σ^2, we study the property of estimators $\tilde{F} = DX$ for any $f \in \Theta$. The maximum risk over Θ is

$$r(D, \Theta) = \sup_{f \in \Theta} r(D, f) \quad \text{with} \quad r(D, f) = E\{\|\tilde{F} - f\|^2\}.$$

The *linear minimax risk* and *nonlinear minimax risk* are the minimum achievable risk, respectively, over the class $\mathcal{O}_l$ of all linear operators and $\mathcal{O}_n$ of all operators (linear and nonlinear) from $\mathbb{C}^N$ to $\mathbb{C}^N$:

$$r_l(\Theta) = \inf_{D \in \mathcal{O}_l} r(D, \Theta) \quad \text{and} \quad r_n(\Theta) = \inf_{D \in \mathcal{O}_n} r(D, \Theta).$$

Sections 11.5.1 and 11.5.2 provide tools to compute linear and nonlinear minimax risks depending on the geometric properties of Θ, and explain how they compare to the risk of diagonal estimators in a basis $\mathcal{B}$. Block thresholding estimators are not specifically studied because they have almost the same asymptotic properties as diagonal thresholding estimators when the noise variance σ tends to zero [130].

Analog Minimax Risk

Discrete signals most often result from the discretization of analog signals. Signal models are defined over analog signals $\bar{f}$, by specifying a prior set of functions $\overline{\Theta}$ where the analog signal belongs. It may, for example, be derived from information on the signal regularity. The discretization of these analog signals defines a set Θ of discrete signals in $\mathbb{C}^N$ where the estimation is computed. Since analog signals are often restored at the end of the processing chain, we must compute the resulting risk and relate it to the risk computed over discrete signals.

Section 11.5.3 computes the risk of linear and thresholding wavelet estimators for different types of signal and image models, by applying the results of Sections 11.5.1 and 11.5.2. For uniformly regular signals and images, linear wavelet estimators are proved to be asymptotically optimal among all linear and nonlinear estimators. However, when the signal regularity is not uniform, thresholding estimators considerably outperform linear estimators. The risk is computed for piecewise regular signals as well as for bounded variation signals and images, where it is proved that wavelet thresholding estimators are nearly minimax optimal. Readers more interested in algorithms and numerical applications may skip the following sections, which are mathematically more involved.

11.5.1 Linear Diagonal Minimax Estimation

To estimate $f[n] \in \Theta$ from noisy measurements $X[n]$, we first study the maximum risk of a linear diagonal operator in an orthogonal basis $\mathcal{B} = \{g_m\}_{0 \leq m < N}$. Such an estimator can be written as

$$\tilde{F} = DX = \sum_{m=0}^{N-1} a_m X_{\mathcal{B}}[m] g_m, \tag{11.111}$$

where each a_m is a constant. Let $\mathcal{O}_{l,d}$ be the set of all linear diagonal operators D. Since $\mathcal{O}_{l,d} \subset \mathcal{O}_l$, the *linear diagonal minimax risk* is larger than the linear minimax risk

$$r_{l,d}(\Theta) = \inf_{D \in \mathcal{O}_{l,d}} r(D, \Theta) \geqslant r_l(\Theta) = \inf_{D \in \mathcal{O}_l} r(D, \Theta).$$

We characterize diagonal estimators that achieve the linear diagonal minimax risk. If Θ is translation invariant, we prove that diagonal operators in a discrete Fourier basis reach the global linear minimax risk: $r_{l,d}(\Theta) = r_l(\Theta)$.

Quadratic Convex Hull

The "square" of a set Θ in the basis $\mathcal{B}$ is defined by

$$(\Theta)^2_{\mathcal{B}} = \{\tilde{f} \,:\, \tilde{f} = \sum_{m=0}^{N-1} |f_{\mathcal{B}}[m]|^2 g_m \quad \text{with} \quad f \in \Theta\}. \tag{11.112}$$

We say that Θ is *quadratically convex* in $\mathcal{B}$ if $(\Theta)^2_{\mathcal{B}}$ is a convex set. A hyperrectangle $\mathcal{R}_h$ in $\mathcal{B}$ of vertex $h \in \mathbb{C}^N$ is a simple example of a quadratically convex set defined by

$$\mathcal{R}_h = \left\{ f \,:\, |f_{\mathcal{B}}[m]| \leqslant |h_{\mathcal{B}}[m]| \text{ for } 0 \leqslant m < N \right\}.$$

The *quadratic convex hull* $\mathrm{QH}[\Theta]$ of Θ in the basis $\mathcal{B}$ is defined by

$$\mathrm{QH}[\Theta] = \left\{ f \,:\, \sum_{m=0}^{N-1} |f_{\mathcal{B}}[m]|^2 g_m \text{ is in the convex hull of } (\Theta)^2_{\mathcal{B}} \right\}. \tag{11.113}$$

It is the largest set with a square $(\mathrm{QH}[\Theta])^2_{\mathcal{B}}$ equal to the convex hull of $(\Theta)^2_{\mathcal{B}}$.

The risk of a diagonal estimator is larger than the risk of an oracle attenuation (11.30). As a result, the oracle risk (11.31) gives a lower bound of the minimax linear diagonal risk $r_{l,d}(\Theta)$:

$$r_{l,d}(\Theta) \geqslant r_{\inf}(\Theta) = \sup_{f \in \Theta} \sum_{m=0}^{N-1} \frac{\sigma^2 |f_{\mathcal{B}}[m]|^2}{\sigma^2 + |f_{\mathcal{B}}[m]|^2}. \tag{11.114}$$

Theorem 11.11 proves that this inequality is an equality if Θ is quadratically convex.

Theorem 11.11. If Θ is a bounded and closed set, then there exists a worst signal $h \in \mathrm{QH}[\Theta]$ such that $r_{\inf}(h) = r_{\inf}(\mathrm{QH}[\Theta])$ in the basis $\mathcal{B}$. Moreover, the linear diagonal operator D defined by

$$a_m = \frac{|h_{\mathcal{B}}[m]|^2}{\sigma^2 + |h_{\mathcal{B}}[m]|^2} \tag{11.115}$$

achieves the linear diagonal minimax risk

$$r(D, \Theta) = r_{l,d}(\Theta) = r_{\inf}\left(\mathrm{QH}[\Theta]\right). \tag{11.116}$$

Proof. The risk $r(D, f)$ of the diagonal operator (11.111) is

$$r(D, f) = \sum_{m=0}^{N-1} \left(\sigma^2 |a_m|^2 + |1 - a_m|^2 |f_{\mathcal{B}}[m]|^2\right). \tag{11.117}$$

Since it is a linear function of $|f_{\mathcal{B}}[m]|^2$, it reaches the same maximum in Θ and in $\mathrm{QH}[\Theta]$. This proves that $r(D, \Theta) = r(D, \mathrm{QH}[\Theta])$ and thus that $r_{l,d}(\Theta) = r_{l,d}(\mathrm{QH}[\Theta])$.

To verify that $r_{l,d}(\Theta) = r_{\inf}(\mathrm{QH}[\Theta])$, we prove that $r_{l,d}(\mathrm{QH}[\Theta]) = r_{\inf}(\mathrm{QH}[\Theta])$. Since (11.114) shows that $r_{\inf}(\mathrm{QH}[\Theta]) \leqslant r_{l,d}(\mathrm{QH}[\Theta])$ to get the reverse inequality, it is sufficient to prove that the linear estimator defined by (11.115) satisfies $r(D, \mathrm{QH}[\Theta]) \leqslant r_{\inf}(\mathrm{QH}[\Theta])$. Since Θ is bounded and closed, $\mathrm{QH}[\Theta]$ is also bounded and closed and thus compact, which guarantees the existence of $h \in \mathrm{QH}[\Theta]$ such that $r_{\inf}(h) = r_{\inf}(\mathrm{QH}[\Theta])$. The risk of this estimator is calculated with (11.117):

$$\begin{aligned} r(D, f) &= \sum_{m=0}^{N-1} \frac{|f_{\mathcal{B}}[m]|^2 \sigma^4 + \sigma^2 |h_{\mathcal{B}}[m]|^4}{(\sigma^2 + |h_{\mathcal{B}}[m]|^2)^2} \\ &= \sum_{m=0}^{N-1} \frac{\sigma^2 |h_{\mathcal{B}}[m]|^2}{\sigma^2 + |h_{\mathcal{B}}[m]|^2} + \sigma^4 \sum_{m=0}^{N-1} \frac{|f_{\mathcal{B}}[m]|^2 - |h_{\mathcal{B}}[m]|^2}{(\sigma^2 + |h_{\mathcal{B}}[m]|^2)^2}. \end{aligned}$$

To show that $r(D, f) \leqslant r_{\inf}(\mathrm{QH}[\Theta])$, we verify that the second summation is negative. Let $0 \leqslant \eta \leqslant 1$ and y be a vector with decomposition coefficients in $\mathcal{B}$ satisfying

$$|y_{\mathcal{B}}[m]|^2 = (1 - \eta) |h_{\mathcal{B}}[m]|^2 + \eta |f_{\mathcal{B}}[m]|^2.$$

Since $\mathrm{QH}[\Theta]$ is quadratically convex, necessarily $y \in \mathrm{QH}[\Theta]$, so

$$J(\eta) = \sum_{m=0}^{N-1} \frac{\sigma^2 |y_{\mathcal{B}}[m]|^2}{\sigma^2 + |y_{\mathcal{B}}[m]|^2} \leqslant \sum_{m=0}^{N-1} \frac{\sigma^2 |h_{\mathcal{B}}[m]|^2}{\sigma^2 + |h_{\mathcal{B}}[m]|^2} = J(0).$$

Since the maximum of $J(\eta)$ is at $\eta = 0$,

$$J'(0) = \sum_{m=0}^{N-1} \frac{|f_{\mathcal{B}}[m]|^2 - |h_{\mathcal{B}}[m]|^2}{(\sigma^2 + |h_{\mathcal{B}}[m]|^2)^2} \leqslant 0,$$

which finishes the proof. ■

The worse signal h, which maximizes $r_{\inf}(h)$ in $\mathrm{QH}[\Theta])$, is a signal with coefficients $|h_{\mathcal{B}}[m]|$ that have a slow decay. It yields conservative amplification factors a_m that keep many coefficients. This theorem implies that $r_{l,d}(\Theta) = r_{l,d}(\mathrm{QH}[\Theta])$. To take advantage of the fact that Θ may be much smaller than its quadratic convex hull, it is thus necessary to use nonlinear diagonal estimators.

Translation-Invariant Set

Signals such as sounds or images are often arbitrarily translated in time or in space, depending on the beginning of the recording or the position of the camera. To simplify border effects, we consider signals of period N. We say that Θ is *circular translation invariant* if for any $f[n] \in \Theta$, then $f[(n-p) \bmod N] \in \Theta$ for all $0 \leq p < N$.

If the set is translation invariant and the noise is stationary, then we show that the best linear estimator is also translation invariant, which means that it is a convolution. Such an operator is diagonal in the discrete Fourier basis $\mathcal{B} = \{g_m[n] = N^{-1/2} \exp(i2\pi mn/N)\}_{0 \leq m < N}$. The decomposition coefficients of f in this basis are proportional to its discrete Fourier transform:

$$f_{\mathcal{B}}[m] = \frac{1}{\sqrt{N}} \sum_{n=0}^{N-1} f[n] \exp\left(\frac{-i2\pi mn}{N}\right) = \frac{\hat{f}[m]}{\sqrt{N}}.$$

For a set Θ, the lower bound $r_{\text{inf}}(\Theta)$ in (11.114) becomes

$$r_{\text{inf}}(\Theta) = \sup_{f \in \Theta} \sum_{m=0}^{N-1} \frac{\sigma^2 N^{-1} |\hat{f}[m]|^2}{\sigma^2 + N^{-1} |\hat{f}[m]|^2}. \tag{11.118}$$

Theorem 11.12 proves that diagonal operators in the discrete Fourier basis achieve the linear minimax risk.

Theorem 11.12. Let Θ be a closed and bounded set. Let $h \in \text{QH}[\Theta]$ be such that $r_{\text{inf}}(h) = r_{\text{inf}}(\text{QH}[\Theta])$ and

$$\hat{h}_0[m] = \frac{|\hat{h}[m]|^2}{N\sigma^2 + |\hat{h}[m]|^2}. \tag{11.119}$$

If Θ is circular translation invariant, then $\tilde{F} = DX = X \circledast h_0$ achieves the linear minimax risk

$$r_l(\Theta) = r(D, \Theta) = r_{\text{inf}}\left(\text{QH}[\Theta]\right). \tag{11.120}$$

Proof. Since $r_l(\Theta) \leq r_{l,d}(\Theta)$, Theorem 11.11 proves in (11.116) that

$$r_l(\Theta) \leq r_{\text{inf}}\left(\text{QH}[\Theta]\right).$$

Moreover, the risk $r_{\text{inf}}\left(\text{QH}[\Theta]\right)$ is achieved by the diagonal estimator (11.115). In the discrete Fourier basis it corresponds to a circular convolution with a transfer function given by (11.119).

We show that $r_l(\Theta) \geqslant r_{\text{inf}}\left(\text{QH}[\Theta]\right)$ by using particular Bayes priors. If $f \in \text{QH}[\Theta]$, then there exists a family $\{f_i\}_i$ of elements in Θ such that for any $0 \leqslant m < N$,

$$|\hat{f}[m]|^2 = \sum_i p_i |\hat{f}_i[m]|^2 \quad \text{with} \quad \sum_i p_i = 1.$$

To each $f_i \in \Theta$ we associate a random shift vector $F_i[n] = f_i[n - Q_i]$ as in (9.27). Each $F_i[n]$ is circular stationary, and its power spectrum is computed in (9.29): $\hat{R}_{F_i}[m] = N^{-1} |\hat{f}_i[m]|^2$. Let F be a random vector that has a probability p_i to be equal to F_i. It

is circular stationary and its power spectrum is $\hat{R}_F[m] = N^{-1}|\hat{f}[m]|^2$. We denote by π_f the probability distribution of F. The risk $r_l(\pi_f)$ of the Wiener filter is calculated in (11.15):

$$r_l(\pi_f) = \sum_{m=0}^{N-1} \frac{\hat{R}_F[m]\,\hat{R}_W[m]}{\hat{R}_F[m] + \hat{R}_W[m]} = \sum_{m=0}^{N-1} \frac{N^{-1}\,|\hat{f}[m]|^2\,\sigma^2}{N^{-1}\,|\hat{f}[m]|^2 + \sigma^2}. \tag{11.121}$$

Since Θ is translation invariant, the realizations of F are in Θ, so $\pi_f \in \Theta^*$. The minimax theorem (11.4) proves in (11.21) that $r_l(\pi_f) \leqslant r_l(\Theta)$. Since this is true for any $f \in \mathrm{QH}[\Theta]$, taking a supremum with respect to f in (11.121) proves that $r_l\left(\mathrm{QH}[\Theta]\right) \leqslant r_l(\Theta)$, which finishes the proof. ■

11.5.2 Thresholding Optimality over Orthosymmetric Sets

We study geometrical conditions on Θ to nearly reach the linear minimax risk $r_l(\Theta)$ and the nonlinear minimax risk $r_n(\Theta)$ with diagonal estimators in a basis $\mathcal{B} = \{g_m\}_{0 \leqslant m < N}$. Since the oracle attenuation (11.30) yields a smaller risk than any linear or nonlinear diagonal estimator, the maximum risk on Θ of any diagonal estimator has a lower bound calculated with the oracle risk (11.31):

$$r_{\inf}(\Theta) = \sup_{f \in \Theta} \sum_{m=0}^{N-1} \frac{\sigma^2\,|f_{\mathcal{B}}[m]|^2}{\sigma^2 + |f_{\mathcal{B}}[m]|^2}.$$

Theorem 11.7 proves that thresholding estimators have a risk that is close to this oracle lower bound. Thus, we need to understand under what conditions $r_n(\Theta)$ is on the order of $r_{\inf}(\Theta)$, and compare it with $r_l(\Theta)$.

Hyperrectangle

We first consider hyperrectangles, which are building blocks for computing the minimax risk over any set Θ. A hyperrectangle in $\mathcal{B}$

$$\mathcal{R}_h = \{f \,:\, |f_{\mathcal{B}}[m]| \leqslant |h_{\mathcal{B}}[m]| \quad \text{for} \quad 0 \leqslant m < N\} \tag{11.122}$$

is a separable set along the basis directions g_m. The risk lower bound for diagonal estimators is

$$r_{\inf}(\mathcal{R}_h) = \sum_{m=0}^{N-1} \frac{\sigma^2\,|h_{\mathcal{B}}[m]|^2}{\sigma^2 + |h_{\mathcal{B}}[m]|^2}.$$

Theorem 11.13 proves that for a hyperrectangle, the nonlinear minimax risk is very close to the linear minimax risk.

Theorem 11.13. On a hyperrectangle $\mathcal{R}_h$ the linear and nonlinear minimax risks are reached by diagonal estimators. They satisfy

$$r_l(\mathcal{R}_h) = r_{\inf}(\mathcal{R}_h), \tag{11.123}$$

and

$$\mu\, r_{\inf}(\mathcal{R}_h) \leqslant r_n(\mathcal{R}_h) \leqslant r_{\inf}(\mathcal{R}_h) \quad \text{with} \quad \mu \leqslant 1/1.25. \tag{11.124}$$

Proof. We first show that a linear minimax estimator is necessarily diagonal in $\mathcal{B}$. Let $\tilde{F} = DX$ be the estimator obtained with a linear operator D represented by the matrix $A = (a_{m,n})_{0 \leqslant n,m \leqslant N}$ in $\mathcal{B}$:

$$\tilde{F}_{\mathcal{B}} = A\, X_{\mathcal{B}}.$$

Let tr$A$ be the trace of A, and A^* be its complex transpose. Since $X = f + W$ where W is a white noise of variance σ^2, a direct calculation shows that

$$r(D, f) = E\{\|\tilde{F} - f\|^2\} = \sigma^2 \operatorname{tr} AA^* + (Af_{\mathcal{B}} - f_{\mathcal{B}})^*\, (Af_{\mathcal{B}} - f_{\mathcal{B}}). \tag{11.125}$$

If D_d is the diagonal operator with coefficients that are $a_m = a_{m,m}$, the risk is then

$$r(D_d, f) = \sum_{m=0}^{N-1} \left(\sigma^2\, |a_{m,m}|^2 + |1 - a_{m,m}|^2\, |f_{\mathcal{B}}[m]|^2 \right). \tag{11.126}$$

To prove that the maximum risk over $\mathcal{R}_h$ is minimized when A is diagonal, we show that $r(D_d, \mathcal{R}_h) \leqslant r(D, \mathcal{R}_h)$. For this purpose, we use a prior probability distribution $\pi \in \mathcal{R}_h^*$ corresponding to a random vector F with realizations that are in $\mathcal{R}_h$:

$$F_{\mathcal{B}}[m] = S[m]\, h_{\mathcal{B}}[m]. \tag{11.127}$$

The random variables $S[m]$ are independent and equal to 1 or -1 with probability $1/2$. The expected risk $r(D, \pi) = E\{\|F - \tilde{F}\|^2\}$ is derived from (11.125) by replacing f by F and taking the expected value with respect to the probability distribution π of F. If $m \neq p$, then $E\{F_{\mathcal{B}}[m]\, F_{\mathcal{B}}[p]\} = 0$, so we get

$$\begin{aligned} r(D, \pi) &= \sigma^2 \sum_{m=0}^{N-1} |a_{m,m}|^2 + \sum_{m=0}^{N-1} |h_{\mathcal{B}}[m]|^2 \left[|a_{m,m} - 1|^2 + \sum_{\substack{p=0 \\ p \neq m}}^{N-1} |a_{m,p}|^2 \right] \\ &\geqslant \sigma^2 \sum_{m=0}^{N-1} |a_{m,m}|^2 + \sum_{m=0}^{N-1} |1 - a_{m,m}|^2 |h_{\mathcal{B}}[m]|^2 \;= r(D_d, h). \end{aligned} \tag{11.128}$$

Since the realizations of F are in $\mathcal{R}_h$, (11.22) implies that $r(D, \mathcal{R}_h) \geqslant r(D, \pi)$, so $r(D, \mathcal{R}_h) \geqslant r(D_d, h)$. To prove that $r(D, \mathcal{R}_h) \geqslant r(D_d, \mathcal{R}_h)$, it is now sufficient to verify that $r(D_d, \mathcal{R}_h) = r(D_d, h)$. To minimize $r(D_d, f)$, (11.126) proves necessarily that $a_{m,m} \in [0, 1]$. In this case, (11.126) implies

$$r(D_d, \mathcal{R}_h) = \sup_{f \in \mathcal{R}_h} r(D_d, f) = r(D_d, h).$$

Now that we know that the minimax risk is achieved by a diagonal operator, we apply Theorem 11.11, which proves in (11.116) that the minimax risk among linear diagonal operators is $r_{\inf}(\mathcal{R}_h)$ because $\mathcal{R}_h$ is quadratically convex. So, $r_l(\mathcal{R}_h) = r_{\inf}(\mathcal{R}_h)$.

To prove that the nonlinear minimax risk is also obtained with a diagonal operator, we use the minimax Theorem 11.4, which proves that

$$r_n(\mathcal{R}_h) = \sup_{\pi \in \mathcal{R}_h^*} \inf_{D \in \mathcal{O}_n} r(D, \pi). \tag{11.129}$$

The set $\mathcal{R}_h$ can be written as a product of intervals along each direction g_m. As a consequence, to any prior $\pi \in \mathcal{R}_h^*$ corresponding to a random vector F, we associate a prior $\pi' \in \mathcal{R}_h^*$ corresponding to F' such that $F'_{\mathcal{B}}[m]$ has the same distribution as $F_{\mathcal{B}}[m]$ but with $F'_{\mathcal{B}}[m]$ independent from $F'_{\mathcal{B}}[p]$ for $p \neq m$. We then verify that for any operator $D, r(D, \pi) \leqslant r(D, \pi')$. The supremum over $\mathcal{R}_h^*$ in (11.129) can thus be restricted to processes that have independent coordinates. This independence also implies that the Bayes estimator that minimizes $r(D, \pi)$ is diagonal in $\mathcal{B}$. The minimax theorem (11.14) proves that the minimax risk is reached by diagonal estimators.

Since $r_n(\mathcal{R}_h) \leqslant r_l(\mathcal{R}_h)$, we derive the upper bound in (11.124) from the fact that $r_l(\mathcal{R}_h) = \mathcal{R}_{\inf}(\mathcal{R}_h)$. The lower bound (11.124) is obtained by computing the Bayes risk $r_n(\pi) = \inf_{D \in \mathcal{O}_n} r(D, \pi)$ for the prior π corresponding to F defined in (11.127), and verifying that $r_n(\pi) \geqslant \mu\, r_{\inf}(\mathcal{R}_h)$. We see from (11.129) that $r_n(\mathcal{R}_h) \geqslant r_n(\pi)$, which implies (11.124). ■

The bound $\mu > 0$ was proved by Ibragimov and Khas'minskii [311], but the essentially sharp bound $1/1.25$ was obtained by Donoho, Liu, and MacGibbon [193]. They showed that μ depends on the variance σ^2 of the noise, and that if σ^2 tends to 0 or to $+\infty$, then μ tends to 1. For hyperrectangles, linear estimators are thus asymptotically optimal compared to nonlinear estimators.

Orthosymmetric Sets

To differentiate the properties of linear and nonlinear estimators, we consider more complex sets that can be written as unions of hyperrectangles. We say that Θ is *orthosymmetric* in $\mathcal{B}$ if for any $f \in \Theta$ and for any a_m with $|a_m| \leqslant 1$, then

$$\sum_{m=0}^{N-1} a_m f_{\mathcal{B}}[m]\, g_m \in \Theta.$$

Such a set can be written as a union of hyperrectangles:

$$\Theta = \bigcup_{f \in \Theta} \mathcal{R}_f. \tag{11.130}$$

An upper bound of $r_n(\Theta)$ is obtained with the maximum risk $r_{\text{th}}(\Theta) = \sup_{f \in \Theta} r_{\text{th}}(f)$ of a hard- or soft-thresholding estimator in the basis $\mathcal{B}$, with a threshold $T = \sigma\sqrt{2 \log_{\text{e}} N}$.

Theorem 11.14. If Θ is orthosymmetric in $\mathcal{B}$, then the linear minimax estimator is reached by linear diagonal estimators and

$$r_{l,d}(\Theta) = r_l(\Theta) = r_{\inf}(\text{QH}[\Theta]). \tag{11.131}$$

The nonlinear minimax risk satisfies

$$\frac{1}{1.25}\, r_{\inf}(\Theta) \leqslant r_n(\Theta) \leqslant r_{\text{th}}(\Theta) \leqslant (2 \log_{\text{e}} N + 1)\left(\sigma^2 + r_{\inf}(\Theta)\right). \tag{11.132}$$

Proof. Since Θ is orthosymmetric, $\Theta = \cup_{f \in \Theta} \mathcal{R}_f$. On each hyperrectangle $\mathcal{R}_f$, we showed in (11.128) that the maximum risk of a linear estimator is reduced by letting it be

diagonal in $\mathcal{B}$. The minimax linear estimation in Θ is therefore diagonal: $r_l(\Theta) = r_{l,d}(\Theta)$. Theorem 11.11 proves in (11.116) that $r_{l,d}(\Theta) = r_{\inf}(\mathrm{QH}[\Theta])$, which implies (11.131).

Since $\Theta = \cup_{f \in \Theta} \mathcal{R}_f$, we also derive that $r_n(\Theta) \geqslant \sup_{f \in \Theta} r_n(\mathcal{R}_f)$. So (11.124) implies that

$$r_n(\Theta) \geqslant \frac{1}{1.25}\, r_{\inf}(\Theta).$$

Theorem 11.7 proves in (11.51) that the thresholding risk satisfies

$$r_{\mathrm{th}}(f) \leqslant (2 \log_{\mathrm{e}} N + 1)\left(\sigma^2 + r_{\mathrm{pr}}(f)\right).$$

A modification of the proof shows that this upper bound remains valid if $r_{\mathrm{pr}}(f)$ is replaced by $r_{\inf}(f)$ [221]. Taking a supremum over all $f \in \Theta$ proves the upper bound (11.132), given that $r_n(\Theta) \leqslant r_{\mathrm{th}}(\Theta)$. ■

This theorem shows that $r_n(\Theta)$ always remains within a factor $2 \log_{\mathrm{e}} N$ of the lower bound $r_{\inf}(\Theta)$ and that the thresholding risk $r_{\mathrm{th}}(\Theta)$ is at most $2 \log_{\mathrm{e}} N$ times larger than $r_n(\Theta)$. In some cases, the factor $2 \log_{\mathrm{e}} N$ can even be reduced to a constant independent of N.

Unlike the nonlinear risk $r_n(\Theta)$, the linear minimax risk $r_l(\Theta)$ may be much larger than $r_{\inf}(\Theta)$. This depends on the convexity of Θ. If Θ is quadratically convex, then $\Theta = \mathrm{QH}[\Theta]$, so (11.131) implies that $r_l(\Theta) = r_{\inf}(\Theta)$. Since $r_n(\Theta) \geqslant r_{\inf}(\Theta)/1.25$, the risk of linear and nonlinear minimax estimators are of the same order. In this case, there is no reason for working with nonlinear as opposed to linear estimators. When Θ is an orthosymmetric ellipsoid, Exercise 11.14 computes the minimax linear estimator of Pinsker [400] and the resulting risk.

If Θ is not quadratically convex, then its hull $\mathrm{QH}[\Theta]$ may be much bigger than Θ. This is the case when Θ has a star shape that is elongated in the directions of the basis vectors g_m, as illustrated in Figure 11.12. The linear risk $r_l(\Theta) = r_{\inf}\left(\mathrm{QH}[\Theta]\right)$

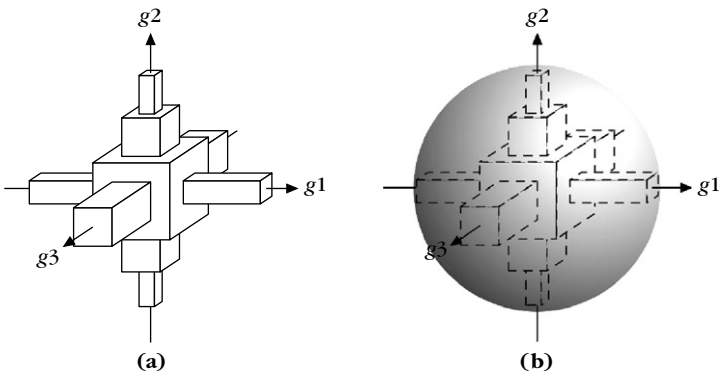

FIGURE 11.12

(a) Example of orthosymmetric set Θ in three dimensions. **(b)** The quadratically convex hull $\mathrm{QH}[\Theta]$ is a larger ellipsoid including Θ.

may then be much larger than $r_{\text{inf}}(\Theta)$. Since $r_n(\Theta)$ and $r_{\text{th}}(\Theta)$ are on the order of $r_{\text{inf}}(\Theta)$, they are then much smaller than $r_l(\Theta)$. A thresholding estimator thus brings an important improvement over any linear estimator.

EXAMPLE 11.2

Let Θ be an ℓ^p ball defined by

$$\Theta = \{f \,:\, \sum_{m=0}^{N-1} \beta_m^p \, |f_{\mathcal{B}}[m]|^p \leqslant C^p\}. \tag{11.133}$$

It is an orthosymmetric set. Its square is

$$(\Theta)^2_{\mathcal{B}} = \{f \,:\, \sum_{m=0}^{N-1} \beta_m^p \, |f_{\mathcal{B}}[m]|^{p/2} \leqslant C^p\}.$$

If $p \geqslant 2$, then $(\Theta)^2_{\mathcal{B}}$ is convex, so Θ is quadratically convex. If $p < 2$, the convex hull of $(\Theta)^2_{\mathcal{B}}$ is $\{f : \sum_{m=0}^{N-1} \beta_m^2 \, |f_{\mathcal{B}}[m]| \leqslant C^2\}$, so the quadratic convex hull of Θ is

$$\text{QH}[\Theta] = \{f \,:\, \sum_{m=0}^{N-1} \beta_m^2 \, |f_{\mathcal{B}}[m]|^2 \leqslant C^2\}. \tag{11.134}$$

The smaller p, the larger the difference between Θ and $\text{QH}[\Theta]$.

Risk Calculation

Let us consider the maximum linear and nonlinear approximation errors on Θ, with M vectors selected from the basis $\mathcal{B}$:

$$\varepsilon_l(M, \Theta) = \sup_{f \in \Theta} \varepsilon_l(M, f) \quad \text{and} \quad \varepsilon_N(M, \Theta) = \sup_{f \in \Theta} \varepsilon_N(M, f).$$

Let $r(D_M, \Theta)$ be the risk associated to a linear diagonal projector

$$\tilde{F} = D_M X = \sum_{m=0}^{M-1} X_{\mathcal{B}}[m] \, g_m.$$

Theorem 11.15 proves that $r(D_M, \Theta)$ depends on the linear approximation error $\varepsilon_l(M, \Theta)$. Similarly, the thresholding risk, which is of the order of $r_{\text{inf}}(\Theta)$, depends on the nonlinear approximation error $\varepsilon_n(M, \Theta)$.

Theorem 11.15. Let $s > 1/2$ and C be such that $1 \leqslant C/\sigma \leqslant N^s$. If $\varepsilon_l(M, \Theta) \leqslant C^2 \, M^{1-2s}$, then

$$r(D_{M_0}, \Theta) \leqslant 3 \, C^{1/s} \, \sigma^{2-1/s} \quad \text{with} \quad (C/(2\sigma))^{1/s} \leqslant M_0 \leqslant (C/\sigma)^{1/s}. \tag{11.135}$$

$$\text{If } \varepsilon_n(M, \Theta) \leqslant C^2 \, M^{1-2s} \quad \text{then} \quad r_{\text{inf}}(\Theta) \leqslant 3 \, C^{1/s} \, \sigma^{2-1/s}. \tag{11.136}$$

In particular, if

$$\Theta_{C,s} = \left\{ f \,:\, \left(\sum_{m=0}^{N-1} |f_{\mathcal{B}}[m]|^{1/s} \right)^s \leqslant C \right\}, \tag{11.137}$$

then $r_{\text{inf}}(\Theta_{C,s}) \sim C^{1/s}\, \sigma^{2-1/s}$.

Proof. The property (11.135) is a consequence of (11.43) in Theorem 11.6. Since $r_{\text{inf}}(f) \leqslant r_{\text{pr}}(f)$, we derive (11.136) from (11.38) in Theorem 11.5.

Theorem 9.9 together with Theorem 9.10 prove that any $f \in \Theta_{C,s}$ satisfies $\varepsilon_n(M,f) \leqslant C^2 M^{1-2s}/(2s-1)$, which implies that $r_{\text{inf}}(\Theta_{C,s}) = O(C^{1/s}\, \sigma^{2-1/s})$. To get a reverse inequality, we consider $f \in \Theta_{C,s}$ such that $|f_{\mathcal{B}}[m]| = \sigma$ for $0 \leqslant m < \lfloor (C/\sigma)^{1/s} \rfloor$ and $f_{\mathcal{B}}[m] = 0$ for $m \geqslant \lfloor (C/\sigma)^{1/s} \rfloor$. In this case,

$$r_p(f) = \lfloor (C/\sigma)^{1/s} \rfloor\, \sigma^2 \sim C^{1/s}\, \sigma^{2-1/s}.$$

Since $r_{\text{inf}}(\Theta_{C,s}) \geqslant r_{\text{pr}}(f)/2$, it follows that $r_{\text{inf}}(\Theta_{C,s}) \sim \sigma^{2-1/s}\, C^{1/s}$. ■

The hypothesis $C/\sigma \geqslant 1$ guarantees that the largest signal coefficient is not dominated by the noise, whereas $C/\sigma \leqslant N^s$ indicates that the smallest coefficient has an amplitude smaller than the noise. This is typically the domain of application for noise-removal algorithms. If s is large, then $r_{\text{inf}}(\Theta)$ is almost on the order of σ^2. This risk is much smaller than the noise energy $E\{\|W\|^2\} = N\sigma^2$, which means that the estimation removes most of the noise.

11.5.3 Nearly Minimax with Wavelet Estimation

Analog signal models are defined over functions by characterizing their regularity. Discrete signal models are derived through the discretization process. We consider uniformly regular and piecewise regular signals as well as bounded variation signals and images. The risk obtained by linear and thresholding wavelet estimators is computed with the tools proved in Sections 11.5.1 and 11.5.2, and their optimality is demonstrated by comparing them to the linear and nonlinear minimax risks.

All asymptotic calculations are performed for a Gaussian white noise, with a variance σ^2 that decreases to zero. We write $r_0(\Theta) \sim r_1(\Theta)$ if there exists two constant $B \geqslant A > 0$ that do not depend on the parameters of the set Θ or on σ such that $A r_0(\Theta) \leqslant r_1(\Theta) \leqslant B r_0(\Theta)$.

Estimation of Discrete Signals and Functions

Let $\overline{\Theta}$ be a set of functions in $\mathbf{L}^2[0,1]$, which defines an analog signal model. A Gaussian white noise model can characterize the random fluctuations of many sensor outputs. The observed noise process is written as

$$dX(dx) = \bar{f}(x)\, dx + \sigma\, dW(dx), \tag{11.138}$$

where the noise $W(dx)$ is a standard Wiener process, and $\bar{f}(x)$ is the analog signal of interest, which belongs to the functional set $\overline{\Theta}$. The acquisition device outputs noisy measurements $X[n] = \langle X, \bar{\phi}_n \rangle$ where the $\bar{\phi}_n(x)$ are the sensor responses. We

suppose here that the acquisition device performs a low-pass filtering and uniform sampling, and thus that $\bar{\phi}_n(x) = \bar{\phi}_s(ns - x)$ where s is the sampling interval. The resulting N noisy measurements can be written as

$$X[n] = f[n] + W[n],$$

where $f[n]$ is the discrete signal and $W[n]$ is the discrete noise:

$$f[n] = \bar{f} \star \bar{\phi}_s(ns) = \int \bar{f}(x)\, \bar{\phi}_s(ns - x)\, dx \quad \text{and} \quad W[n] = \sigma \int \bar{\phi}_s(ns - x)\, dW(dx). \tag{11.139}$$

The resulting set of possible discrete signals is

$$\Theta = \{f \in \mathbb{C}^N \ : f[n] = \bar{f} \star \bar{\phi}_s(ns) \quad \text{with} \quad \bar{f} \in \overline{\Theta}\}.$$

The properties of the Wiener process imply that if $\{\bar{\phi}_n(x) = \bar{\phi}_s(ns - x)\}_n$ is an orthonormal family of a space $\mathbf{U}_N$ in $\mathbf{L^2}[0, 1]$, then $W[n]$ is a Gaussian white noise of variance σ^2.

Let us consider a wavelet orthonormal basis of $\mathbf{L^2}[0, 1]$. To simplify explanations, we suppose that $\bar{\phi}_s(ns - x) = \phi_L(x - 2^L n)$ where ϕ_L is the scaling function at a scale $s = 2^L = N^{-1}$ associated to this wavelet orthonormal basis. As a result, $\{\bar{\phi}_s(ns - x) = \phi_{L,n}(x)\}_{0 \leq n < N}$ is a scaling orthonormal basis. The discretized signal then corresponds to scaling coefficients $f[n] = \langle \bar{f}\, \phi_{L,n} \rangle$, and the sampling approximation space $\mathbf{U}_N$ is a multiresolution approximation space $\mathbf{V}_L$. This hypothesis can be relaxed without modifying the theorems, as long as $\bar{\phi}_s$ has a fast decay and defines a Riesz basis.

Since $f[n]$ are the decomposition coefficients of $\bar{f}$ in the orthonormal basis $\{\phi_{L,n}\}_{0 \leq n < N}$, from any discrete estimator $\tilde{F}[n] = DX[n]$ of $f[n]$, an analog estimator of $\bar{f}(x)$ is derived:

$$\bar{F}(x) = \sum_{n=0}^{2^{-L}-1} \tilde{F}[n]\, \phi_{L,n}(x). \tag{11.140}$$

The resulting risk is

$$E\{\|\bar{f} - \bar{F}\|^2\} = E\{\|P_{\mathbf{V}_L}\bar{f} - \bar{F}\|^2\} + \|\bar{f} - P_{\mathbf{V}_L}\bar{f}\|^2.$$

Since $f[n]$ and $\tilde{F}[n]$ are the coefficients of $P_{\mathbf{V}_L}\bar{f}$ and $\bar{F}$ in an orthonormal basis, the $\mathbf{L^2}$ error norm is equal to the coefficient error norm in $\mathbb{C}^N$: $\|P_{\mathbf{V}_L}\bar{f} - \bar{F}\|^2 = \|f - \tilde{F}\|^2$, and thus

$$E\{\|\bar{f} - \bar{F}\|^2\} = E\{\|f - \tilde{F}\|^2\} + \|\bar{f} - P_{\mathbf{V}_L}\bar{f}\|^2. \tag{11.141}$$

Taking a supremum over $\bar{f} \in \overline{\Theta}$, we get

$$r(D, \Theta) \leq r(D, \overline{\Theta}) \leq r(D, \Theta) + \varepsilon_l(N, \overline{\Theta}), \tag{11.142}$$

where $\varepsilon_l(N, \overline{\Theta})$ is the maximum linear approximation when projecting functions in $\overline{\Theta}$ over the space $\mathbf{U}_N = \mathbf{V}_L$ of dimension N. We typically have $\varepsilon_l(N, \overline{\Theta}) = O(N^{-\beta})$ for

some $\beta > 0$, and since $r(D, \Theta)$ typically decays like σ^γ for some $\gamma > 0$, by choosing $N \sim \sigma^{-\gamma/\beta}$ the linear approximation error is of the same order as the estimation risk, and we get

$$r(D, \Theta) \sim r(D, \overline{\Theta}). \tag{11.143}$$

For a sufficiently large resolution N, the estimation errors over discrete and analog signals are of the same order.

Uniformly Regular Signals

Models of uniformly regular signals are defined with a bound over their Hölder norm. Section 9.1.3 proves that such functions have optimal linear approximations in a wavelet basis. We derive that linear wavelet estimators have a maximum risk that is nearly minimax among all linear and nonlinear estimators.

The homogeneous Hölder norm of a uniformly Lipschitz α function $\bar{f}$ is the infimum $\|\bar{f}\|_{\tilde{\mathbf{C}}^\alpha}$ of all K that satisfy

$$\forall (t, v) \in [0, 1]^2, \quad |\bar{f}(t) - p_v(t)| \leq K\, |t - v|^\alpha,$$

where $p_v(t)$ is a polynomial of degree $\lfloor \alpha \rfloor$. A set of uniformly Lipschitz α functions provides a good model for uniformly regular signals:

$$\overline{\Theta}_\alpha = \{\bar{f} \in \mathbf{L^2}[0, 1] \,:\, \|\bar{f}\|_{\tilde{\mathbf{C}}^\alpha} \leq C_\alpha\}, \tag{11.144}$$

where α and C_α measure this uniform regularity.

Since $f[n] = \langle \bar{f}\, \phi_{L,n} \rangle$, we derive in Section 7.3.1 that the orthogonal wavelet coefficients and scaling coefficients of $\bar{f}(x)$ in $\mathbf{L^2}[0, 1]$ at a scale $2^j > 2^L$ are the discrete wavelet coefficients of f in $\mathbb{C}^N$:

$$\langle \bar{f}(x), \psi_{j,m}(x) \rangle = \langle f[n], \psi_{j,m}[n] \rangle \quad \text{and} \quad \langle \bar{f}(x), \phi_{j,m}(x) \rangle = \langle f[n], \phi_{j,m}[n] \rangle.$$

Estimating wavelet or scaling coefficients of $\bar{f}$ at scales $2^j > 2^L$ is thus equivalent to estimating the coefficients of f from the noisy observation X.

A linear wavelet projector over a family of $2^{-k} < 2^{-L} = N$ scaling functions is defined by

$$\tilde{F}[n] = D_k X[n] = \sum_{m=0}^{2^{-k}-1} \langle X, \phi_{k,m} \rangle\, \phi_{k,m}[n]. \tag{11.145}$$

It can also be rewritten as a projection over wavelets at scales $2^j > 2^k$:

$$\tilde{F}[n] = D_k X[n] = \sum_{j=k+1}^{J} \sum_{m=0}^{2^{-j}-1} \langle X, \psi_{j,m} \rangle\, \psi_{j,m} + \sum_{m=0}^{2^{-J}-1} \langle X, \phi_{J,m} \rangle\, \phi_{J,m}. \tag{11.146}$$

This amounts to setting all wavelet coefficients $\langle X, \psi_{j,n} \rangle$ at scales $2^j \geq 2^k$ to zero. An analog estimator $\tilde{F}(x)$ is associated to $\tilde{F}[n] = D_k X[n]$ with (11.140). Theorem 11.16 proves that if the projection scale 2^k is appropriately adjusted, then

this linear estimator produces a maximum risk over uniformly Lipschitz α functions, which is nearly minimax among all linear and nonlinear operators. The proof follows a typical approach to compute minimax rates for such estimators. The set Θ_α is embedded in hyperrectangles over which calculations can be carried. Asymptotic risk decays are computed when the noise variance σ^2 decreases to zero.

Theorem 11.16. Over uniformly Lipschitz α functions, a linear wavelet projector with cut-off scale $2^k \sim (\sigma/C_\alpha)^{1/(\alpha+1/2)}$ satisfies

$$r(D_k, \overline{\Theta}_\alpha) \sim r_l(\overline{\Theta}_\alpha) \sim r_n(\overline{\Theta}_\alpha) \sim C_\alpha^{1/(\alpha+1/2)}\, \sigma^{2-1/(\alpha+1/2)}. \tag{11.147}$$

Proof. We shall prove that

$$r(D_k, \Theta_\alpha) \sim r_l(\Theta_\alpha) \sim r_n(\Theta_\alpha) \sim C_\alpha^{1/(\alpha+1/2)}\, \sigma^{2-1/(\alpha+1/2)} \tag{11.148}$$

by showing that Θ_α is nearly a hyperrectangle in a wavelet basis. Theorem 9.7 proves that $\varepsilon_l(N, \overline{\Theta}_\alpha) = O(N^{-2\alpha})$. For N sufficiently large, the theorem result (11.147) is derived from (11.148), by verifying that the maximum risk over $\overline{\Theta}_\alpha$ is of the same order as the maximum risk over Θ_α, with the same argument as in (11.143).

Theorem 9.6 proves in (9.22) that there exists $B \geqslant A > 0$ such that

$$A\, \|\bar{f}\|_{\tilde{\mathbf{C}}^\alpha} \leqslant \sup_{j \geqslant J, 0 \leqslant n < 2^{-j}} 2^{-j(\alpha+1/2)}\, |\langle f, \psi_{j,n}\rangle| \leqslant B\, \|\bar{f}\|_{\tilde{\mathbf{C}}^\alpha}. \tag{11.149}$$

Let us define

$$\mathcal{R}_\lambda = \{ f \in \mathbb{C}^N \,:\, \sup_{j \geqslant J, 0 \leqslant n < 2^{-j}} |\langle f, \psi_{j,n}\rangle| \leqslant \lambda\, C_\alpha\, 2^{j(\alpha+1/2)} \}.$$

This set is hyperrectangles in a wavelet basis, as defined in (11.122). We know that $\langle f, \psi_{j,n}\rangle = \langle \bar{f}, \psi_{j,n}\rangle$ for $j > L$, and that $f \in \Theta_\alpha$ if and only if $\bar{f} \in \overline{\Theta}_\alpha$, thus $\|\bar{f}\|_{\tilde{\mathbf{C}}^\alpha} \leqslant C_\alpha$. It results from (11.149) that

$$\mathcal{R}_A \subset \Theta_\alpha \subset \mathcal{R}_B.$$

Theorem 11.13 proves in (11.123) that $r_{\inf}(\mathcal{R}_A)/1.125 \leqslant r_n(\mathcal{R}_A)$, so as a consequence of this embedding, the maximum risk over Θ_α satisfies

$$r_{\inf}(\mathcal{R}_A)/1.125 \leqslant r_n(\mathcal{R}_A) \leqslant r_n(\Theta_\alpha) \leqslant r_l(\Theta_\alpha) \leqslant r(D_k, \mathcal{R}_B). \tag{11.150}$$

Let us compute

$$r_{\inf}(\mathcal{R}_A) \leqslant A^2 \sum_{j=L+1}^{J} \sum_{m=0}^{2^{-j}} \min(\sigma^2,\, C_\alpha^2\, 2^{j(2\alpha+1)}) \sim A^2\, \sigma^2\, 2^{-k} \quad \text{with} \quad 2^k = (\sigma/C_\alpha)^{1/(\alpha+1/2)}. \tag{11.151}$$

Theorem 9.7 proves that the linear approximation error over Θ_α satisfies $\varepsilon_l(M, \Theta_\alpha) = O(C_\alpha^2 M^{-2\alpha})$. Theorem 11.15 derives in (11.135) for $s = \alpha + 1/2$ that the linear projector corresponding to $2^{-k} \sim M_0 \sim (C/\sigma)^{1/(\alpha+1/2)}$ yields a maximum risk that satisfies $r(D_k, \Theta_\alpha) \sim \sigma^2\, (\sigma/C_\alpha)^{-1/(\alpha+1/2)}$. Inserting this and (11.151) in (11.150) proves (11.148). ■

This theorem proves that for uniformly regular images, it is not worth using sophisticated nonlinear estimators. Linear estimators are optimal and a simple projector in a wavelet basis is nearly optimal. This theorem remains valid in two dimensions for images. For images, Theorem 9.16 proves that over a set $\overline{\Theta}_\alpha^2$ of uniformly Lipschitz α images with a homogeneous Hölder norm bounded by C_α, the linear approximation error has a different decay than in one dimension, and satisfies

$$\varepsilon_l(N, \overline{\Theta}_\alpha^2) = O(C_\alpha^2 N^{-\alpha}).$$

The same proof as in Theorem 11.16 shows that linear estimators remain optimal with a risk that satisfies

$$r(D_k, \overline{\Theta}_\alpha^2) \sim r_l(\overline{\Theta}_\alpha^2) \sim r_n(\overline{\Theta}_\alpha^2) \sim C_\alpha^{2/(\alpha+1)}\, \sigma^{2-2/(\alpha+1)}, \tag{11.152}$$

with a linear wavelet projector D_k the cut-off scale of which satisfies $2^k \sim (\sigma/C_\alpha)^{2/(\alpha+1)}$.

Piecewise Regular Signals

When signals are not uniformly regular, linear estimators are not optimal anymore. For piecewise regular signals, optimal nonlinear estimators average the noisy data $X = f + W$ over domains where f is regular, but avoid averaging X across the discontinuities of f. These adaptive smoothing algorithms require estimating the positions of the discontinuities of f from X. A wavelet thresholding algorithm implements a similar adaptive averaging and produces a nearly minimax risk.

A piecewise uniformly Lipschitz α function is defined as a function with a Hölder norm bounded on consecutive intervals $[t_k, t_{k+1}]$, where the t_k are the locations of at most K discontinuities:

$$\overline{\Theta}_{\alpha,K} = \{\bar{f} \in \mathbf{L^2}[0,1] : \exists \{t_k\}_{0 \leqslant k < K} \in [0,1]^K \quad \text{with} \quad \|\bar{f}\|_{\tilde{\mathbf{C}}^\alpha([t_k, t_{k+1}])} \leqslant C_\alpha \text{ for } 0 \leqslant k < K\}. \tag{11.153}$$

This model uses a standard Hölder norm $\|f\|_{\mathbf{C}^\alpha} = \|f\|_{\tilde{\mathbf{C}}^\alpha} + \|f\|_\infty$, which imposes that f is uniformly Lipschitz α and uniformly bounded, so that the amplitudes of all discontinuities are bounded. The discretization of signals $\bar{f}(x) \in \overline{\Theta}_{\alpha,K}$ defines a discrete set of signals $f[n] \in \Theta_{\alpha,K}$. Figure 11.2 shows a piecewise regular signal with $K = 9$.

A wavelet thresholding estimator of $f[n]$ is defined by

$$\tilde{F}[n] = \sum_{j > L, m} \rho_T(\langle X, \psi_{j,m} \rangle)\, \psi_{j,m}[n]. \tag{11.154}$$

An analog thresholding estimator $\bar{F}(x)$ is associated to $\tilde{F}[n]$ with (11.140). Theorem 11.17 proves that such thresholding estimators yield a nearly minimax risk, and that this risk is almost the same as the minimax risk in (11.147) for functions having no discontinuities. Linear estimators blur singularities and thus produce a much larger risk.

Theorem 11.17. Over piecewise Lipschitz α functions, a linear wavelet projector with cut-off scale $2^k \sim \sigma / C_\alpha$ satisfies

$$r(D_k, \overline{\Theta}_{\alpha,K}) \sim r_l(\overline{\Theta}_{\alpha,K}) \sim C_\alpha K \sigma. \tag{11.155}$$

For any $\sigma > 0$, a thresholding wavelet estimator with $N \sim (C_\alpha/\sigma)^{2-1/(\alpha+1/2)}$ and $T = \sigma \sqrt{2 \log_e N}$ satisfies

$$r_{\text{th}}(\overline{\Theta}_\alpha) = O\Big(C_\alpha^{1/(\alpha+1/2)} \, \sigma^{2-1/(\alpha+1/2)} \, |\log(\sigma/C_\alpha)| \Big). \tag{11.156}$$

Proof. We shall first show that

$$r(D_k, \Theta_{\alpha,K}) \sim r_l(\Theta_{\alpha,K}) \sim C_\alpha K \sigma. \tag{11.157}$$

Theorem 9.12 proves that $\varepsilon_l(N, \overline{\Theta}_\alpha) = O(N^{-1})$. For N sufficiently large, (11.155) is derived from (11.157) by proving that the maximum risk over $\overline{\Theta}_{\alpha,K}$ is equivalent to the maximum risk over $\Theta_{\alpha,K}$, with the same argument as in (11.143).

One can verify that $h[n] = C_\alpha N^{-1/2} \mathbf{1}_{[0,N/2]}[n] \in \Theta_{\alpha,K}$ for any $K \geqslant 1$ and $\alpha > 0$. An upper bound of the linear minimax risk is computed over a smaller translation-invariant set obtained by translating h modulo N:

$$\Theta_0 = \Big\{ f \in \mathbb{C}^N \,:\, \exists p \in [0, N-1] \quad \text{with} \quad f[n] = h[(n-p) \bmod N] \Big\} \subset \Theta_{\alpha,K}.$$

It results that $r_l(\Theta_{\alpha,K}) \geqslant r_l(\Theta_0)$. Theorem 11.12 proves that the linear minimax risk over this translation-invariant set is reached by a diagonal operator in the discrete Fourier basis. Any $f \in \Theta_0$ satisfies $|\hat{f}[2m]|^2 = |\hat{h}[2m]| = C_\alpha N^{-1/2} \, |\sin(2\pi m/N)|^{-1}$ and $|\hat{f}[2m+1]|^2 = |\hat{h}[2m+1]| = 0$. Since Θ_0 is included in a hyperrectangle defined by $\hat{h}$, we derive from (11.120) and (11.118) that

$$r_l(\Theta_0) = r_{\text{inf}}(\text{QH}[\Theta]_0) = \sum_{m=0}^{N/2-1} \frac{\sigma^2 N^{-2} C_\alpha^2 \, |\sin(2\pi m/N)|^{-2}}{\sigma^2 + N^{-2} C_\alpha^2 \, |\sin(2\pi m/N)|^{-2}} \sim C_\alpha \sigma.$$

A similar calculation shows that if Θ_0 is generated by a signal h having K discontinuities of amplitude C_α instead of a single one, then $r_l(\Theta_0) \sim K C_\alpha \sigma$.

Theorem 9.12 proves that the linear approximation error over $\Theta_{\alpha,K}$ satisfies $\varepsilon_l(M, \Theta_{\alpha,K}) = O(K C_\alpha^2 M^{-1})$. Theorem 11.15 derives in (11.135) for $s = 1$ that the linear projector corresponding to $2^{-k} \sim M_0 \sim C/\sigma$ yields a maximum risk that satisfies $r(D_k, \Theta_{\alpha,K}) \sim C_\alpha \sigma$. Since $r_l(\Theta_{\alpha,K}) \geqslant r_l(\Theta_0) \sim K C_\alpha \sigma$ and $r(D_k, \Theta_{\alpha,K}) \leqslant r_l(\Theta_{\alpha,K})$, we derive (11.157).

Let us now prove the nonlinear minimax risk result (11.156). For $T = \sigma \sqrt{2 \log_e N}$, the thresholding risk satisfies

$$r_{\text{th}}(\Theta) \leqslant (2 \log_e N + 1) \Big(\sigma^2 + r_{\text{inf}}(\Theta) \Big).$$

Moreover, Theorem 9.12 proves that $\varepsilon_n(M, \Theta_{\alpha,K}) = O(C_\alpha^2 M^{-2\alpha})$. Thus, we derive from (11.136) in Theorem 11.15 for $s = \alpha + 1/2$ that $r_{\text{inf}}(\Theta_{\alpha,K}) = O(C_\alpha^{1/(\alpha+1/2)} \, \sigma^{2\alpha/(\alpha+1/2)})$, so

$$r_{\text{th}}(\Theta_\alpha) = O\Big(\log_e N \, C_\alpha^{1/(\alpha+1/2)} \, \sigma^{2-1/(\alpha+1/2)} \Big).$$

Theorem 9.12 proves that $\varepsilon_l(N, \overline{\Theta}_\alpha) = O(C_\alpha^2 N^{-1})$. We derive (11.156) with the same argument as in (11.143), by having $\varepsilon_l(N, \overline{\Theta}_\alpha) = O(C_\alpha^{1/(\alpha+1/2)} \, \sigma^{2-1/(\alpha+1/2)})$, which is achieved with $N \sim (C_\alpha/\sigma)^{2-1/(\alpha+1/2)}$ and thus $|\log N| \sim |\log(\sigma/C_\alpha)|$. ■

Bounded Variation Signals

Bounded variation signals may have discontinuities and include piecewise regular signals. However, it defines a more general model that does not impose any uniform regularity between singularities. The total variation of a signal over $[0, 1]$ is defined by

$$\|\bar{f}\|_V = \int_0^1 |\bar{f}'(x)|\, dx,$$

for which we derive a set of bounded variation signals

$$\overline{\Theta}_V = \left\{ \bar{f} \in \mathbf{L^2}[0, 1] \,:\, \|\bar{f}\|_V \leqslant C_V \right\}.$$

Theorem 11.18 proves that nonlinear estimators can have much lower risk than linear estimators for bounded variation functions. It also shows that wavelet thresholding estimations nearly reach the nonlinear minimax rate.

Theorem 11.18: *Donoho, Johnstone.* Over bounded variation functions, a linear wavelet projector with cut-off scale $2^k \sim \sigma / C_\alpha$ satisfies

$$r(D_k, \overline{\Theta}_V) \sim r_l(\overline{\Theta}_V) \sim C_V\, \sigma. \tag{11.158}$$

There exists $B \geqslant A > 0$ such that for any $\sigma > 0$, a thresholding wavelet estimator for $N \sim (C_V/\sigma)^{4/3}$ and $T = \sigma \sqrt{2 \log_e N}$ satisfies

$$A\, C_V^{2/3}\, \sigma^{4/3} \leqslant r_n(\overline{\Theta}_V) \leqslant r_{\text{th}}(\overline{\Theta}_V) \leqslant B\, C_V^{2/3}\, \sigma^{4/3}\, |\log(\sigma/C_V)|, \tag{11.159}$$

Proof. We first prove that

$$r(D_k, \Theta_V) \sim r_l(\Theta_V) \sim C_V\, \sigma \quad \text{with} \quad 2^{-k} \sim \sigma / C_\alpha. \tag{11.160}$$

Theorem 9.14 proves that $\varepsilon_l(\overline{\Theta}_V) = O(C_V^2\, N^{-1})$. For N sufficiently large, (11.158) is derived from (11.160) by verifying that the maximum risk over $\overline{\Theta}_{\mathbf{V}}$ and Θ_V is equivalent, with the same argument as in (11.143).

To compute the risk over Θ_V, this set is embedded in two sets that are orthosymmetric in the wavelet basis. This embedding is derived from an upper bound and a lower bound of the wavelet coefficients of $\bar{f}$. Theorem 9.13 proves that there exists $A_2 > 0$ and $B_2 > 0$ such that

$$\|\bar{f}\|_V \leqslant B_2 \sum_{j=-\infty}^{J+1} \sum_{n=0}^{2^{-j}-1} 2^{-j/2}\, |\langle \bar{f}, \psi_{j,n} \rangle| \tag{11.161}$$

and

$$\|\bar{f}\|_V \geqslant A_2 \sup_{j \leqslant J} \left(\sum_{n=0}^{2^{-j}-1} 2^{-j/2}\, |\langle \bar{f}, \psi_{j,n} \rangle| \right). \tag{11.162}$$

We know that $\langle f, \psi_{j,n} \rangle = \langle \bar{f}, \psi_{j,n} \rangle$ for $j > L$, and $f \in \Theta_V$ if and only if $\bar{f} \in \overline{\Theta}_V$. Thus, it results from (11.161) and (11.162) that for any $q \geqslant L$,

$$\Theta_q \subset \Theta_V \subset \Theta_\infty, \tag{11.163}$$

with

$$\Theta_q = \left\{ f \in \mathbb{C}^N \;:\; \sum_{m=0}^{2^{-q}-1} 2^{-q/2} \, |\langle f, \psi_{q,m} \rangle| \leqslant B_2^{-1} \, C_V \quad \text{and} \quad \langle f, \psi_{j,m} \rangle = 0 \text{ for } j \neq q \right\}$$

and

$$\Theta_\infty = \left\{ f \in \mathbb{C}^N \;:\; \sup_{j \leqslant J} \left(\sum_{m=0}^{2^{-j}-1} 2^{-j/2} \, |\langle f, \psi_{j,m} \rangle| \right) \leqslant A_2^{-1} \, C_V \right\}.$$

These two sets are orthosymmetric in the wavelet basis because they only depend on the modulus of wavelet coefficients. If f is in one of these sets, it remains in these sets when reducing the amplitude of its wavelet coefficients.

It results from (11.131) in Theorem 11.14 that

$$r_{\inf}(\mathrm{QH}[\Theta_q]) = r_l(\Theta_q) \leqslant r_l(\Theta_V) \leqslant r_l(\Theta_\infty) = r(D_k, \Theta_\infty). \tag{11.164}$$

The proof of (9.50) in Theorem 9.14 proceeds by showing that there exists B_3 such that for all $f \in \Theta_\infty$, the linear approximation error satisfies

$$\varepsilon_l(M, f) \leqslant B_3 \, \|f\|_V^2 \, M^{-1}.$$

Theorem 11.15 derives in (11.6) for $s = 1$ that

$$r(D_k \Theta_\infty) \leqslant 3 B_3 C_V \sigma \quad \text{with} \quad 2^{-k} \sim \sigma / C_\alpha. \tag{11.165}$$

Property (11.134) implies that

$$\mathrm{QH}[\Theta_q] = \left\{ f \in \mathbb{C}^N \;:\; \sum_{m=0}^{2^{-q}-1} 2^{-q} \, |\langle f, \psi_{q,m} \rangle|^2 \leqslant B_2^{-2} \, C_V^2 \quad \text{and} \quad \langle f, \psi_{j,m} \rangle = 0 \text{ for } j \neq q \right\}.$$

For $2^q = B_2 \sigma / C_V$, if $\langle f, \psi_{q,m} \rangle = \sigma$ and $\langle f, \psi_{j,m} \rangle = 0$ for $j \neq q$, then $f \in \mathrm{QH}[\Theta_q]$, and thus

$$r_{\inf}(\mathrm{QH}[\Theta_q]) \geqslant r_{\inf}(f) = 2^{-q-1} \sigma^2 = 2^{-1} \, B_2^{-1} \, C_V \, \sigma.$$

Together with (11.164) and (11.165) it implies (11.160).

To prove the nonlinear minimax risk result (11.156), we first show that

$$A \, C_V^{2/3} \, \sigma^{4/3} \leqslant r_n(\Theta_V) \leqslant r_{\mathrm{th}}(\Theta_V) \leqslant \log N \, B \, C_V^{2/3} \, \sigma^{4/3}. \tag{11.166}$$

Theorem 11.14 implies that

$$\frac{1}{1.25} \, r_{\inf}(\Theta_q) \leqslant r_n(\Theta_q)$$

and

$$r_{\mathrm{th}}(\Theta_\infty) \leqslant (2 \log_{\mathrm{e}} N + 1) \left(\sigma^2 + r_{\inf}(\Theta_\infty) \right).$$

Since $\Theta_q \subset \Theta_V \subset \Theta_\infty$, it results that

$$\frac{1}{1.25}\, r_{\inf}(\Theta_q) \leqslant r_n(\Theta_V) \leqslant r_{\text{th}}(\Theta_V) \leqslant (2\log_e N + 1)\left(\sigma^2 + r_{\inf}(\Theta_\infty)\right). \tag{11.167}$$

Theorem 9.14 proves that there exists B_4 such that for each $f \in \Theta_\infty$, the nonlinear approximation error satisfies

$$\varepsilon_n(M, f) \leqslant B_4\, C_V^2\, M^{-2}.$$

Applying (11.136) in Theorem 11.15 for $s = 3/2$ shows that

$$r_{\inf}(\Theta_\infty) \leqslant 3 B_4^{2/3}\, C_V^{2/3}\, \sigma^{2-2/3}. \tag{11.168}$$

Inserting this in (11.167) proves the right upper bound of (11.166).

To prove the left lower bound of (11.166), we choose $2^q = (B_2\sigma/C_V)^{2/3}$. If $\langle f, \psi_{q,m}\rangle = \sigma$ and $\langle f, \psi_{j,m}\rangle = 0$ for $j \neq q$, then $f \in \Theta_q$, so

$$r_{\inf}(\Theta_q) \geqslant r_{\inf}(f) = 2^{-q-1}\sigma^2 = 2^{-1}\, B_2^{-2/3}\, C_V^{2/3}\, \sigma^{4/3}.$$

Inserting this inequality in (11.167) proves the left lower bound of (11.166).

Theorem 9.14 proves that $\varepsilon_l(\overline{\Theta}_V) = O(N^{-1})$. Thus, we derive (11.159) from (11.166) by verifying that the maximum risk over Θ_V and $\overline{\Theta}_V$ is equivalent, with the same argument as in (11.143). Indeed, the linear approximation risk is sufficiently small for $N \sim (C_V/\sigma)^{4/3}$, and thus $|\log N| \sim |\log(\sigma/C_V)|$. ■

This theorem proves that when the noise variance σ decreases, the nonlinear minimax risk has a faster asymptotic decay than the linear minimax risk and the thresholding risk is asymptotically equivalent to the nonlinear minimax risk up to a $|\log\sigma|$ factor. The proof shows that the set of bounded variation functions Θ_V can be embedded in two sets that are close enough and that are orthosymmetric in a wavelet basis. It computes the linear and nonlinear risk from the linear and nonlinear approximation errors in these orthosymmetric sets. Similar minimax and thresholding risks can also be calculated in balls of any Besov space, introduced in Section 9.2.3, leading to similar near-optimality results [223].

For $\alpha > 1$, a piecewise regular signal with K discontinuities has a total variation that satisfies $\|f\|_V \leqslant B\,K\,\|f\|_{\mathbf{C}^\alpha}$ for some constant $B > 0$. The linear minimax rate is the same for piecewise regular signals in (11.155) and for the much larger class of bounded variation signals in (11.158), because the risk is dominated by the error in the neighborhood of singularities. However, the nonlinear minimax rate for a piecewise regular signal in (11.156) decays faster than for bounded variation signals in (11.159), because nonlinear estimators take advantage of the signal regularity between singularities.

Bounded Variation Images

Images with edges of finite length and no highly irregular textures have level sets of finite average length. Theorem 2.9 proves that this average length is equal to the total image variation defined by

$$\|f\|_V = \int_0^1 \int_0^1 |\vec{\nabla} f(x_1, x_2)|\, dx_1\, dx_2. \tag{11.169}$$

The partial derivatives of $\vec{\nabla} f$ are understood in the general sense of distributions to include discontinuous functions. Images also have bounded intensity values. A simple and yet quite powerful image model is thus obtained with functions having a bounded total variation and a bounded amplitude:

$$\overline{\Theta}_V = \left\{ \bar{f} \in \mathbf{L^2}[0,1]^2 \,:\, \|f\|_V \leq C_V,\ \|f\|_\infty \leq C_\infty \right\}.$$

A camera outputs discrete images obtained by a local averaging of the incoming light intensity. According to (11.138), with a white noise model, the noisy image can be written as $X[n] = f[n] + W[n]$ for $n = (n_1, n_2)$, with $f[n] = \bar{f} \star \bar{\phi}_s(ns)$ and $W[n] = \int \bar{\phi}_s(ns - x)\, dW(dx)$ for $x = (x_1, x_2)$.

Let us consider a separable wavelet orthonormal basis of $\mathbf{L^2}[0,1]^2$. Like in one dimension, we suppose that the low-pass filter is a two-dimensional scaling function $\bar{\phi}_s(x) = \phi_L^2(-x)$ associated to this wavelet orthonormal basis at a scale $s = 2^L = N^{-1/2}$. The discrete image obtained at the camera output can thus be considered as scaling coefficients $f[n] = \langle \bar{f}\, \phi^2_{L,n} \rangle$, and the resulting wavelet coefficients of $\bar{f}(x)$ are the discrete wavelet coefficients of $f[n]$ in $\mathbb{C}^N$:

$$\langle \bar{f}(x), \psi^l_{j,m}(x) \rangle = \langle f[n], \psi^l_{j,m}[n] \rangle \quad \text{for} \quad j > L, 2^j m \in [0,1]^2 \quad \text{and} \quad l = 1, 2, 3.$$

We suppose that $\phi_L^2(x)$ has a compact support and a finite total variation. Let Θ_V be the set of images $f[n]$ obtained by discretizing analog functions $\bar{f} \in \overline{\Theta}_V$. One can verify that Θ_V is a set of discrete images having a bounded amplitude and a bounded discrete total variation as defined by (2.70).

Similar to (11.154), a wavelet thresholding estimator $\tilde{F}[n]$ is computed from the wavelet coefficients of a noisy image X at scales $2^j > 2^L$, from which an analog estimator $\bar{F}(x) = \sum_n \tilde{F}[n]\, \phi^2_{L,n}(x)$ is recovered like in (11.140). Theorem 11.19 proves that this wavelet thresholding estimation of bounded variation images is more efficient than any linear estimation, and yields a risk that is nearly minimax.

Theorem 11.19: *Donoho, Johnstone.* Let $C = C_V + C_\infty$. Over bounded variation images, a linear wavelet projector with cut-off scale $2^k \sim (\sigma/C)^{4/3}$ satisfies

$$r(D_k, \overline{\Theta}_V) \sim r_l(\overline{\Theta}_V) \sim C^{4/3}\, \sigma^{2/3}. \tag{11.170}$$

There exists $B \geq A > 0$ such that for any $\sigma > 0$, a thresholding wavelet estimator for $N \sim (C/\sigma)^2$ and $T = \sigma \sqrt{2 \log_e N}$ satisfies

$$A\, C\, \sigma \leq r_n(\overline{\Theta}_V) \leq r_{\text{th}}(\overline{\Theta}_V) \leq B\, C\, \sigma\, |\log(\sigma/C)|. \tag{11.171}$$

Proof. We first prove

$$r(D_k, \Theta_V) \sim r_l(\Theta_V) \sim C^{4/3}\, \sigma^{2/3} \quad \text{with} \quad 2^k \sim (\sigma/C)^{4/3}. \tag{11.172}$$

Theorem 9.18 proves in (9.64) that

$$\varepsilon_l(N, \overline{\Theta}_V) = O(C^2\, N^{-1/2}) \quad \text{with} \quad C = C_V + C_\infty.$$

For N sufficiently large, the theorem result (11.170) is derived from (11.172), with the same argument as in (11.143).

The risk over Θ_V is calculated by embedding this set in two orthosymmetrics in the wavelet basis. Let us define

$$\Theta_q = \Big\{ f \in \mathbb{C}^N \;:\; \sum_{\substack{2^q m \in [0,1]^2 \\ 1 \leqslant l \leqslant 3}} |\langle f, \psi^l_{q,m} \rangle| \leqslant B_2^{-1} C \quad \text{and} \quad |\langle f, \psi^l_{q,m} \rangle| \leqslant B_2^{-1} C\, 2^q \quad \text{and} \quad \langle f, \psi^l_{j,m} \rangle = 0 \quad \text{for} \quad j \neq q \Big\}$$

and

$$\Theta_\infty = \left\{ f \in \mathbb{C}^N \;:\; \sup_{\substack{j \leqslant J \\ 1 \leqslant l \leqslant 3}} \left(\sum_{2^j m \in [0,1]^2} |\langle f, \psi^l_{j,m} \rangle|^2 \right) \leqslant A_2^{-2} C^2\, 2^j \right\}.$$

The upper bound (9.61) of Theorem 9.17 implies that there exists $B_2 > 0$ such that $\Theta_q \subset \Theta_V$ for any $q \geqslant L$ with $N = 2^{-2L}$. One can also derive from (9.67) that $\Theta_V \subset \Theta_\infty$ for some $0 < A_2 < B_2$. This embedding implies that

$$r_{\text{inf}}(\text{QH}[\Theta_q]) \leqslant r_l(\Theta_V) \leqslant r(D_k, \Theta_\infty). \tag{11.173}$$

The proof of (9.64) in Theorem 9.18 proceeds by showing that there exists B_3 such that the linear approximation error of any $f \in \Theta_\infty$ satisfies

$$\varepsilon_l(M, f) \leqslant B_3 \, \|f\|_V \, \|f\|_\infty M^{-1/2} \leqslant B_3 C^2 M^{-1/2}.$$

Theorem 11.15 derives in (11.135) for $s = 3/4$ that

$$r(D_k, \Theta_\infty) \leqslant 3 B_3^{2/3} C^{4/3} \sigma^{2/3} \quad \text{with} \quad 2^{-k} \sim (C/\sigma)^{4/3}. \tag{11.174}$$

Using the inequality $\sum_n |c_n|^2 \leqslant \sup_n |c_n| \sum_n |c_n|$, one can also verify that

$$\text{QH}[\Theta_q] = \left\{ f \in \mathbb{C}^N \;:\; \sum_{2^q m \in [0,1]^2} 2^{-q} |\langle f, \psi^l_{q,m} \rangle|^2 \leqslant B_2^{-2} C^2 \right\}.$$

For $2^q = (B_2 \sigma / C)^{2/3}$, if $\langle f, \psi_{q,m} \rangle = \sigma$ and $\langle f, \psi_{j,m} \rangle = 0$ for $j \neq q$, then $f \in \text{QH}[\Theta_q]$, so

$$r_{\text{inf}}(\text{QH}[\Theta_q]) \geqslant r_{\text{inf}}(f) = 2^{-2q-1} \sigma^2 = 2^{-1} B_2^{-4/3} C^{4/3} \sigma^{2/3}.$$

Inserting this result and (11.174) in (11.173) proves (11.172).

To prove the nonlinear minimax risk result (11.171), we first show that

$$A\, C\, \sigma \leqslant r_n(\Theta_V) \leqslant r_{\text{th}}(\Theta_V) \leqslant B\, C\, \log N \sigma. \tag{11.175}$$

This requires a different embedding of Θ_V. Let $f^r_{\mathcal{B}}[k]$ be the sorted wavelet coefficients in decreasing amplitude order. Theorem 9.17 proves that there exists $A_4 > 0$ such that

$$\Theta_V \subset \Theta_1^* = \left\{ f \in \mathbb{C}^N \;:\; |f^r_{\mathcal{B}}[k]| \leqslant A_4^{-1} C_V\, k^{-1} \right\},$$

where Θ_1^* is also an orthosymmetric set. Theorem 11.14 implies that

$$\frac{1}{1.25}\, r_{\text{inf}}(\Theta_q) \leqslant r_n(\Theta_q)$$

and

$$r_{\text{th}}(\Theta_1^*) \leqslant (2 \log_{\text{e}} N + 1)\left(\sigma^2 + r_{\text{inf}}(\Theta_1^*)\right).$$

Since $\Theta_q \subset \Theta_V \subset \Theta_1^*$, it results that

$$\frac{1}{1.25}\, r_{\text{inf}}(\Theta_q) \leqslant r_n(\Theta_V) \leqslant r_{\text{th}}(\Theta_V) \leqslant (2 \log_{\text{e}} N + 1)\left(\sigma^2 + r_{\text{inf}}(\Theta_1^*)\right). \qquad \textbf{(11.176)}$$

Theorem 9.17 proves that there exists B_4 such that for each $f \in \Theta_1^*$, the nonlinear approximation error satisfies

$$\varepsilon_n(M, f) \leqslant B_4\, C_V^2\, M^{-1}.$$

Applying (11.136) in Theorem 11.15 for $s = 1$ shows that

$$r_{\text{inf}}(\Theta_1^*) \leqslant 3 B_4^{1/2}\, C_V\, \sigma. \qquad \textbf{(11.177)}$$

Inserting this in (11.176) proves the right upper bound of (11.175).

To prove the left lower bound of (11.175), we choose $2^q = B_2 \sigma / C$. If $\langle f, \psi_{q,m} \rangle = \sigma$ for 2^{-q} indexes m, and if $\langle f, \psi_{q,m} \rangle = 0$ for the $2^{-2q} - 2^{-q}$ others, and if $\langle f, \psi_{j,m} \rangle = 0$ for $j \neq q$, then we verify that $f \in \Theta_q$ and thus that

$$r_{\text{inf}}(\Theta_q) \geqslant r_{\text{inf}}(f) = 2^{-q-1}\sigma^2 = 2^{-1}\, B_2^{-1}\, C\, \sigma.$$

Inserting this inequality in (11.176) proves the left lower bound of (11.175).

Theorem 9.18 proves that $\varepsilon_l(\overline{\Theta}_V) = O(C^2\, N^{-1/2})$. We derive (11.171) from (11.175) with the same argument as in (11.143), by setting $N \sim (C/\sigma)^2$ and thus $|\log N| \sim |\log(\sigma / C_V)|$, so that $\varepsilon_l(\overline{\Theta}_V) = O(C\sigma)$. ■

This theorem proves that wavelet thresholding estimators are nearly minimax over bounded variation images and yield a risk with a decay that is faster than any linear estimator. In two dimensions, the hypothesis that images have a bounded amplitude is important to control linear approximation errors that play a role both for linear and nonlinear estimators.

For images having some geometric regularity, such as the $\mathbf{C}^2$ piecewise regular images in Section 11.3.2, a thresholding estimator in a curvelet frame has a risk with an asymptotic decay that is faster for small σ. Indeed, curvelet frames yield nonlinear approximations with a smaller asymptotic error for such images. This is also valid for bandlet estimations presented in Section 12.2.4.

11.6 EXERCISES

11.1 [2] *Linear prediction.* Let $F[n]$ be a zero-mean, wide-sense stationary random vector with covariance $R_F[k]$. We predict the future $F[n+l]$ from past values $\{F[n-k]\}_{0 \leqslant k < N}$ with $\tilde{F}[n+l] = \sum_{k=0}^{N-1} a_k\, F[n-k]$.

(a) Prove that $r = E\{|F[n+l] - \tilde{F}[n+l]|^2\}$ is minimum if and only if

$$\sum_{k=0}^{N-1} a_k \, R_F[q-k] = R_F[q+l] \quad \text{for} \quad 0 \leqslant q < N.$$

Verify that $r = R_F[0] - \sum_{k=0}^{N-1} a_k \, R_F[k+l]$ is the resulting minimum risk. *Hint:* Use Proposition 11.2.

(b) Suppose that $R_F[n] = \rho^{|n|}$ with $|\rho| < 1$. Compute $\tilde{F}[n+l]$ and r.

11.2 [1] Let $X = F + W$ where the signal F and the noise W are zero-mean, wide-sense circular stationary random vectors. Let $\tilde{F}[n] = X \circledast h[n]$ and $r(D, \pi) = E\{\|F - \tilde{F}\|^2\}$. The minimum risk $r_l(\pi)$ is obtained with the Wiener filter (11.14). A frequency selective filter h has a discrete Fourier transform $\hat{h}[m]$ that can only take the values 0 or 1. Find the frequency selective filter that minimizes $r(D, \pi)$. Prove that $r_l(\pi) \leqslant r(D, \pi) \leqslant 2\, r_l(\pi)$.

11.3 [2] Let $\{g_m\}_{0 \leqslant m < N}$ be an orthonormal basis. We consider the space $\mathbf{V}_p$ of signals generated by the first p vectors $\{g_m\}_{0 \leqslant m < p}$. We want to estimate $f \in \Theta = \mathbf{V}_p$ from $X = f + W$, where W is a white Gaussian noise of variance σ^2.

(a) Let $\tilde{F} = DX$ be the orthogonal projection of X in $\mathbf{V}_p$. Prove that the resulting risk is minimax among linear operators:

$$r(D, \Theta) = r_n(\Theta) = p\, \sigma^2.$$

(b) Find the linear minimax estimator over the space of discrete polynomial signals of size N and degree d. Compute the linear minimax risk.

11.4 [1] Let $|\langle f, g_{m_k} \rangle| \geqslant |\langle f, g_{m_{k+1}} \rangle|$ for $k \geqslant 1$ be the sorted decomposition coefficients of f in $\mathcal{B} = \{g_m\}_{0 \leqslant m < N}$. We want to estimate f from $X = f + W$ where W is a Gaussian white noise of variance σ^2. If $|\langle f, g_{m_k} \rangle| = 2^{-k/2}$, compute the oracle projection risk r_p in (11.34) as a function of σ^2 and N. Give an upper bound on the risk r if we threshold at $T = \sigma\sqrt{2 \log_e N}$ the decomposition coefficients of X. The same question if $|\langle f, g_{m_k} \rangle| = k^{-1}$. Explain why the estimation is more precise in one case than in the other.

11.5 [3] Let $\Theta_{d,K}$ be a set of signals that are piecewise polynomial of degree q, with at most K discontinuities with N samples. Let $X = f + W$ where W is a Gaussian white noise of variance σ^2.

(a) Prove that the minimax risk satisfies $r_n(\Theta_{d,K}) \geqslant K(d+1)\sigma^2$.

(b) Prove that a thresholding risk in a Daubechies wavelet basis with $d+1$ vanishing moments satisfies $r_{\text{th}}(\Theta_{d,K}) = O(K(d+1)(\log_e N)^2 \sigma^2)$.

11.6 [2] Let $F = f[(n - P) \bmod N]$ be the random-shift process (11.17) obtained with a Dirac doublet $f[n] = \delta[n] - \delta[n-1]$. We want to estimate F from $X = F + W$ where W is a Gaussian white noise of variance $\sigma^2 = 4\, N^{-1}$.

(a) Specify the Wiener filter $\tilde{F}$ and prove that the resulting risk satisfies $r_l(\pi) = E\{\|F - \tilde{F}\|^2\} \geqslant 1$.

(b) Show that one can define a thresholding estimator $\tilde{F}$ with a risk

$$E\{\|F-\tilde{F}\|^2\} \leq 12\,(2\,\log_e N+1)\,N^{-1}.$$

11.7 [2] Let $f=\mathbf{1}_{[0,P-1]}$ be a discrete signal of $N>P$ samples. Let $F=f[(n-P) \bmod N]$ be the random-shift process defined in (11.17). We measure $X=F+W$ where W is a Gaussian white noise of variance σ^2.

(a) Suppose that $\tilde{F}=F \circledast h$. Compute the transfer function $\hat{h}[m]$ of the Wiener filter and the resulting risk $r_l(\pi)=E\{\|F-\tilde{F}\|^2\}$.

(b) Let $\tilde{F}$ be the estimator obtained by thresholding the decomposition coefficients of each realization of F in a Haar basis, with $T=\sigma\sqrt{2\log_2 N}$. Prove that $E\{\|F-\tilde{F}\|^2\} \leq \sigma^2(2\log_e N+1)^2$.

(c) Compare the Wiener and Haar thresholding estimators when N is large.

11.8 [2] *Two-dimensional wavelet tight frame.* Implement a translation-invariant wavelet thresholding estimator for images. The translation-invariant dyadic wavelet transform is computed similarly to a separable orthogonal wavelet image transform. The filtering and subsampling by conjugate mirror filters along rows and columns are replaced by nondecimated filterings with the same filters, according to the *algorithme à trous* in Section 5.2.2.

11.9 [2] Compare the SNR and the visual quality of hard and soft thresholding estimators in a wavelet Orthonormal basis and hard- and soft-thresholding estimators in translation-invariant wavelet frames for images contaminated by an additive Gaussian white noise. Perform numerical experiments on the Lena, Barbara, and peppers images. Find the best threshold values T as a function of the noise variance.

11.10 [2] For audio denoising, implement a soft-thresholding estimator in a windowed Fourier transform tight frame. Compare the audio quality and the SNR with a block thresholding estimator, over time-frequency blocks of fixed size.

11.11 [3] Let $g(t)$ be a Gaussian of variance 1. Let $g_s[n]=K_s\,g(n/s)$, where K_s is adjusted so that $\sum_n g_s[n]=1$. An adaptive smoothing of $X=f+W$ is calculated by adapting the scale s as a function of the abscissa:

$$\tilde{F}[l]=\sum_{n=0}^{N-1} X[n]\,g_{s(l)}[l-n]. \tag{11.178}$$

The scale $s(l)$ should be large where the signal f seems to be regular, whereas it should be small if we guess that f may have a sharp transition in the neighborhood of l.

(a) Find an algorithm that adapts $s(l)$ depending on the noisy data $X[n]$, and implement the adaptive smoothing (11.178). Test your algorithm on the Piece-polynomial and Piece-regular signals in WaveLab as a function of the noise variance σ^2.

(b) Compare your numerical results with a translation-invariant hard wavelet thresholding. Analyze the similarities between your algorithm that computes $s(l)$ and the strategy used by the wavelet thresholding to smooth or not to smooth certain parts of the noisy signal.

11.12 [3] *Risk of frame thresholding.* Let $\{\phi_p\}_{0 \leqslant p < P}$ with $P \geqslant N$ be a frame of $\mathbb{C}^N$ with frame bounds $B \geqslant A > 0$. For $X = f + W$ where W is a Gaussian white noise of variance σ^2, prove that the risk of a thresholding estimator (11.68) satisfies $r_{\text{th}}(f) \geqslant B^{-1} \sum_{p=0}^{P-1} \min(|\langle f, \phi_p \rangle|^2, \sigma^2)$.

11.13 [3] Let $r_{\text{th}}(f, T)$ be the risk of an estimator of f obtained by hard thresholding at T the decomposition coefficient of $X = f + W$ in a basis $\mathcal{B}$. The noise W is Gaussian white with a variance σ^2. This risk is estimated by

$$\tilde{r}(X, T) = \sum_{m=0}^{N-1} C(X_{\mathcal{B}}[m]),$$

with

$$C(u) = \begin{cases} u^2 - \sigma^2 & \text{if } u \leqslant T \\ \sigma^2 & \text{if } u > T \end{cases}.$$

(a) Justify qualitatively the definition of this estimator as it is done for (11.71) in the case of a soft-thresholding estimator.

(b) Let $\phi_\sigma(x) = (2\pi\sigma^2)^{-1/2} \exp(-x^2/(2\sigma^2))$. With calculations similar to the proof of Theorem 11.9, show that

$$r_{\text{th}}(T) - E\{\tilde{r}(X, T)\} = 2\, T\, \sigma^2 \sum_{m=0}^{N-1} \Big[\phi_\sigma(T - f_{\mathcal{B}}[m]) + \phi_\sigma(T + f_{\mathcal{B}}[m]) \Big].$$

(c) Implement an algorithm that finds $\tilde{T}$ that minimizes $\tilde{r}(X, T)$. Study numerically the performance of $\tilde{T}$ to estimate noisy signals with a hard thresholding in a wavelet basis.

11.14 [2] We want to estimate a signal f that belongs to an ellipsoid

$$\Theta = \left\{ f \,:\, \sum_{m=0}^{N-1} \beta_m^2 \, |f_{\mathcal{B}}[m]|^2 \leqslant C^2 \right\}$$

from $X = f + W$, where W is a Gaussian white noise of variance σ^2. We denote $x_+ = \max(x, 0)$.

(a) Using Proposition 11.14, prove that the minimax linear risk on Θ satisfies

$$r_l(\Theta) = \sigma^2 \sum_{m=0}^{N-1} a[m], \qquad \textbf{(11.179)}$$

with $a[m] = (\frac{\lambda}{\beta_m} - 1)_+$ where λ is a Lagrange multiplier calculated with

$$\sum_{m=0}^{N-1} \beta_m \left(\frac{\lambda}{\beta_m} - 1 \right)_+ = \frac{C^2}{\sigma^2}. \tag{11.180}$$

(b) By analogy to Sobolev spaces, the set Θ of signals having a discrete derivative of order s with an energy bounded by C^2 is defined from the discrete Fourier transform:

$$\Theta = \{ f : \sum_{m=-N/2+1}^{N/2} |m|^{2s} N^{-1} |\hat{f}[m]|^2 \leqslant C^2 \}. \tag{11.181}$$

Show that the minimax linear estimator D in Θ is a circular convolution $DX = X \circledast h$. Explain how to compute the transfer function $\hat{h}[m]$.

(c) Show that the minimax linear risk satisfies

$$r_l(\Theta) \sim C^{2/(2s+1)} \sigma^{2-2/(2s+1)}.$$

11.15 [3] Let $h \in \mathbb{C}^N$, then consider the set of shift signals $\Theta_h = \{h_p[n] = h[(n-p) \bmod N] \text{ for } 0 \leqslant p < N\}$. Let $X = f + W$ with $f \in \Theta_h$.

(a) Find a linear estimator that is diagonal in the Fourier basis and that yields a minimax risk over Θ_h.

(b) For $h[n] = 1_{[0,N/2]}[n]$, prove that $r_l(\Theta_h)/(N\sigma^2) \sim N^{-1/2}$ for all $N > 0$.